EXPERIMENTS ON NUCLEAR STRUCTURE

by

D. J. Pullen, B.Sc.

A thesis submitted for the degree of
Doctor of Philosophy in the
University of Oxford

Trinity College
Oxford

July, 1963

ACKNOWLEDGEMENTS

It is with pleasure that I acknowledge the advice and encouragement of Professor Denys H. Wilkinson, under whose supervision this research has been carried out.

Many of the experiments were performed in collaboration with Dr. Roy Middleton to whom I am deeply indebted for his friendly guidance and assistance. I also wish to express my appreciation to Dr. S. Hinds and Dr. A.E. Litherland for their help and collaboration at various stages of the work. I am grateful to Dr. J.R. Rook for helpful discussions on the interpretation of the results. My thanks are due to Dr. B. Buck, Dr. P.E. Hodgson, Mr. B.E.F. Macefield and Mr. R.N. Maddison for the use of their computer programmes.

I am indebted to Mr. H. Marchant for his valuable assistance with the experiments and analysis of the data, and to Mr. A.H.F. Muggleton who prepared many of the targets. I thank Mrs. J. Redding and Miss J. Homer and their staff for their cooperation in scanning the nuclear emulsion plates. Thanks are also due to Mr. D. Akers and his staff for operating the A.W.R.E. Aldermaston Tandem accelerator.

I gratefully acknowledge the financial assistance given me by the U.K. Department of Scientific and Industrial Research.

ABSTRACT

Magnetic deflection techniques have been employed to measure proton angular distributions from some (d,p) and (t,p) reactions. In many cases the distributions exhibit typical stripping patterns and their analysis in terms of plane wave and distorted wave theories of stripping has enabled spin and parity assignments to be made for a number of excited nuclear levels. These theories are briefly outlined in Chapter 1 of this thesis and the experimental procedures are described in Chapter 2.

The (d,p) reaction has been studied at an incident energy of 3 MeV with target nuclei B^{10}, B^{11}, C^{12}, C^{14} and O^{16} and an account of this investigation is given in Chapter 3. Although the plane wave theory gives a good account of the angular distributions corresponding to the low-Q transitions (say $Q \leq 2$ MeV) it is not a good approximation for the high-Q transitions. This is in accord with Wilkinson's suggestion that distortion effects should be quite small even at low deuteron bombarding energies providing also that the reaction Q-value is low. Agreement with the high-Q ground state distribution for B^{11} could only be obtained with distorted wave theory if a cut-off radius were used. This may indicate the need for taking into account finite range effects in this theory.

The $Se^{76}(d,p)Se^{77}$ reaction has been studied at 7.8 MeV bombarding energy and eleven angular distributions corresponding to the ground and ten excited states of Se^{77} have been analysed using distorted wave theory. This investigation is described in Chapter 4. Deuteron and proton elastic scattering measurements have also been made from Se^{76} and Se^{77}, respectively. The optical model potentials required to describe the stripping distributions are found to be entirely consistent with those derived from the elastic scattering data.

In Chapter 5 an account is given of a systematic study of the (t,p) reaction for target nuclei B^{10}, B^{11}, C^{12}, C^{14}, O^{16}, O^{18} Si^{28}, Si^{29} and Ca^{40}. This investigation was carried out at triton energies between 8 and 13 MeV. In the majority of cases the angular distributions are observed to be strongly forward peaked and these have been analysed in terms of Newns' plane wave theory of double stripping. With the exception of the $B^{10}(t,p)B^{12}$ and $C^{12}(t,p)C^{14}$ reactions the agreement in general is found to be very satisfactory. In addition to the ground state, nine excited states of B^{13} were observed and information on the spins and parities of six of them have been obtained. The excitation energies of only four excited states were

previously known. C^{16} had not previously been observed and the present investigation has shown this to be stable by 4.25 MeV against neutron emission, in good agreement with the predictions of Zel'dovich. The ground state was confirmed to be O^{+} and the first excited state at 1.753 MeV excitation is probably 2^{+}. The delayed neutron emission for C^{16} has also been studied and its measured half-life found to be 0.74 ± 0.03 seconds. Angular distributions were measured for the ground and nine excited states of O^{18} and ground and four excited states of O^{20}. Only one state, at 4.45 MeV excitation in O^{18}, could not be interpreted by a double stripping process. Spin-parity assignments from the reactions $Si^{28}(t,p)Si^{30}$, $Si^{29}(t,p)Si^{31}$ and $Ca^{40}(t,p)Ca^{42}$ are in good agreement with earlier measurements.

The Be^{11} nucleus has been studied using the $Be^{9}(t,p)Be^{11}$ reaction at 6 and 10 MeV triton energies. This investigation is described in Chapter 6. At the higher bombarding energy six energy levels of Be^{11} were observed and three of these were found to have natural widths in excess of 10 keV. Proton distributions were measured at both energies for the ground and first excited states. Their interpretation in terms of a double stripping mechanism is complicated by the presence of large backward peaks but the distributions are not inconsistent with the spins of $\frac{1}{2}^{-}$ and $\frac{1}{2}^{+}$, respectively, predicted by Talmi and Unna. Angular distributions from the $C^{12}(t,\alpha)B^{11}$ reaction at 10 MeV triton energy were also studied in an attempt to obtain information on the spins and parities of some of the states in B^{11} which are involved in the beta-decay of Be^{11}.

In Chapter 7 an account is given of triton elastic scattering measurements made at incident energies 6.4, 6.8 and 7.2 MeV from C^{12}, O^{16}, O^{18}, F^{19} and Ca^{40}. Only the scattering from F^{19} and Ca^{40} can be readily described by the optical model, although the optical parameters are ambiguous. The scattering distributions from O^{16} at all three energies exhibit large backward peaks suggestive of compound resonance scattering.

Optical model parameters derived from the triton scattering data have been used by Rook and Mitra to analyse the proton distributions from $Ca^{40}(t,p)Ca^{42}$, using distorted wave theory. A brief account of the results is given in Appendix C.

TABLE OF CONTENTS

Page No.

CHAPTER I

GENERAL INTRODUCTION

The work described herein is concerned mainly with an experimental study of some of the level properties of light nuclei, in particular the spins and parities of excited states, and of the mechanisms of the nuclear reactions employed in their investigation. Considerable data has accumulated during this last decade on both the static and dynamic properties of nuclear energy levels. Although in principle these could be calculated from a detailed knowledge of the internucleon forces the solution of the many-body problem involved is prohibitively complex. Instead, models of the nucleus have been constructed whose physical properties can be calculated and compared with experiment. The extent to which the predictions of a model are confirmed by experiment is then a test of its validity.

In the first part of this chapter a brief description is given of some of the nuclear models which have been particularly successful. This is then followed by a discussion of the nuclear reactions employed in the present investigations.

1.1 The Nuclear Shell Model

It was early recognised that strong discontinuities occur in the properties of nuclei with certain numbers of neutrons and protons - the 'magic' numbers - and this suggested a shell model structure for the nucleus whereby the nuclear discontinuities arise as a result of shell closures. In the simplest form of the shell model, the single particle model, an even number of nucleons of a given kind are assumed to pair off to form an 'inert core' having zero angular momentum. Any remaining nucleon then moves in an average spherically symmetric potential well due to this core and the properties of the nucleus are taken to be due only to this single nucleon. By a suitable choice of well shape, e.g. square well or harmonic oscillator potential, the ordering of the energy levels may be calculated, but as it stands this model is unable to predict the correct energy gaps required to explain the magic numbers. These arise quite naturally, however, if in addition to the static potential an interaction between the intrinsic spin and orbital angular momentum of each nucleon is also assumed. This spin-orbit interaction or j-j coupling scheme, which was introduced by Mayer [(1)] and Haxel, Jensen and Suess [(2)], gives rise to an energy difference between the states

j=l+½ and j=l-½ which increases with l, the former being more strongly bound. In addition now to yielding the magic numbers this model correctly predicts, though with some exceptions, the ground state spins and parities of even-even and odd-A nuclei and gives at least a qualitative understanding of their magnetic moments.

There are, nevertheless, serious objections to this simple model. For example, it is clearly unable to predict the spins of odd-odd nuclei where there are two unpaired nucleons, since there is nothing to indicate which of the various possible resultants of the two j-vectors has lowest energy. There are also a number of cases where the observed ground state spins of odd-A nuclei are one unit less than predicted by the single particle model (e.g. Ne^{21} and Na^{23} both have spin 3/2 whereas the model predicts $d_{5/2}$ ground states). Also, the model is limited to a description of excited nuclear states in terms of only single particle excitations.

A more refined version of the shell model is the independent particle model. In this, the residual two-body interactions between the 'loose' particles in an unfilled shell are introduced as a perturbation and only the filled shells are assumed to form an inert core. The total wave function for the individual particles in a particular state is obtained, in either the L-S or j-j coupling schemes, by an expansion in terms of a single particle wave function. This expansion contains a sum of terms, each a product of the single particle wave function and a properly antisymmetrized wave function representing the remaining (n-1) particles. The summation extends over all possible wave functions for the (n-1) particles and these are referred to as the parent states of the state in question. The coefficients of the terms in the expansion are the coefficients of fractional parentage (Lane and Wilkinson [3]) which ensure correct overall antisymmetrization.

In a review of the energy levels of light nuclei, Inglis [4] showed that neither j-j coupling nor L-S coupling can alone account for the observed level spectra for nuclei in the 1p-shell between He^4 and O^{16}. To obtain reasonable agreement it is necessary to assume a mode of coupling intermediate between these two extremes. Furthermore, Lane [5] has demonstrated that the observed dynamic properties of these nuclei, such as radiative transition widths and particle decay widths, are consistent only with intermediate coupling. Calculations involving intermediate coupling in the 1p-shell depend on only three parameters, L, K and a. The parameters L and K are the direct and exchange radial integrals which arise from the central potential and ‘a’ is a measure of the strength of the spin-orbit force. For a reasonable choice of potential and wave function the ratio L/K is found to be approximately 6. The value K fixes the energy scale and a/K is the intermediate coupling parameter, i.e. for predominantly j-j coupling a/K>>1 and for predominantly L-S coupling

a/K<<1. Kurath [6] has calculated the energy levels in the 1p-shell as a function of a/K and comparison with experiment indicates that a gradual transition from L-S to j-j coupling takes place through the shell. More generally, the j-j coupling model becomes a better approximation with increasing mass number, and beyond about A = 40 it is a very reasonable approximation. (This is to be expected since it is required to reproduce the proper shell closures in the heavier nuclei.)

For nuclei just beyond O^{16} the situation is complicated by the fact that the $2s_{1/2}$ and $1d_{5/2}$ levels are nearly degenerate which results in a high degree of configuration mixing between these states. Nevertheless, intermediate coupling calculations have been carried out by Elliot and Flowers [7] for nuclei up to A = 19.

1.2 The Nuclear Collective Model

Detailed calculations with the independent particle model become extremely complex when the number of particles outside a closed shell (or holes within a shell) is not very small. However, for nuclei sufficiently far from a closed shell the energy spectra exhibit features that may be interpreted in terms of rotational bands. These arise from collective motion of the nucleons corresponding to variations in the shape of the nucleus, i.e. departures of the binding field from spherical symmetry. Furthermore, such nuclear distortions are also suggested by the large electric quadrupole moments observed in many nuclei that cannot readily be accounted for by the independent particle model.

In the collective model of Bohr and Mottelson [8] the nucleus is considered as made up of a more or less stable core of nucleons formed into closed shells, with the extra nucleons moving in the potential of the core, but then includes the deformation of the core caused by its interaction with the extra nucleons. This deformed core thus amounts to a modification of the field in which the nucleons move. The nuclear spin is then given by the resultant of the deformation oscillations and the intrinsic motion of the individual nucleons.

A detailed model of the intrinsic level structure in a deformed potential has been constructed by Nillson [9] using a single particle Hamiltonian with an ellipsoidal oscillator potential, together with a spin-orbit term and a term depending on l (which compensates for the tendency of the oscillator well to give too small a binding energy for states with high l). Nillson gives the single particle levels as a function of the deformation and the results are presented in an extensive set of level diagrams. If the deformation is known, for example from the measured quadrupole moment, then the ground state spin of a particular nucleus can be obtained by counting up the occupied levels

in the level diagram for that value of the deformation parameter and determining the orbit of the last unpaired nucleon. This intrinsic state can then form the basis of a rotational band. As in the 'undistorted' shell model, excited states can arise from the odd nucleon moving to higher unfilled orbits in the Nillson model. This 'Unified' model, which effectively couples the independent particle model with the collective model, has proved capable of explaining an impressive array of nuclear properties.

Although the collective model had its earliest successes with heavier nuclei it has also been successfully applied to a number of nuclei in the (2s,1d)-shell. For example, Litherland et al [(10)] have shown that the lower-lying levels of nuclei of masses 25 and 31 can be well described as overlapping systems of rotational bands, and Paul [(11)] has obtained very good agreement with the observed properties of F^{19} by applying the Nillson model.

1.3 Direct Nuclear Reactions and Plane Wave Theory

In the experimental studies of the properties of nuclear energy levels, direct reactions have played a particularly important role. In these, the initial nuclear state proceeds directly to the final state without the intermediate formation of a compound nucleus. A distinctive feature of such reactions is then the strong dependence of the cross section on the direction of emission of the reaction products.

A particularly well-known example of this class of reactions is the deuteron stripping reaction. In this, one or other of the component particles of the deuteron is stripped off and captured by the target nucleus to form a definite quantum state of the residual nucleus, leaving the other to continue in the forward or near-forward direction. Calculations of the angular distributions of the particles emitted from such a process were first made by Butler [(12)], and by Bhatia, Huang, Huby and Newns [(13)] who used the Born approximation. These theories showed that the distribution is characteristic of the orbital angular momentum, l (in units of $\hbar$), taken into the nucleus by the captured nucleon. The selection rules require the final state spin, J_f, to be given by the vector addition of the initial spin, J_i, the intrinsic spin of the captured nucleon (½) and the value of l, i.e.

$$\vec{J}_f = \vec{J}_i + \vec{\ell} + \vec{\tfrac{1}{2}}$$

and hence

$$(J_i + \ell + \tfrac{1}{2}) \geq J_f \geq \left|\vec{J}_i + \vec{\ell} + \vec{\tfrac{1}{2}}\right|_{min}$$

If the parities of the initial and final states are π_i and π_f then

$$\pi_i \pi_f = (-1)^{\ell}$$

and there is a change of parity only if *l* is odd. Thus, if the spin and parity of the target nucleus are known and if the *l*-value can be obtained from the measured distribution of the emitted particles, then the parity of the final state can be determined, together with limits on the value of J_f.

In the theories of Butler and Bhatia et al., coulomb forces are neglected, interactions between the neutron and proton after stripping and between the emitted particle and residual nucleus are disregarded, and it is assumed that the effects of elastic and inelastic scattering of the deuterons can be neglected. Thus the waves in the incident and exit channels are represented by plane waves. It is also assumed that the capture takes place at a radius R, whose value must be chosen so as to give agreement with the experimental data. For the Butler theory the Gamow-Critchfield radius, [14] $R = (1.7 + 1.22\ A^{1/3}) \times 10^{-13}$ cm, is usually found to give reasonable agreement providing distortion effects are not too severe. The angular dependence of the cross sections from the Butler and Born approximation theories are generally found to be similar providing the radius used for the latter is about 1fm (1 fermi (fm) = 10^{-13}cm) larger than that used for the Butler theory.

The differential cross section predicted by Butler may be expressed for a (d,p) reaction (the (d,n) case is similar) in the form*

$$\sigma(\theta) = \frac{8N^2R^3}{\hbar^2}\left(\frac{m_d^* m_p^*}{m_n^*}\right)\left(\frac{k_p}{k_d}\right)\left(\frac{2J_f+1}{2J_i+1}\right)\frac{1}{(q^2+k_n^2)^2}\sum_{\ell_n}\left[q.\,j_{\ell_n-1}(qR) - ik_n\, j_{\ell n}(qR)\frac{h^{(1)}_{\ell_n-1}(ik_nR)}{h^{(1)}_{\ell_n}(ik_nR)}\right]^2\gamma^2_{\ell_n}$$

where the term N^2 is related [12] to the normalization of the asymptotic state of the deuteron and is given by $2\alpha/(1-\alpha\rho_t)$, where $\hbar^2\alpha^2/m$ is the deuteron binding energy, ε_d, and ρ_t is the effective range of the triplet neutron-proton interaction. The quantities m_d, m_p and m_n are the reduced masses of the deuteron, proton and captured neutron, and k_p, k_d are the wave numbers of the emitted proton and incident deuteron. Quantity q is the momentum with which the captured neutron approaches the nuclear surface i.e. $q = \left|\vec{k}_d - \vec{k}_p\right|$, and ik_n the wave number of the captured neutron in its final state, calculated from energy conservation. $j_\nu(qR)$ is a spherical Bessel function and $h_\nu^{(1)}(ik_nR)$ a spherical Hankel function. The factor $\gamma^2_{\ell n}$ is the reduced width of the energy level into which the

* In practice the summation over l_n usually reduces to only one term.

neutron is captured. For a virtual state it is related to the partial width, $\Gamma_{\ell n}$, for the decay of that state back to the initial state, by a barrier penetration factor [15]. For a bound state $\gamma^2_{\ell n}$ is defined formally. In the theory of Bhatia et al., the cross-section is expressed in a similar form but is dependent on only one Bessel function, $j_{\ell n}$. It also contains a term $\Omega_{\ell n}$, the neutron capture probability analogous to $\gamma^2_{\ell n}$. (Occasionally $\Lambda_{\ell n}$ is used where $\Lambda_{\ell n} = (2J_f + 1)\,\Omega_{\ell n}$).

Since stripping is a one-particle process it may only lead to states where the captured nucleon is in a single-particle level with orbital angular momentum *l*, outside a core comprising the target nucleus in its ground state i.e. without change of parent [3]. Thus the stripping reduced width is expected to be large for a transition leading to a state whose configuration is predominantly single-particle. Providing the stripping mechanism is well understood, the reduced level widths obtained from these reactions may thus be compared with the values predicted by a nuclear model, and this provides a stringent test of the model. The expected reduced width for a single-particle level is $3\hbar^2/2mR^2$ where m is the reduced nucleon mass. It is thus convenient to define a dimensionless reduced width, θ^2_ℓ, as the ratio of the measured $\gamma^2_{\ell n}$ (in absolute units) to this value.

Despite the far reaching nature of the assumption used to derive the Butler-Born formulae, the angular distributions so calculated have been very successful in describing at least the general features of a large number of experimental distributions. Also, in addition to the (d,p) and (d,n) processes, angular distributions from many other one-nucleon transfer processes exhibit Butler-type patterns, for example (p,d), (n,d), (He^3,d), (t,α), etc. The first two are simply the reverse of the (d,p) and (d,n) reactions and, as for the (t,α) reaction, have been interpreted in terms of a direct 'pick-up' mechanism.

In view of the underlying assumptions made, however, it is not surprising that some departures from the simple theory are observed. For example, the measured distributions for *l*=1 transitions are frequently observed to dip below the theoretical curve in the forward direction, and *l*=2 distributions sometimes exhibit a subsidiary peak at 0^o which is not accounted for by the theory. The theory also fails to account for the detailed structure observed in the distribution at angles beyond the position of the principal stripping peak. In the case of positive Q-value transitions, the stripping peaks corresponding to different *l*-values are sufficiently well separated to enable unambiguous determinations of *l*. For negative Q-values, however, and moderate deuteron energies, all distributions with $l \leq 2$ tend to peak at 0° and it is possible to obtain agreement with

any of these *l*-values for quite small changes in the radius R. In view of this, the *l*-value assignments are not so definite as for positive Q-values and the effects of the stripping assumptions are more important.

The major difficulty encountered with plane wave theory, however, is that it produces reduced widths about an order of magnitude smaller than the values expected on the basis of some reasonable potential-well model of the nucleon-transfer process. Also, in a few cases reduced level widths have been extracted from stripping results and compared with values obtained from nucleon resonance scattering experiments on virtual mirror states, the conclusion again being that stripping widths are markedly smaller, i.e. the Butler theory overestimates cross sections.

The normal procedure for extracting a reduced width is by measuring the ratio of the experimental and calculated differential cross-section at the stripping peak. Other methods have been suggested, however, in attempts to improve the agreement. For example, Bowcock [16] has suggested that a partial wave analysis of the experimental and calculated differential cross sections be made by a Legendre polynomial expansion and the ratio of corresponding coefficients examined as a function of polynomial order. Since non-direct amplitudes and distortion effects are expected to affect this ratio seriously for only low partial waves then the higher order ratios should approach a constant value close to the actual reduced width. Although in general this method does give larger reduced widths the improvement does not seem very significant (e.g. Kuehner et al [17]). Amado [18] has noted that a pole occurs in the Butler expression corresponding to non-physical momentum transfers $k^2 = -q^2$, and suggests that by extrapolating the experimental data to these poles all non-direct contributions to the reduced width can be eliminated since they remain finite. However, the values so obtained do not appear to differ markedly from those extracted by the straightforward peak-fitting procedure [17].

A reduced width may be expressed in the form [19] $\theta^2 = S\theta_0^2$ where S is the relative reduced width or spectroscopic factor, which measures the degree of overlap of the initial and final state wavefunctions, and θ_0^2 is the single-particle reduced width. MacFarlane and French [19] have extracted reduced widths from stripping data using the Butler theory and peak-fitting technique, and treated θ_0^2 as an empirical parameter incorporating the inadequacies of the plane wave theory. By determining S from shell model calculations, they were able to obtain values of θ_0^2 for a wide variety of transitions and demonstrate its dependence on the incident deuteron energy and reaction Q-value.

Exchange interactions have been considered by a number of authors in plane wave Born approximation (e.g. French,[20] Evans and French,[21] and Owen and Madansky [22]). In these it is assumed that the emitted proton (assuming a (d,p) reaction) comes not from the incident deuteron but from the target nucleus. Thus they are expected to play an important role only when the target nucleus can be reasonably well described by a core plus a rather loosely bound proton. If the deuteron interacts strongly with the core, this leads to 'heavy-particle' stripping [22] with the proton distribution peaked in the backward direction. However, backward peaks are not necessarily indicative of heavy-particle stripping since they may arise quite naturally as a result of distortion effects in ordinary deuteron stripping [23]. If the deuteron interacts instead with the loosely bound proton this leads to a 'knock-out' process in which the proton is ejected mainly in the forward direction. The angular distribution of these protons, however, cannot easily be distinguished from that due to ordinary stripping [24].

Since the plane wave theory takes no account of the distortions of the incoming and outgoing waves, it is normally expected to be a reasonable approximation only at moderate deuteron energies (say ~10 MeV) where the distortions should be less severe. However, as has been pointed out by Wilkinson [25], even at low energies the Butler theory should give a good description of the stripping patterns providing the reaction Q-value is also low. To test this theory an experimental investigation of (d,p) stripping has been carried out at a deuteron energy of 3 MeV and for a range of Q-values, and an account of this is given in Chapter 3.

1.4 Distorted Wave Theory

A more accurate theory of the stripping process takes into account the distortions of the incoming deuteron wave and outgoing proton wave in the coulomb and nuclear fields of the target and residual nuclei. Such a theory, which is referred to as the distorted wave Born approximation (D.W.B.A.) theory, has been developed by a number of authors, notably Thomas [26], Tobocman and Kalos [27], Huby, Refai and Satchler [28], and Buck and Hodgson [29]. These treatments all assume weak coupling, that is, that the most important process that occurs when a deuteron is incident on a target nucleus is elastic scattering, so that stripping can be treated as a perturbation on this. From general reaction theory the cross-section for a (d,p) stripping process may be expressed approximately [29] as,

$$\sigma(\theta) = \frac{m_p^* m_d^*}{4\pi^2 \hbar^4} \left(\frac{k_p}{k_d} \right) \left| I(\vec{k}_p, \vec{k}_d) \right|^2$$

In which the transition amplitude I is given by:

$$I(\vec{k}_p, \vec{k}_d) = \int f^*_{kp}(\vec{r}_p') \chi_s^*(p) \psi^*(R : \xi, \vec{r}_n, \vec{\sigma}_n) V f_{kd}(\vec{r}_n, \vec{r}_p) \chi_s(d) \psi(T, \xi) d\vec{r}_n \, d\vec{r}_p \, d\xi$$

$\psi(T)$ and $\psi(R)$ are, respectively, the internal wave functions of the target and residual nuclei and f_{kd} and f_{kp} are the spatial wave functions of the deuteron and proton; $\chi_s(p)$ is the proton spin function and $\chi_s(d)$ the triplet deuteron spin function (the small D-state component is assumed negligible); ξ represents the internal coordinates of the target nucleus; $\vec{r}_n$ and $\vec{r}_p$ are the position coordinates of the proton and neutron relative to the centre-of-mass of the residual nucleus and $\vec{r}_p' = \vec{r}_p - (m_n/m_R)\vec{r}_n$. If plane waves are assumed for f_{kp} and f_{kd} then this expression reduces to the original Butler form. However, in the D.W.B.A. theory these wave functions are distorted by suitable potentials due to the nuclear and coulomb interactions. V is the interaction in the final state between the proton and residual nucleus. This may be expressed in the form $V = V_{pn} + V_{pT}$ where V_{pn} is the proton-neutron interaction and V_{pT} the proton-target interaction. In the calculations, it is assumed that V_{pT} has already been taken completely into account in the construction of the distorted proton waves, i.e. that inelastic effects due to excitation of the target-core by the outgoing proton are negligible, and therefore V reduces to V_{pn}. (In plane wave theory V_{pT} is disregarded entirely and consequently predicts zero polarization of the outgoing protons.)

The D.W.B.A. theory has been extremely successful in removing many of the shortcomings of the plane wave theory, and in general gives much improved agreement to the detailed structure in the experimental distributions. The calculations may be carried through to the centre of the nucleus to include contributions to stripping from the nuclear interior, thereby removing the rather arbitrary cut-off radius employed in the Butler theory. However, in order to make the evaluation of the transition amplitude practicable it is necessary to assume V_{pn} to be of zero range, and Rook (ref. 30 and private communication) has suggested that the effect of a finite range interaction may be simulated by using a cut-off radius close to the nuclear surface. Some evidence for this is discussed in Chapter 3. Of particular importance, however, is the fact that much smaller cross-sections are predicted by the D.W.B.A. theory than the Butler theory and this leads to more realistic estimates of reduced widths.

It is apparent [29] from D.W.B.A. calculations that individually the two types of distortions i.e. coulomb and nuclear, produce an angular distribution markedly different from the Butler

distribution but that together they tend to have opposite effects and give a final distribution very similar to the Butler form (but with reduced cross-section). The success of the plane wave theory in correctly predicting the general features of the distributions therefore appears to be somewhat fortuitous.

In the present work, distorted wave calculations have been carried out using the Buck-Hodgson [29] computer programme as modified by Macefield [31]. The distorted deuteron and proton waves are generated by an optical model such as describes the observed elastic scattering of these particles. This model (e.g. Feshbach, Porter and Weisskopf,[32] Bjorklund and Fernbach [3]) effectively replaces the nucleus by a central potential well having both refracting (real) and absorbing (imaginary) parts and the interaction is assumed to have the form

$$V(r) = V_c(r) - U\ f(r) - iW\ g(r)$$

The real potential U elastically scatters the particles and the imaginary potential W takes into account all the inelastic processes. $V_c(r)$ is the coulomb potential, taken to be that due to a uniformly charged sphere of radius $r_cA^{1/3}$, and f(r), g(r) are functions describing the radial dependences of U and W, respectively. For these the same Saxon-Woods form factors have been assumed, i.e.

$$f(r) = g(r) = \left[1 + \exp\left\{\frac{(r-R)}{a}\right\}\right]^{-1}$$

with nuclear surface diffuseness a and radius $R = r_0A^{1/3}$. The deuteron and proton distorted waves are, therefore, each characterised by the four parameters U, W, r_o and a. To the central distorting potential may also be added a spin orbit term. However, although this may have an important effect on the polarization of the emitted particles, in general it does not significantly affect the angular distribution. (Some indication of its possible effect is given in Chapter 4.)

To carry out a distorted wave analysis of a (d,p) stripping reaction thus requires a knowledge of the deuteron and proton elastic scattering from the target and residual nuclei, respectively. Furthermore, the scattering measurements should be carried out at the energies appropriate to the (d,p) study. In order to determine whether the distortions in stripping are due only to elastic scattering processes the $Se^{76}(d,p)Se^{77}$ reaction has been studied together with the deuteron and proton elastic scattering from Se^{76} and Se^{77}, respectively. The elastic measurements have been analysed with the optical model and the parameters compared with those which give best agreement

to the stripping distributions. An account of this investigation, part of which has already been published, [34, 35] is given in Chapter 4.

1.5 Double Stripping Reactions

Recently, considerable interest has centred on reactions involving the transfer of two nucleons, such as (t,p), (He^3,p), (d,α), … etc. The earlier experimental studies were carried cut mainly with the (He^3, p) reaction [36 - 39] and in a number of cases the distributions were found to exhibit strong forward peaking, suggestive of a two-nucleon stripping mechanism. Theoretical treatments of double stripping have been given by El Nadi, [40] Newns, [41] and Glendenning [24] using plane wave Born approximation theory. An approximate form for the angular dependence of the emitted particles is [41]

$$\sigma(\theta) \propto \exp\left(\frac{-K^2}{4\gamma^2}\right)\sum_L \alpha_L \, j_L^2(ka)$$

If we consider outgoing protons, then the exponential factor represents the probability that the proton has initially a momentum $\hbar K$, due to the internal motion of the projectile, required for stripping to occur, i.e. $\bar{K} = \bar{k}_p - \bar{k}_3/3$ where k_p, k_3 are the wave numbers of the emitted proton and incident (mass-3) particle. $\hbar^2\gamma^2/m$ is the binding energy of the projectile, ε_3, and α_L is a constant analogous to the capture probability occurring in the Born approximation deuteron stripping theory. $j_L(ka)$ is the usual spherical Bessel function evaluated for an interaction radius a, and $\bar{k} = \bar{k}_3 - \bar{k}_p$ is the wave number of the two captured particles, which are assumed captured as a 'lump'.

A more detailed expression for the distribution which takes into account the structure of the captured particles has also been derived by Newns [41]. However, as has been shown by Hinds and Middleton, [37] the two expressions predict sufficiently similar distributions as to justify the use of the approximate expression alone, particularly in view of the plane wave assumption.

The selection rules require the final nuclear spin to be given by:

$$\bar{J}_f = \bar{J}_i + \bar{L} + \bar{S}$$

where S is the total spin of the two captured nucleons and $\bar{L} = \bar{\ell}_1 + \bar{\ell}_2$ where ℓ_1, ℓ_2 are the two nucleon orbital angular momenta. The initial and final states have the same parity or not according to L is even or odd. In the case of (He^3, p) and (t,n) reactions, S may be either 0 or 1. The selection

rules are particularly restrictive, however, in the case of (t,p) and (He^3,n) reactions, since for these the Pauli principle allows only S = 0 (providing that the triton and He^3 are spatially symmetric and that there is no mechanism for flipping the spin of one of the captured nucleons.) Furthermore, if the target spin is zero then at most only one L-value is allowed which uniquely determines the spin and parity of the final state. These reactions therefore provide extremely valuable tools for determining nuclear level properties.

A systematic study of the (t,p) reaction is reported in Chapter 5 of this thesis. This has been carried cut for a range of nuclei, principally in the (1p) and (2s,1d) shells, and the proton distributions have been analysed with plane wave double stripping theory. The (t,p) reaction is of particular interest since it may lead to highly neutron-rich nuclei which are not easily accessible by other reactions. For example, C^{16} (which had not previously been observed) has been studied by means of the C^{14}(t,p)C^{16} reaction. The published account of this investigation is given in Appendix B. Information concerning the spin-parity of Be^{11} has also been obtained by means of the Be^9(t,p)Be^{11} reaction (Chapter 6 and ref. 42). Although the simple shell model predicts odd parity for this nucleus the β^--decay measurements of Wilkinson and Alburger [43] suggested that it might in fact have positive parity, though this assignment was only very tentative. The present study was undertaken primarily in view of this uncertainty in the parity.

Rook and Mitra [30] have recently developed a distorted wave formalism for (t,p) double stripping using the zero-range approximation for the triton. No previous measurements of elastic triton scattering had been made, however, from which the optical model distorting parameters could be determined. For this reason triton elastic scattering measurements have been made for a number of nuclei and the results are described in Chapter 7, together with an account of the optical model analyses. The distorting parameters extracted from these measurements have been used by Rook and Mitra [30] to analyse the proton distributions from the Ca^{40}(t,p)Ca^{42} reaction described in Chapter 5. A brief account of this analysis is given in Appendix C.

C H A P T E R II

EXPERIMENT PROCEDURES

Most of the experimental investigations to be described in the following chapters were carried out using ion beams from the AWRE Aldermaston Tandem accelerator, and the charged reaction products were analysed with a multi-channel broad-range magnetic spectrograph. In some of the earlier experiments, however, the Aldermaston and AERE Harwell Van de Graaff generators were employed, together with a single-channel broad-range spectrograph and 180° double-focusing magnetic spectrometer.

2.1 The Multi-Channel Broad-range Magnetic Spectrograph

This instrument was designed by Middleton [44] and permitted the simultaneous recording of particle energy spectra at twenty-four different angles. Essentially it consisted of twenty-four broad range magnetic spectrographs which utilized the focusing property of a homogeneous magnetic field with circular boundary (Bainbridge,[45] Browne and Buechner [46]). A schematic diagram of the magnet is shown in fig. 2.1.

The magnet consisted of a low-carbon steel torus formed from 48 segments with the pole shape shown in the lower half of the figure. The segments in the first and third quadrants were separated by brass spacers to form 24 radial air gaps, or channels, each 0.95 cm wide, and these channels were spaced at 7.5° intervals in the angular ranges 5° to 87.5° and 92.5° to 175°. The pole radius was 50.8 cm, but to allow for the effect of fringing field at the gaps the effective radius of the magnetic field was assumed to be given by this pole radius plus one gap width, i.e. a radius of 51.75 cm.

Excitation of the magnet was provided by 26 coils which were situated flanking the channels. The energising current, and therefore magnetic field, was held constant to less than one part in 10^4 by an electronic feedback control system. Field strengths between 6.0 and 11.5 kilogauss were normally used and these were measured with a proton magnetic resonance frequency probe placed in the fifth channel. The maximum field strength enabled particles with an equivalent proton energy up to 21.8 MeV to be recorded.

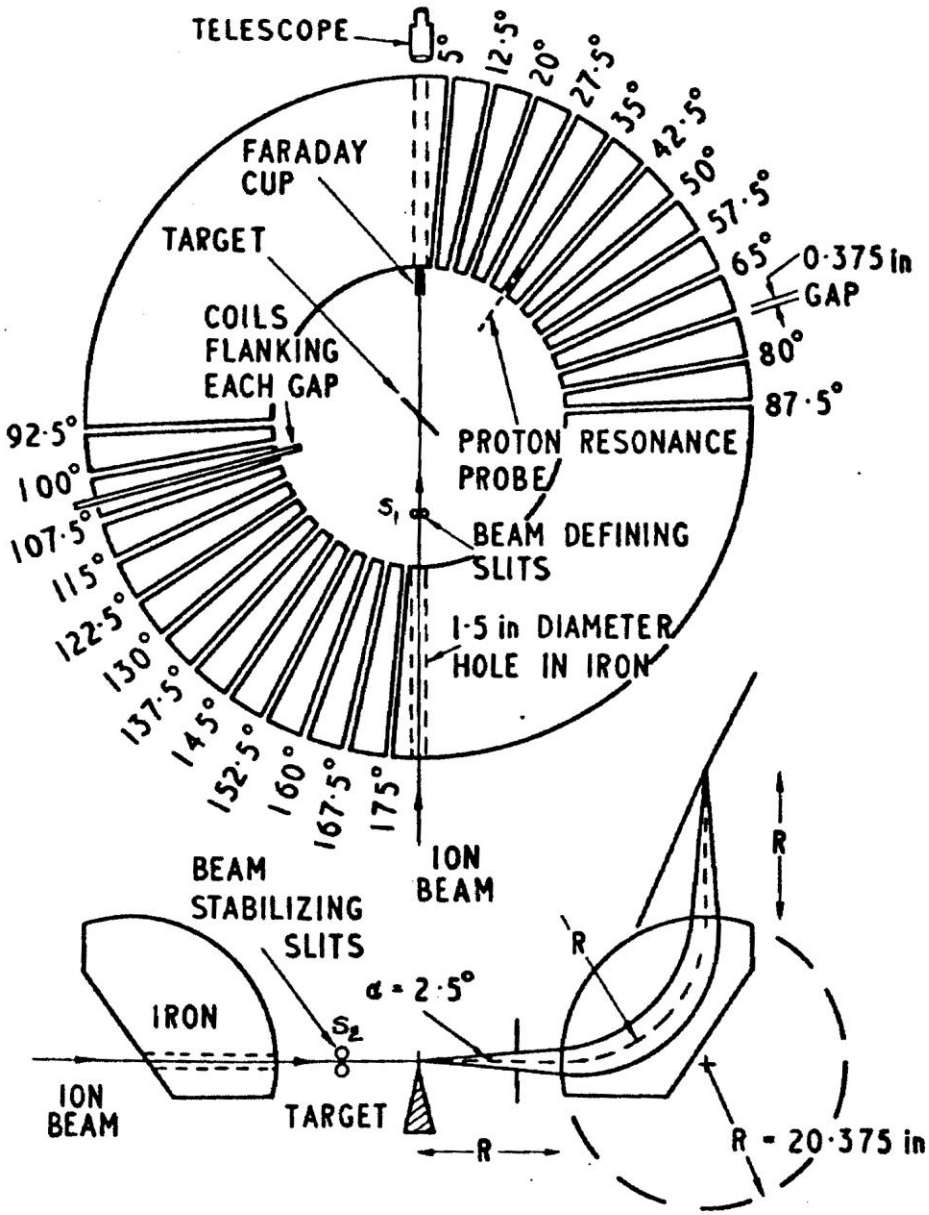

Fig. 2.1 *Schematic of Aldermaston Multi-Channel Broad-Range Magnetic Spectrograph*

The incident ion beam from the Tandem accelerator, after deflection through 90° by the beam analysing magnet, entered the spectrograph through a field-free hole bored through one of the segments. Prior to striking the target, which was mounted at the center of the torus, the beam was defined by a slit system to rectangular shape 1.5mm wide and 0.5mm high. The edges of this slit were defined by four gold-plated cylinders each having a radius of 0.5cm. One pair, S_1, was mounted with axes vertical and the other pair, S_2, with axes horizontal, the latter also supplying the error signal for stabilizing the center-terminal voltage of the accelerator. An anti-scatter slit was also placed between this slit system and the target to prevent any degraded energy particles scattered off the slit edges from reaching the target frame. Typical beam currents after collimation were about 0.15 microampere.

After passing through the target the beam was collected by a Faraday cup which was electron suppressed by the fringing field of the magnet. The current from the cup was then electronically integrated to give a measure of the total exposure strength. By raising the cup out of alignment the target could be viewed directly through a telescope mounted along the beam axis. A small retractable perspex viewer was situated immediately behind the target and the procedure for aligning the beam was facilitated by observing the position of the burn mark produced by the beam on the viewer.

Charged particles from the target entered the channels normal to the magnetic field and were brought to a focus along the 101.6 cm long nuclear emulsion plates. To minimize the background caused by particles scattered from the pole faces a series of neoprene rubber baffles were mounted on each face. The nuclear plates were bent to this form by pressing them against shoulders in the plate holders, which were precision machined to the correct contour. Two plates, 2.54 cm wide and 50.8 cm long, were placed end to end in each plate holder and the total range of particle energies which could be accommodated in one exposure was 3.5:1.

The magnet, coils and plate holder assembly were contained in a 3m diameter by 2.5m high vacuum vessel, the general arrangement being shown in fig. 2.2. The vessel was evacuated to a pressure of 5×10^{-5} mm of Hg by a 24-in. oil diffusion pump. The target and slit system were situated in a light alloy drum (centre of assembly in fig. 2.2) and reaction products from the target entered the channels through rectangular apertures in the side wall of the drum. Surrounding this was a steel ring containing a corresponding set of apertures which, during an exposure, were aligned with those in the drum. However, this could be made to rotate through a small angle by

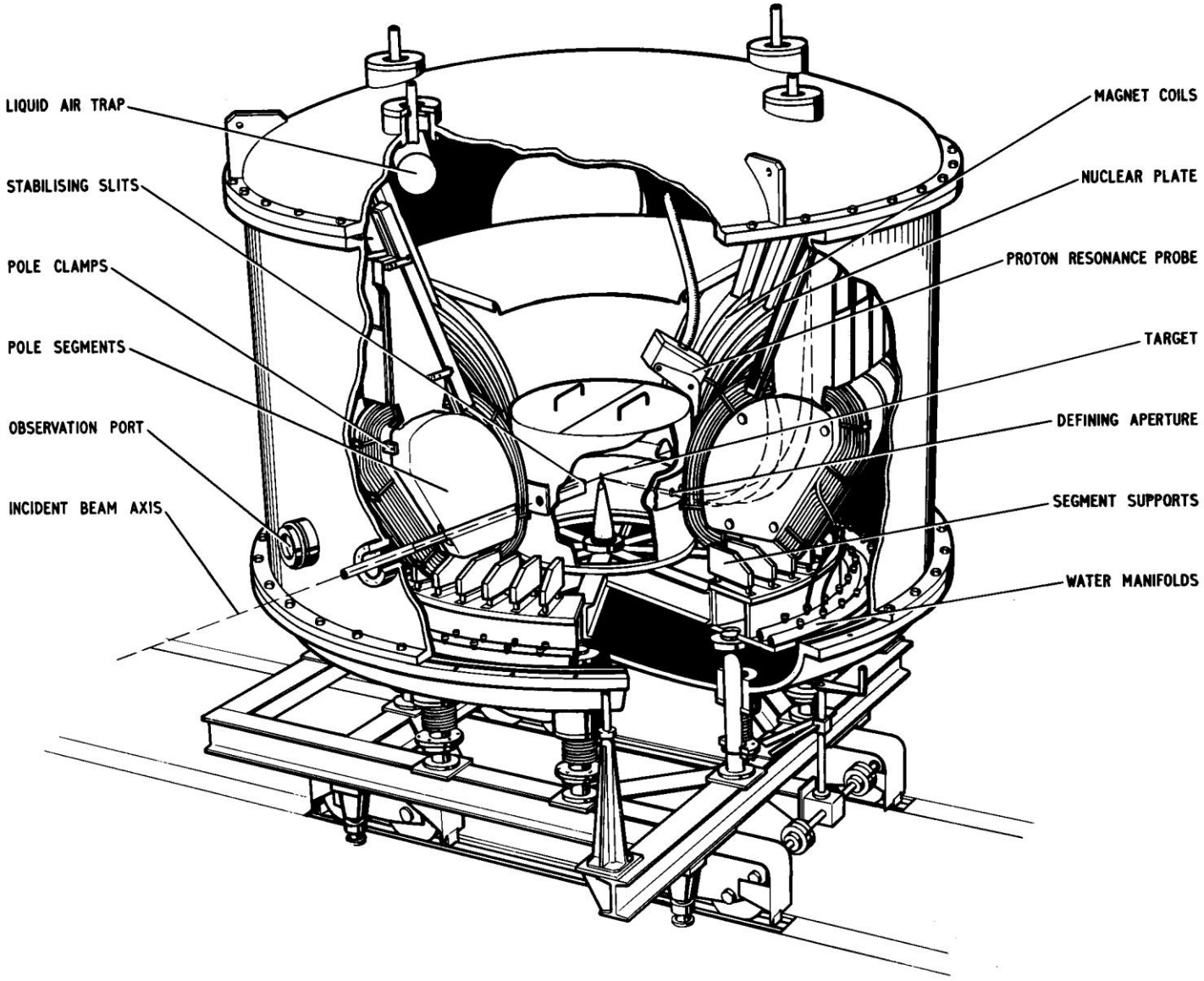

Fig. 2.2 *Aldermaston Multi-Channel Broad-Range Magnetic Spectrograph*

means of a remote controlled actuator and thus acted as a shutter which could open or close the entrance to all channels simultaneously.

In most channels the rectangular apertures were 0.64 cm wide by 3.18 cm high, the latter defining a total angle of acceptance in the vertical plane of 5.0°. In the horizontal plane, the acceptance angle was limited by a 6 mm wide slit situated immediately in front of the nuclear plates. Since the flight path to this slit varied according to the trajectory radius in the field, this angle was a slowly varying function of the radius, or distance along the plates. For particles deflected through 90° the total solid angle of acceptance was 3.01×10^{-4} steradian.

Since in many of the reactions studied the particle angular distributions were strongly forward peaked, this frequently resulted in very intense particle groups in the forward direction with comparatively weak groups at large angles. To overcome the problem of scanning such intense groups, it was found expedient to reduce the angular acceptances in the first three channels, at 5°, 12.5° and 20°, to 1/4, 1/2, and 3/4 the normal value. For elastic scattering measurements, however, where the differential cross-sections can differ by a factor 10^5 or more between 5° and 175°, the first two channels were not normally employed and the acceptance angles in the next four channels were suitably reduced to prevent over exposure. In addition, a remote controlled shutter was employed in the third channel which provided an independent control of the exposure strength at that angle. With these modifications elastic scattering distributions could be measured between 20° and 175° in one exposure.

Ilford K2 nuclear emulsions with thicknesses of 50 or 100 μm were used for the detection of protons, deuterons and tritons. In the (t, α) reaction studies, 25 μm thick Ilford K-1 alpha-sensitive emulsions were employed. For reactions such as (d, p) or (t, p) it was normally found advantageous to use thin absorbers placed in direct contact with the emulsions to prevent particles other than protons from being recorded. A particularly convenient absorber was found to be 0.007 in. thick polythene tape which allowed protons through with an energy greater than 5.1 MeV, but was sufficient to stop all deuterons, tritons and alpha-particles with energies less than 6.9, 8.3, and 28 MeV, respectively. For proton energies much less than this the use of an absorber became impracticable. In such cases discrimination between different particles was made on the basis of their different track lengths and specific ionization in the emulsions.

Prior to mounting in the spectrograph, the plate holders with the nuclear plates in position were mounted on an indexing jig which contained eight fine slits, spaced at 12.7 cm intervals,

through which narrow beams of light could pass. This enabled a set of index lines to be photographed directly on to the emulsions and these served as a reference scale for determining the position of any particle group along the plates.

The spectrograph had been previously calibrated by Hinds and Middleton using the 8.784 MeV alpha-particles from Po^{212} and 6.048 MeV alphas from Bi^{212}. By recording the groups at different positions along the focal planes this gave the desired relationship between the radius of curvature of particle orbits and the distance along the plates.

During normal operation the overall energy resolution of the spectrograph, defined as $E/\Delta E$ where ΔE is the full width at half-maximum for a particle group, was about 1000. The principal factors determining this were the beam spot (or object) height, the effective target thickness, the beam energy spread and the spectrograph aberrations. The object height was fixed at 0.5mm and this determined an image width which was an appreciable fraction of the total width. For 10 MeV protons deflected through 90° and incident on the nuclear plates at a grazing angle of 30°, the magnification was unity and the energy dispersion 11.0cm/MeV, so that the finite object height contributed about 9 keV to the total image half-width. Compared with this the effect due to aberrations was quite small. The beam energy spread was also limited by the 0.5m slit. However, for a typical beam energy of 10 MeV this introduced a spread of only about 2 keV.

The target thickness gave rise to an energy spread due to the difference in energy between particles emitted from the front and back faces of the target. If the target were made very thin then this spread could be made very small, but only at the cost of a considerable loss in reaction yield. It was therefore necessary to compromise between resolving power and yield. Whenever possible self-supporting targets were employed and typical thicknesses were about 50 $\mu g\ cm^{-2}$. A further factor which affected the resolution, though not specifically instrumental in nature, was the width of the strip scanned across the nuclear plates. This was normally 1/4 mm and generally contributed less than 3 keV to the total half-width.

Plate Scanning.

After processing, each nuclear plate was cut into two 25.4 cm lengths and these were scanned using Cooke, Troughton and Simms' M4000 microscopes with x10 eyepieces and x20 objectives. The microscope stages, which were designed at Aldermaston to accommodate this length of plate, provided movement in two perpendicular directions by means of two micrometers. By moving the

plate transversely the tracks inside a 1/4 mm wide strip were counted for a total strip length of 6 mm i.e. over the width of plate used for particle detection. Energy spectra were then obtained by plotting successive counts in these strips as a function of distance along the plate, at the same time noting the position of each strip relative to one of the index lines. From the known position of a group the corresponding trajectory radius, ρ, could be determined. The measured field strength then yielded the value of $H\rho$ for the group, from which its energy could be obtained. The position of a group was determined by extrapolating the maximum slope of its high energy edge to the base line.

Only those particle tracks were counted which started at the surface of the emulsion with their lengths parallel with the length of the plate, and which had the correct angle of dip. When absorbers were not employed the protons, deuterons and alpha-particles had sufficiently different ranges in the emulsion at any one position on the plate that particle identification could be readily made. These criteria ensured that the number of spurious tracks counted e.g. from neutron recoils, was quite negligible.

2.1.2 Data Processing

(a) Energy Measurements

From the measured energy spectra the observed particle groups were correlated with energy levels in the residual nuclei. The excitation energies for these levels were then obtained from the difference in reaction Q-values for the ground and excited state transitions.

If we consider a reaction in which the target nucleus, incident particle, emitted particle and residual nucleus have masses M_0, M_1, M_2 and M_3 and energies (in the laboratory system) E_0, E_1, E_2 and E_3, the Q-value is

$$Q = E_2 + E_3 - E_1 - E_0$$

where E_0 may be assumed zero since the thermal energy is negligible. In an experiment the energies E_1 and E_2 are measured and these are related to the Q-value through the classical equation

$$M_3Q = (M_2 + M_3)E_2 - (M_3 - M_1)E_1 - 2\sqrt{M_1M_2E_1E_2}\cos\theta$$

where θ is the angle between the directions of motion of the incident and emitted particles.

In the present work, incident energies up to about 10 MeV have been used and the relativistic correction to the Q-value equation for these energies can amount to as much as 10 keV for reactions with light nuclei. However, since the determination of excitation energies involves the difference between two Q-values, then providing these are not very different the relativistic correction in such cases is negligible compared with other inaccuracies. Furthermore, in measuring the differences between Q-values any systematic errors which may arise in their absolute values, in particular the error in beam energy, tend to cancel. The accuracy of an excitation energy measurement is therefore better than that of an absolute Q-value.

In determining the beam energy E_1, the Q-value of a well known ground state or low-lying excited state transition was frequently used. For this purpose the usual presence of oxygen and carbon in the targets* was particularly convenient, since the (d,p) and (t,p) reaction Q-values are accurately known for these nuclei. By observing the positions of the proton groups arising from these reactions the energies E_2 could be found directly from the energy calibration. Substitution of the known values of E_2, Q, and the various masses into the Q-value equation then yielded E_1. The Q-values for the reactions under investigation were then found from a similar procedure using this value of E_1.

(b) Angular Distributions.

The angular distribution of a group was obtained by counting the total number of particle tracks in the group at each angle. Since measurements were made simultaneously at all the angles then these were normalised to precisely the same exposure strength, as measured by the total charge collected by the Faraday cup.

The errors given on the experimental points in the angular distributions are generally only statistical (standard deviation). However, in a few cases, where two or more groups overlap, the error has been increased by an amount depending on the extent of overlap and on the relative intensities of the groups involved. The error may also have been increased as a result of uncertain background subtraction. All angular distributions are presented in the centre-of-mass system of coordinates.

* The oxygen probably arose mainly from a surface oxide layer on the targets and carbon was frequently used as a target backing material. Even in the case of self-supporting targets, however, carbon was frequently observed and was probably deposited on the target surface due to the cracking of the oil- and grease vapours by the beam.

(c) Cross-section Determinations.

The differential cross-section for the reaction $M_0(M_1, M_2)M_3$ is given by -

$$\sigma(\theta) = \frac{N(\theta)}{I\, n\, \Delta\Omega}$$

in which N(θ) is the number of particles scattered at an angle θ for a given number of incident particles, n is the number of target nuclei per unit area presented to the beam and ΔΩ is the solid angle subtended by the detector system. Of these quantities the most difficult to measure with any degree of accuracy is n. The most direct method, that of determining the surface density, involves an accurate weight measurement, assumes a certain chemical composition and is only suitable for self-supporting targets. The main errors in this method then arise from the weight measurement itself, from an estimate of the area of the target weighed and from the assumption of uniform target thickness. These probably amount to an error of about ± 20%.

The solid angle subtended by the nuclear plate detectors varied according to the position along the plates. For reaction products detected at the lower end of the plates this was 5.38×10^{-4} steradian and for those detected at the upper end 2.16×10^{-4} steradian. The number of particles incident on the target during an exposure, I, was determined from the total charge collected in the Faraday cup, a typical exposure strength for a reaction study being about 500 microcoulombs. The estimated total error in the absolute differential cross-section so measured is about ± 25%.

In a number of cases, the same target as used in a reaction study was later used to measure the angular distributions of elastically scattered charged particles, these distributions being analysed by means of the optical model. Since the absolute elastic cross-sections are accurately predicted by this model, particularly at small angles where the scattering is close to the Rutherford form, then the absolute reaction differential cross-section, $\sigma(\theta)_R$, may be obtained in terms of the elastic cross-section, $\sigma(\theta)_{El}$, i.e. since n is the same in both cases, then

$$\sigma(\theta)_R = \sigma(\theta)_{El} \cdot f \cdot \frac{N(\theta)_R}{N(\theta)_{El}} \cdot \frac{I_{El}}{I_R}$$

f (= $\Delta\Omega_{El} / \Delta\Omega_R$) is unity only if the elastic and reaction particle groups are detected at the same position on the nuclear plates.

The assumption that n is the same in both measurements is reasonable only if the target has uniform thickness and remains stable during bombardment. Absolute cross-sections measured in this way are estimated to have a maximum total error of only ± 10%.

Where absolute cross-sections have been determined, reference is made as to which of these two methods has been employed.

2.2 The Single-channel Broad-range Magnetic Spectrograph

This instrument was used only in the earlier studies of the $Be^{9}(t,p)Be^{11}$ and $C^{14}(t,p)C^{16}$ reactions and has been described elsewhere [37]. A general view of the spectrograph and scattering chamber is shown in fig. 2.3. The magnet had a pole radius 50 cm and the distance between the pole faces was 0.95 cm.

After deflection through 90° by the beam analysing magnet, the triton beam from the Aldermaston 6 MV Van de Graaff generator was directed on to the target located at the center of the scattering chamber. Prior to striking the target the beam was collimated by a slit system similar to that used with the multi-channel spectrograph. This defined an object 2 mm wide by 0.25 mm high and the incident beam spread resulting from this object height was less than 2 keV for 6 MeV tritons.

After magnetic analysis, charged reaction products from the target were recorded on a 76.2 cm long by 5.08 cm wide nuclear emulsion plate mounted along the focal surface. A rectangular aperture, 0.64 cm wide and 3.18 cm high, placed at the entrance to the spectrograph, and an 8mm-wide slit situated in front of the nuclear plate, defined a total solid angle acceptance of 3.5×10^{-4} steradian for particles deflected through 90°. Particles extending over a range 2.4:1 were detected on the plate in one exposure. Provision was made for moving the plate holder laterally without breaking the vacuum seal, so that four different strips of the emulsion could be successively exposed.

The scattering chamber, which had a diameter of 30 cm, is shown in more detail in fig 2.4. The lid was of plate glass and so permitted visual observation of the target. To minimise carbon build-up on the target an oil-vapour trap, cooled externally by liquid nitrogen, was mounted in the chamber. After passing through the target the direct beam was collected by a Faraday cup and the current integrated, so making possible the normalisation of all data to a predetermined total number

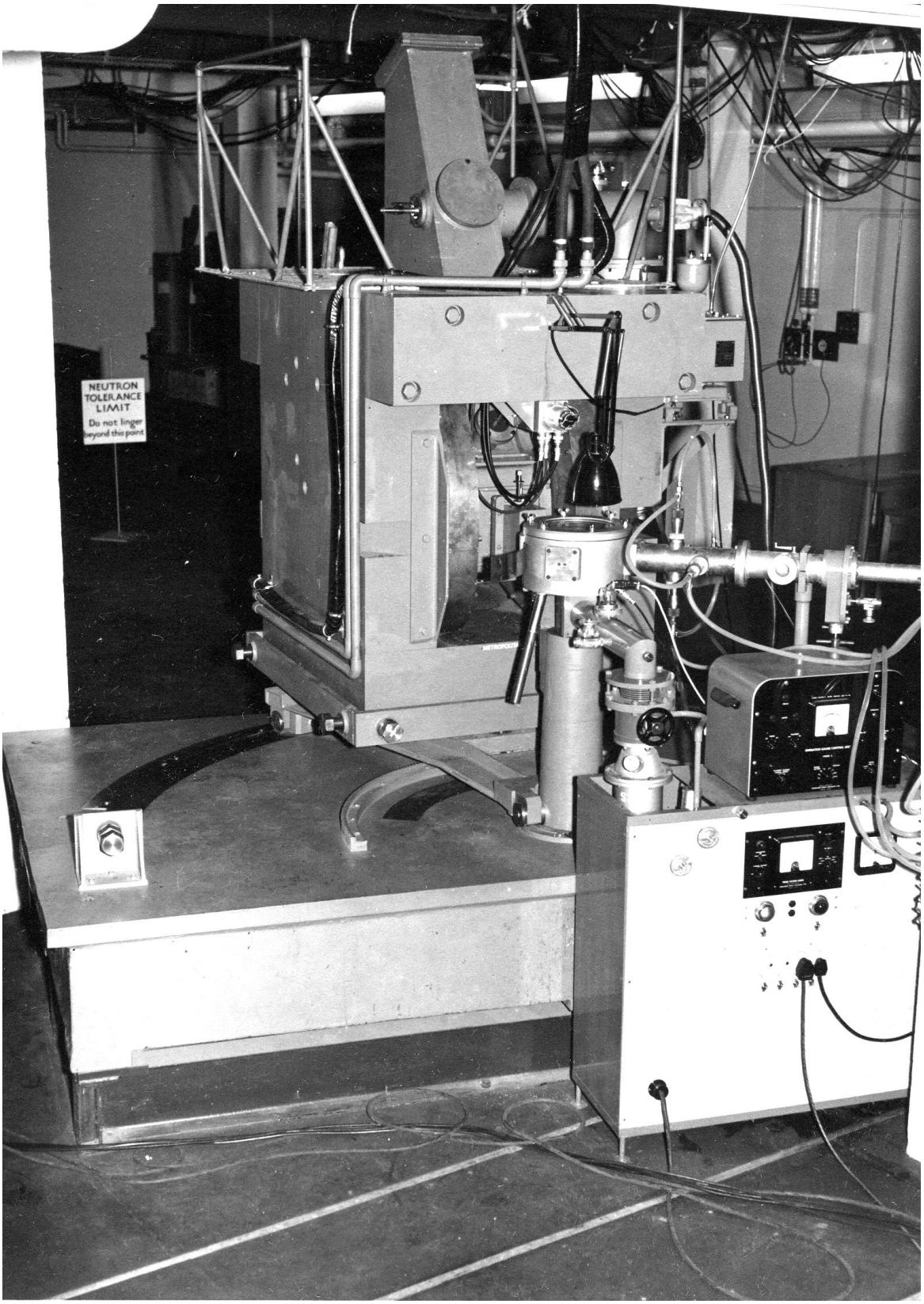

Fig. 2.3 *Aldermaston Single-Channel Broad-Range Magnetic Spectrograph*

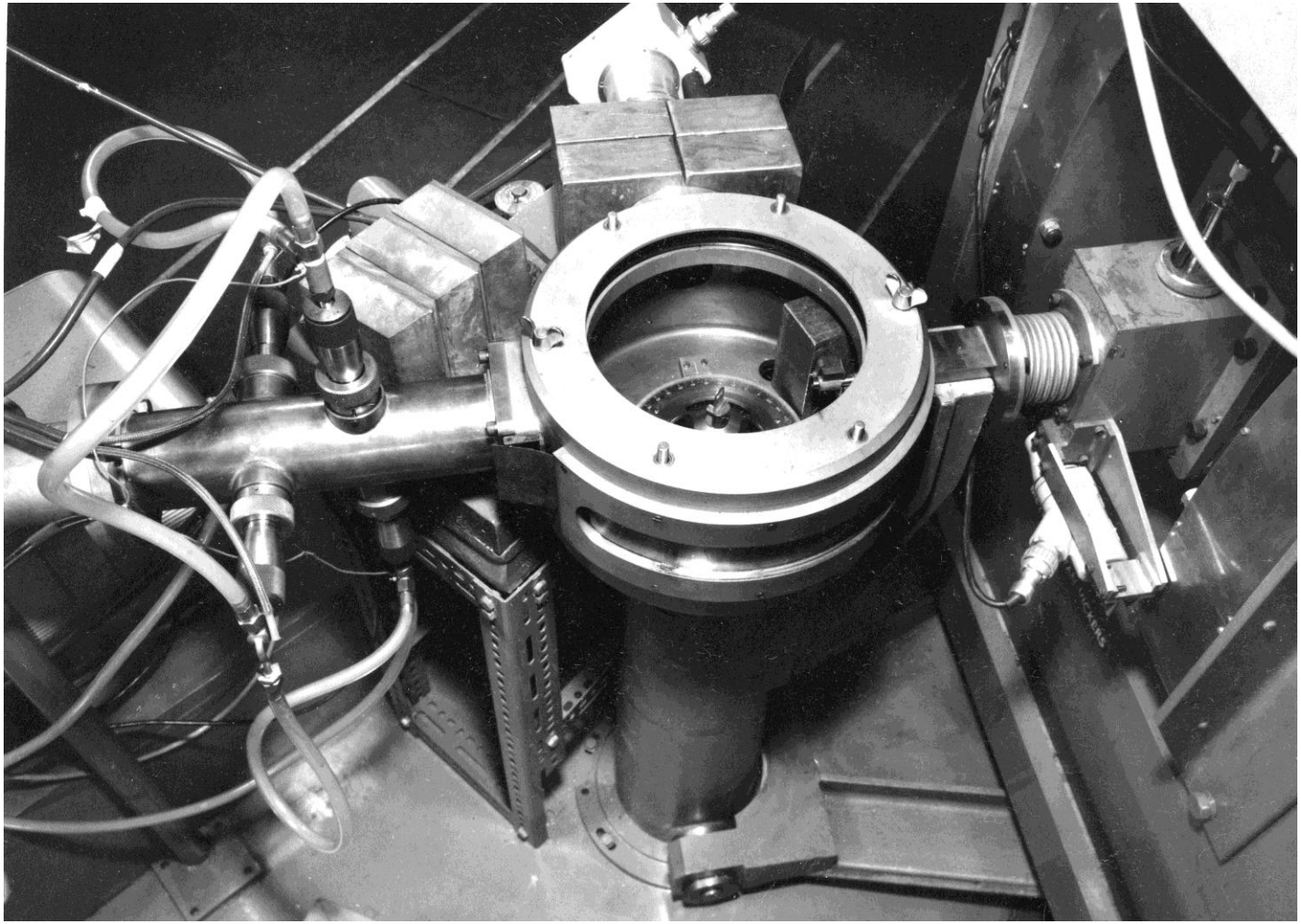

Fig. 2.4 *Single-Channel Spectrograph Scattering Chamber*

of incident particles. Suitable electron suppression was provided by a small permanent magnet mounted on the cup with its field normal to the beam direction.

Reaction products passed from the chamber into the spectrograph through a tube, which was fixed to a stainless steel strip held by a guide over a horizontal slot cut into the wall of the chamber. As the spectrograph was rotated about the target this strip moved over the slot and, relative to the incident beam direction, angles from -5° to 127° could be obtained. The maximum angle was determined by the magnet yoke meeting the beam entry tube. Measurements could thus be made over this angular range except for ± 2° about 0° where the particles were obscured by the Faraday cup. To determine the zero angle a small quartz viewer was placed successively in the target position and at the rear of the Faraday cup and bombarded with low energy (approximately 2 MeV) protons. The positions of the beam spot on the viewer were then observed directly through a telescope which was carefully aligned in the median plane of the magnet.

Since, during a long exposure, there was some danger of the target breaking under bombardment it was desirable to maintain a continuous check on its stability. This was done by means of a monitor detector positioned to view the target at an angle of -90°. A CsI(Tl) crystal was directly mounted on a Du Mont 6292 photomultiplier and pulses from this were linearly amplified and fed into a scaler and 100-channel pulse-height analyser. The scaler bias was set to record only elastically scattered tritons. Gamma-ray background which originated mainly from the collimating slits and Faraday cup was reduced by a suitable arrangement of lead shielding.

The plate scanning and analysis of data followed the same general procedure as described previously for the multi-channel spectrograph.

The 180° Double-focusing Magnetic Spectrometer.

This instrument was used only for some of the earlier investigations of low-Q (d,p) stripping reactions and elastic deuteron scattering described in Chapter 3, and will therefore be only briefly described. The spectrometer was similar in design to the instrument described by Snyder et al [47], and utilised the double-focusing property of a magnetic field whose value varies as $r^{1/2}$ about a mean radius. A general view of the spectrometer, whose magnetic field extended over 180° with a mean radius of 32 cm, and of the scattering chamber is shown in fig 2.5.

The deuteron beam from the Harwell 5 MV Van de Graaff generator entered the scattering chamber at an angle of 15° to the horizontal and prior to striking the target was collimated by a

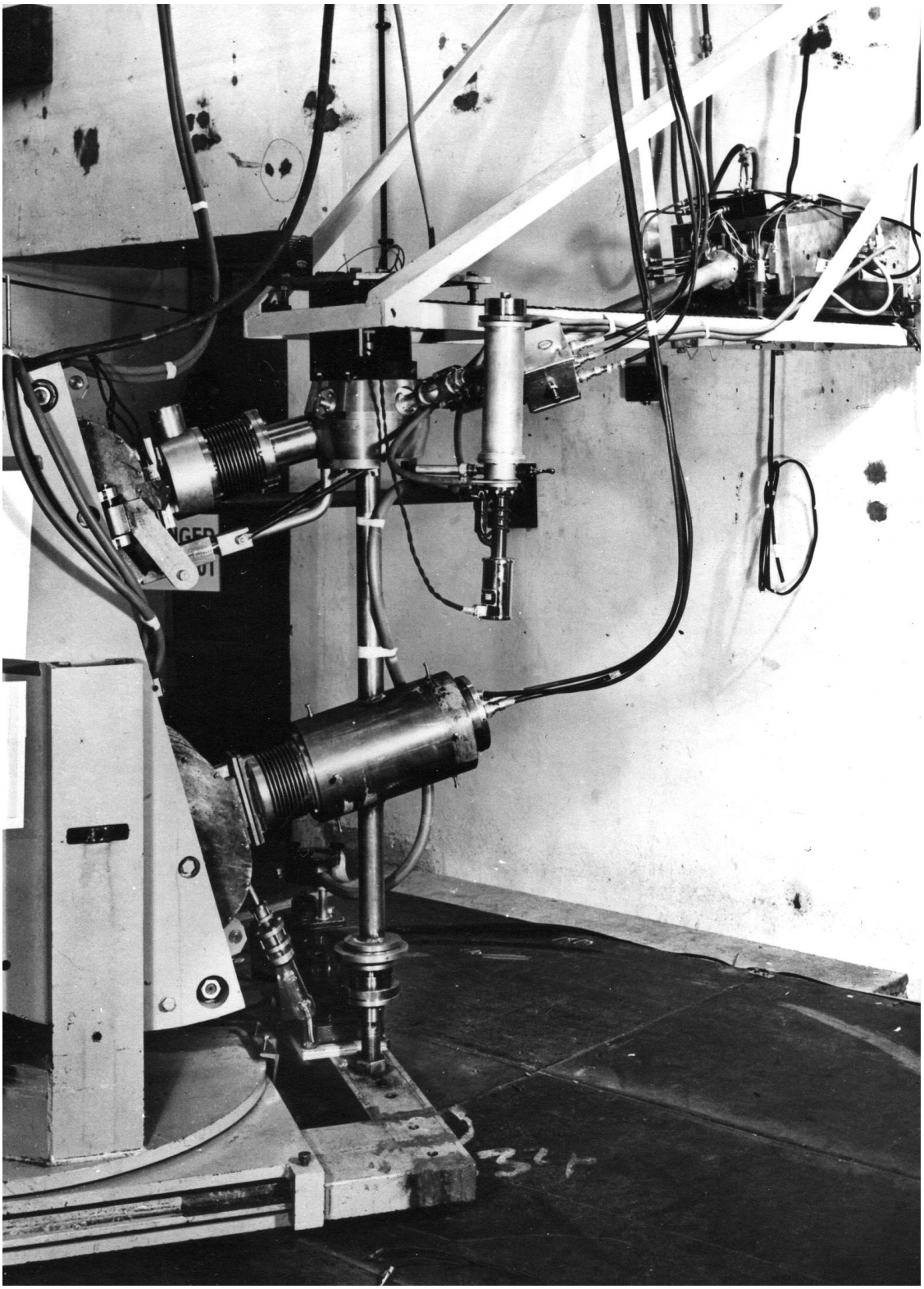

Fig. 2.5 *Harwell Double-Focusing Magnetic Spectrometer*

series of 3 mm diameter apertures. The upper half of the chamber was held fixed whilst the lower half, which was connected to the spectrometer by a brass tube and flexible bellows, could be rotated in the horizontal plane about the target as centre. The maximum angle relative to the incident beam direction was limited to 150°. After passing through the target the direct beam was collected by a Faraday cup and the current integrated to give the total charge. An electron-suppressor ring, held at -300 volts, ensured accurate determination of this charge.

Charged reaction products from the target were magnetically analysed in the spectrometer and detected by a CsI(Tl) crystal and photomultiplier placed directly beyond a 2 mm wide defining slit. Particles with an equivalent proton energy of up to 6 MeV could be analysed in the instrument. The energy resolution was about 150 and the total solid angle of acceptance of the spectrometer, which was defined by a series of apertures in the entrance to the magnet, was 23.3×10^{-4} steradian. The 1-mm thick CsI(Tl) scintillation crystal was mounted on a 30 cm long perspex light guide, this assembly then being coupled to and E.M.E. 6097 photomultiplier which was placed well outside the magnetic field. After amplification the pulses from the photomultiplier were fed into a scaler and 100-channel pulse-height analyser.

Particle energy spectra were obtained by observing the counting rate as the magnetic field was reduced in small steps, each observation consisting of the number of particles counted in a predetermined time interval. This counting time was normally determined by the integrated beam current so that the observations were normalised to the same number of incident deuterons. However, the Faraday cup obscured particles scattered at angles less than 15° and it was necessary to raise the cup to allow observation of these particles down to 0°. Under this condition the measurements were normalised by means of a monitor detector mounted at -140°. As for the spectrometer, this detector consisted of a CsI(Tl) crystal cemented on the face of an E.M.I. 6097 photomultiplier and pulses from this were similarly amplified and fed into a scaler and pulse-height analyser. A 5 mm diameter aperture, placed approximately 5 cm from the crystal, ensured that the crystal was illuminated only by the central region of the target and so prevented detection of particles scattered from other sources. The scaler bias was set so as to record a suitable proton group or elastically scattered deuteron group. The monitor was first calibrated by noting the average number of counts recorded on the scaler for a given incident charge. The Faraday cup was then removed from the beam and the measurements continued down to small angles using the monitor to normalise the data.

At scattering angles of about 10° and less a rather intense background was observed in the (d,p) reaction studies due to spuriously scattered deuterons reaching the spectrometer detector. This was reduced by placing a 17.5 mg cm^{-2} gold foil in front of the crystal, which was sufficient to prevent deuterons of energies less than 2.1 MeV from being detected but transmitted protons with energies greater than 1.7 MeV.

C H A P T E R III

DEUTERON STRIPPING AT LOW ENERGIES

3.1 Introduction

The Butler theory of deuteron stripping is normally expected to be a good approximation only for incident energies well above the coulomb barrier where distortion effects are not too severe. However, Wilkinson [25] has suggested that even for low deuteron bombarding energies (d,p) and (d,n) reactions should exhibit well developed stripping patterns, close to the undistorted Butler form, providing the Q-value for the reaction is low, but not if the Q-value is high. The general line of reasoning which Wilkinson gives is as follows. If the deuteron energy is low and the Q-value high, then the departing energetic proton (assuming a (d,p) reaction) must obtain most of its high linear momentum from the deuteron ground-state wave function since there is little to be had from the bulk motion of the deuteron. In order for this to occur the neutron-proton separation must be small so that the interaction between the two particles is sufficiently strong for the proton to receive this high momentum. Since, however, the neutron must approach close to the nuclear surface before stripping can occur then so also must the proton, and the resulting strong interaction with the nucleus will give rise to a badly distorted stripping pattern, if not to compound nucleus formation. If now the Q-value is low, the correspondingly low linear momentum of the proton can be readily obtained from the deuteron wave function for much larger separations of the two particles. In this case the proton can be well removed from the target nucleus at the instant of stripping and the distortions of the stripping pattern should be much less than for the high-Q case. More generally, the best stripping patterns are expected to occur when the linear momentum of the outgoing proton is equal to about half that of the incident deuteron i.e. for a deuteron energy $E_d \approx -2Q$.

In addition to the above considerations, when the Q-value is low the binding energy of the captured neutron is also low so that its wave function has a long relaxation length outside the nucleus. Stripping can therefore take place when the neutron is anywhere in this tail, not necessarily at the nuclear surface, with the proton a correspondingly further distance away from the nucleus. Furthermore, competition through compound nucleus formation should be much less

serious for low-Q stripping, since for this to occur the proton must penetrate through the coulomb barrier well beyond the point where it could have stripped.

Amado [18] first pointed out that the presence of the energy denominator term $(q^2 + k^2)^{-2}$ in the Butler formula results in a pole when $q^2 = -k^2$ where the Butler theory must be exactly correct. Since this occurs for scattering angles with $\cos\theta > 1$, then in practice the pole is nearest at 0°. Warburton and Chase [48] have shown that under this condition the pole is most closely approached when $E_d \approx -2Q$ for negative Q-values, and $E_d \approx Q$ for positive Q-values. Thus, in accord with Wilkinson's hypothesis, if the deuteron energy is low then the Butler theory should be valid if the Q-value also is low, since stripping can then take place close the pole.

Experimental support for Wilkinson's hypothesis is found in the work of Sellschop [49] on the reactions $Li^7(d,p)Li^8$ (ground state) and $C^{12}(d,p)C^{13}$ (3.09 MeV level), which were studied at deuteron energies between 1.0 and 2.5 MeV, and also of Rout et al [30] on the $N^{14}(d,p)N^{15}$ reaction at 2 MeV. The investigations to be described in this chapter were carried out mainly at a deuteron energy of 3.0 MeV and cover a wider range of Q-values than in the previous work. This has therefore enabled a closer study to be made of the dependence of the stripping patterns on Q-value.

The (d,p) reaction has been studied on B^{10}, B^{11}, C^{12}, C^{14} and O^{16} and the proton angular distributions have been analysed using the Butler and D.W.B.A. stripping theories. As already mentioned (Section 1.4), the latter theory assumes the proton and deuteron waves to be distorted only by elastic scattering processes and are represented by the same optical model parameters as are required to describe the observed scattering. Although there is now a wealth of data on proton elastic scattering (e.g. ref. 51) there was none available on deuteron scattering under the conditions employed in this study. Some elastic deuteron scattering has therefore also been studied to obtain the necessary distorting parameters.

3.2 Procedure

The low-Q (d,p) reactions were first studied with the Harwell 180° magnetic analyser and 5-MV Van de Graaff generator. Most of these measurements were later repeated, however, using the multi-channel spectrograph and 3.02 MeV deuterons from the Aldermaston Tandem accelerator, during a more extensive study which included the high-Q transitions from the $B^{10}(d,p)B^{11}$ reaction. With some exceptions the results presented here are from this later work. The exceptions are the reactions $B^{10}(d,p)B^{11}$ (8.92 MeV level) at $E_d = 3.5$ and 4.0 MeV and $C^{14}(d,p)C^{15}$ (ground state) at

E_d = 3.0 MeV, which were only measured with the Harwell magnetic analyser.

The (d,p) reaction studies on B^{10}, B^{11}, C^{12} and O^{16} were made using a composite target. This was prepared by evaporating boron, containing approximately equal proportions of B^{10} and B^{11}, from a tantalum crucible on to a glass slide containing a thin carbon film. The resulting layer was then stripped off in the usual way and transferred to a target frame. The evaporation was carried out using the electron bombardment technique described by Muggleton and Howe [52] and the oxygen was present in the target only as a contaminant. A precise mass analysis was later made from a measurement of the deuteron elastic scattering from the same target and this gave the following mass values: 28 ± 2 μgm cm^{-2} (B^{10}) and 26 ± 2 μgm cm^{-2} (B^{11}), 7.7 ± 0.7 μgm cm^{-2} (C^{12}) and 5.8 ± 0.5 μgm cm^{-2} (O^{16}). The estimated accuracy of the differential cross-sections obtained from these values is ± 10%.

Two separate exposures were made with the multi-channel spectrograph. The first used a relatively low magnetic field strength of 5637 gauss to study the low-Q reactions from all four target constituents, and the second a high strength of 8690 gauss to study the high-Q reactions from B^{10}, and also the $C^{12}(d,p)C^{13}$ (ground state) reaction. The total exposure strengths were 140 and 350 microcoulombs, respectively.

The $C^{14}(d,p)C^{15}$ reaction was studied using a target prepared from acetylene gas enriched to about 43% in C^{14}. An account of its preparation is given in Appendix A.

Deuteron elastic scattering measurements from B^{10} were carried out at 2.5 and 3.0 MeV using the Harwell magnetic analyser and a self-supporting target of the enriched (approximately 93%) isotope. Measurements were also later made at 3.5 MeV with the multi-channel spectrograph using the composite target.

3.3 Elastic Deuteron Scattering from B^{10}, B^{11}, C^{12} and O^{16}

The differential cross-sections for deuterons elastically scattered from B^{10} at 2.5, 3.0 and 3.5 MeV and from B^{11}, C^{12} and O^{16} at 3.5 MeV are shown plotted on a logarithmic scale in fig. 3.1. (The arbitrary units of cross-section are not the same for all cases.)

The results have been analysed using an optical model parameter search programme developed by Maddison.[53] No spin-orbit term was used and the optical model potential was assumed to have the form (Section 1.4):

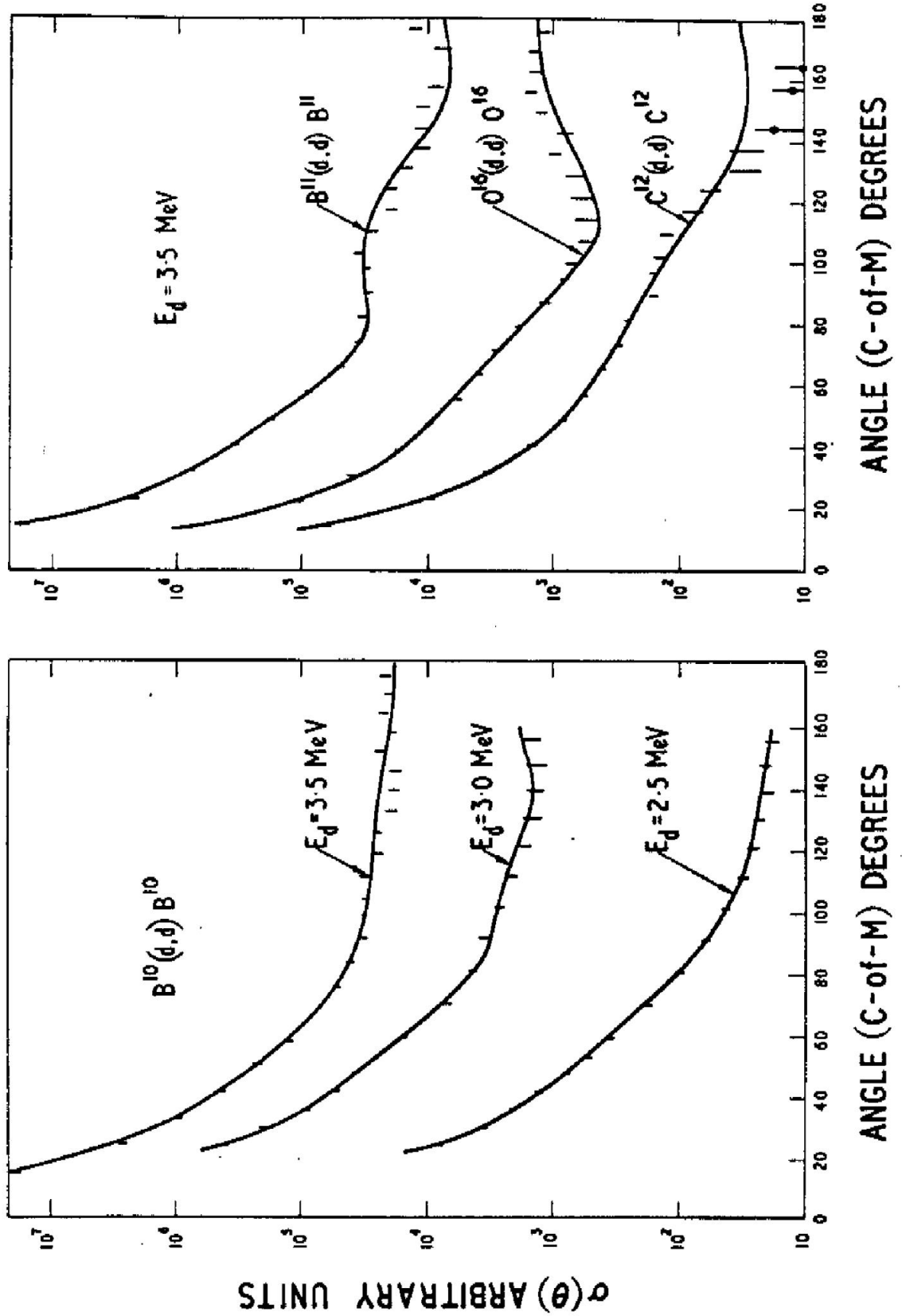

Fig. 3.1 *Measured angular distributions of elastically scattered deuterons and their optical model fits.*

$$V(r) = V_c(r) - (U + iW)\, f(r)$$

in which f(r) is the Saxon-Woods form factor. The calculations were carried out on Oxford's 'Mercury' computer. The search programme has been described in detail by Maddison.[53] By systematically varying the four parameters U, W, r_o and a, it searches for a minimum value of

$$\Delta = \sum_{i=1}^{N} \Delta_i$$

where,

$$\Delta_i = \left(\frac{\sigma(\theta_i)_{Exp} - \sigma(\theta_i)_{Theor}}{\delta\sigma(\theta_i)_{Exp}} \right)^2$$

The quantity $\delta\sigma(\theta_i)_{Exp}$ is the expected error in the observed value of $\sigma(\theta_i)_{Exp}$ and the summation extends over all (i.e. N) experimental points. As the agreement between theory and experiment improves, Δ tends to χ^2 where χ^2 is defined in the usual way,

$$\chi^2 = \sum_{i=1}^{N} \Delta_i \frac{\sigma(\theta_i)_{Exp}}{\sigma(\theta_i)_{Theor}}$$

The curves shown in fig. 3.1 are the best fits which could be obtained and the corresponding parameters are given in Table 3.1. In all cases U, W, r_o and a were initially allowed to vary independently, but for the B^{10} data at 2.5 and 3.5 MeV considerable ambiguity was found among the parameters U, r_o and a and for these sets r_o was maintained constant at 1.5 fm. This value seemed reasonable from previously published measurements.[53]

Although the fits in general are reasonably satisfactory, some deviations among the parameters should not be too surprising for such light nuclei and low energies. In particular, the diffuseness for C^{12} (0.1 fm) and imaginary potential for O^{16} (0.1 MeV) are unusually small compared with the values normally observed. However, it is significant that in these two cases the excitations in the compound systems for 3.5 MeV incident deuterons are only 13.3 MeV (in N^{14}) and 10.6 MeV (in F^{18}), compared with 28.1 MeV (in C^{12}) and 21.6 MeV (in C^{13}) for B^{10} and B^{11}, respectively. At these low excitation energies a significant contribution to the observed scattering may therefore arise from compound elastic scattering, which is not accounted for in the optical model. Thus, the anomalous values for the above parameters may be due to efforts by the optical model to simulate the effects of compound elastic scattering.

T A B L E 3.1

Optical Model Parameters from Deuteron Elastic Scattering Measurements

Target Nucleus	Deuteron Energy (MeV)	U (MeV)	W (MeV)	r (fm)	a (fm)	χ^2
B^{10}	2.5	27	16.1	1.5	0.77	18
B^{10}	3.0	34	7.7	1.28	0.80	24
B^{10}	3.5	28	4.6	1.5	0.48	82
B^{11}	3.5	26	5.3	1.51	0.43	122
C^{12}	3.5	30	4.5	1.70	0.10	90
O^{16}	3.5	42	0.1	1.45	0.30	88

In determining the deuteron parameters for the D.W.B.A. calculations, only the scattering measurements from B^{10} were considered reliable. The parameters so chosen were thus taken to be the mean values obtained from these four sets of data, viz; U = 30 MeV, W = 8 MeV, r_o = 1.5 fm and a = 0.6 fm.

3.4 The (d,p) Reaction Studies

3.4.1 Proton Energy Spectrum

Measurements of proton energy spectra from the composite target were made at both magnetic field strengths with the multi-channel spectrograph. Spectra obtained with the higher field were relatively simple since only those groups were present which corresponded to the ground and first five excited states of B^{11} and the ground state of C^{13}.

A typical spectrum measured with the lower field strength and at an angle of observation of 27.5° is shown in fig. 3.2. The groups were identified by their characteristic rate of change of energy with angle and in the figure are labeled according to the final nuclear states formed in the (d,p) reactions. In addition to the groups arising from the known target constituents an intense proton group was also observed corresponding to the recoil protons from the H(d,p)D reaction.

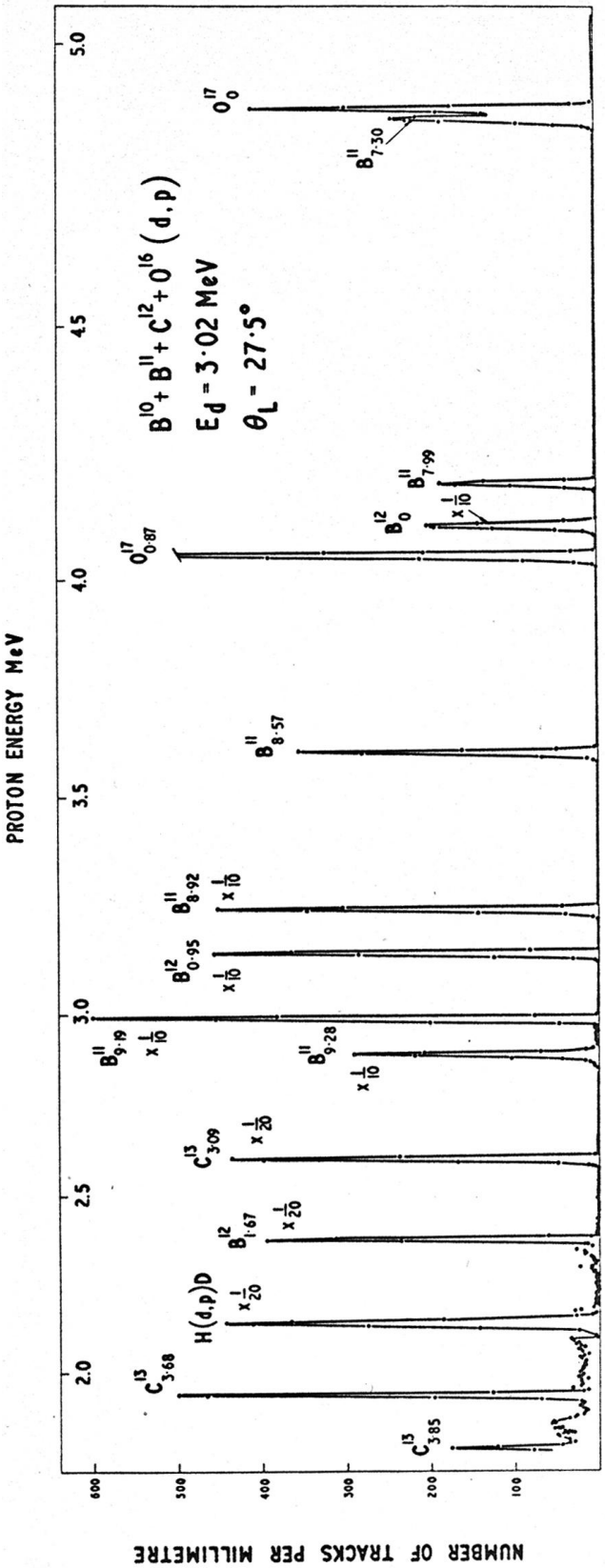

Fig. 3.2 *Proton energy spectrum from the (d,p) reaction using a composite target.*

Fortunately, this group did not overlap with any other at the angles of observation employed and therefore did not present any serious problem.

No new levels were observed and since the level excitations were already well known no precise energy determinations were made. The values assumed in this work were taken from Ajzenberg-Selove and Lauritsen.[54]

3.4.2 Angular Distributions

Proton angular distributions from the (d,p) reactions have been analysed using the Butler and D.W.B.A. stripping theories, the former calculations being performed with a computer programme compiled by Buck.[55] In nearly all cases deuteron optical model parameters used in the distorted wave calculations were maintained fixed at the measured values. The general features of the optical model for proton elastic scattering are quite well known (e.g. refs 33, 51) and Hodgson[56] has given a general relation for determining U_p and W_p, viz: $U_p = 58 - 0.3\,E_p$ and $W_p = 3E_p$ with $r_o = 1.25$ fm and $a = 0.65$ fm. The values U_p and W_p assumed in the present calculations were 55 MeV and 5 MeV, respectively, for all except the B^{11} ground and 4.46 MeV level distributions. In these cases $W_p = 8$ MeV was used to allow for the increased proton energy. The parameters are summarised in Table 3.II. In all calculations presented in this section zero cut-off radius was used.

Since in most cases absolute differential cross-sections have been measured, this has enabled absolute values of the spectroscopic factor (or relative reduced width [19]) S, where $\theta^2(n,l) = S\theta_0^2(n,l)$, to be extracted from the data. These have been obtained using the normal peak fitting procedure described in Section 1.3. In extracting values of S from the Butler analyses, values of the single-particle reduced widths, θ_0^2, were taken from the work of MacFarlane and French [19] in which empirical values of θ_0^2 are given as a function of the binding energy of the captured nucleon.

T A B L E 3.II

Optical Model Parameters used in the D.W.B.A. Analyses

Neutron Well Shape: r_n = 1.3 fm; a_n = 0.7 fm			
Deuteron		Proton	
Parameter	**Value**	**Parameter**	**Value**
U_d (MeV)	30	U_p (MeV)	55
W_d (MeV)	8	W_p (MeV)	5 or 8
r_{od} (fm)	1.5	r_{op} (fm)	1.25
a_d (fm)	0.6	a_p (fm)	0.65
r_{cd} (fm)	1.3	r_{cp} (fm)	1.3

(a) $B^{10}(d,p)B^{11}$

Angular distributions for the proton groups corresponding to the ground and first eleven excited states of B^{11} are shown in the centre-of-mass system in figs. 3.3a and 3.3b. The distribution for the 7.30 MeV level could not be reliably measured at angles less than 30° owing to interference from the ground state proton group from the $O^{16}(d,p)O^{17}$ reaction. The proton group from the 7.99 MeV level was also obscured at angles greater than 107° by the much more intense ground state group from $B^{11}(d,p)B^{12}$.

The broken line curves shown for the more intense transition were calculated from the Butler theory and these have been normalised to the experimental peaks in the distributions. The assumed l-values are noted in the figure. A Butler radius of 5.0 fm was found to give the best fit in all cases except the 6.76 MeV level, for which a larger radius of 5.6 fm was found necessary. The full line curves were calculated from D.W.B.A. theory using the parameters of table 3.II. These have again been normalised to the experimental peaks.

The ground, 4.46, 6.76 and 8.92 MeV levels are all formed by l = 1 transitions and the levels at 9.19 and 9.28 MeV by l = 0. For the two latter transitions, which have Q-values of 0.044

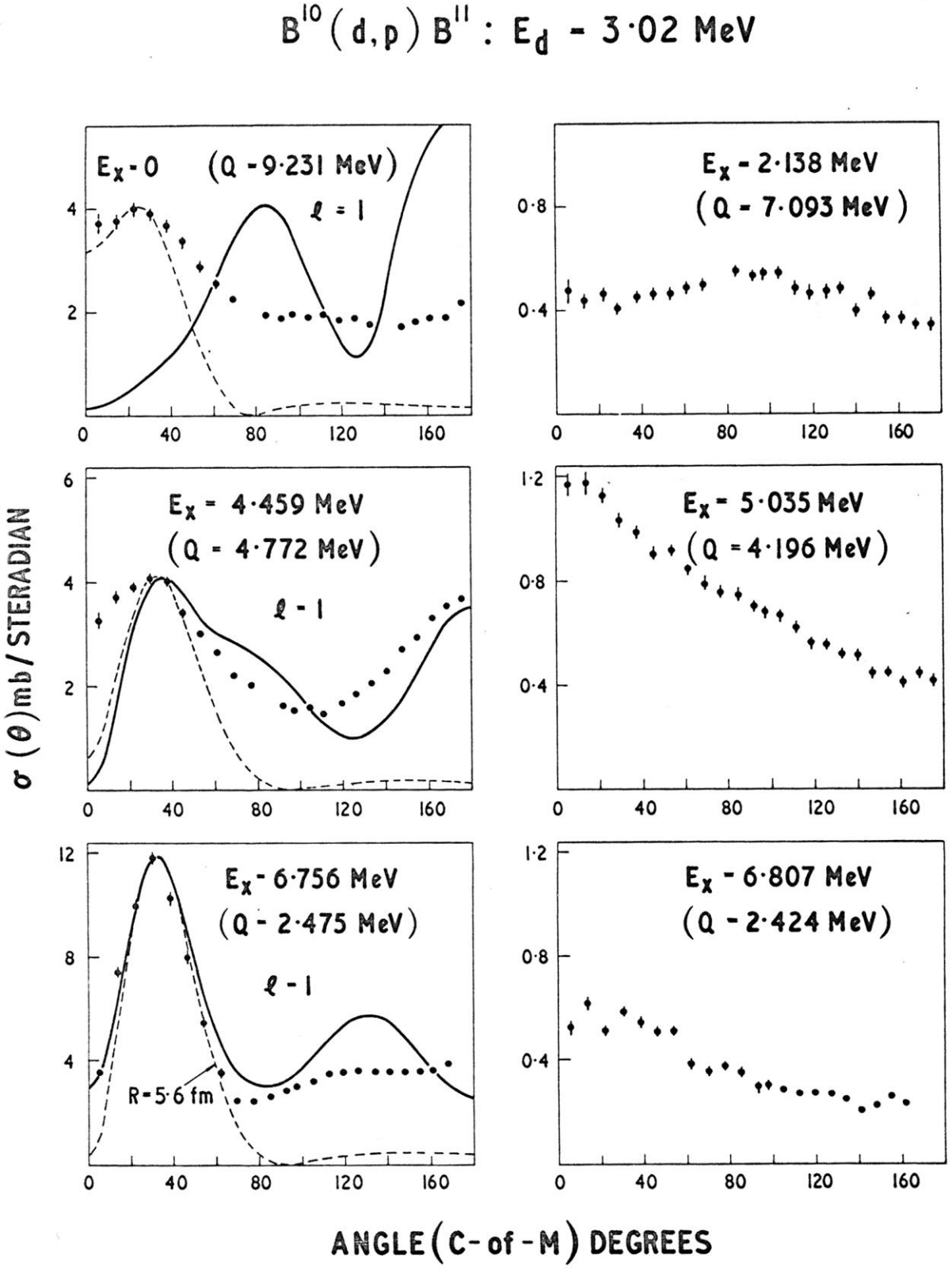

Fig. 3.3a *Proton angular distributions from $B^{10}(d,p)B^{11}$. The dashed curves are from the Butler theory and the full curves were calculated from D.W.B.A. theory.*

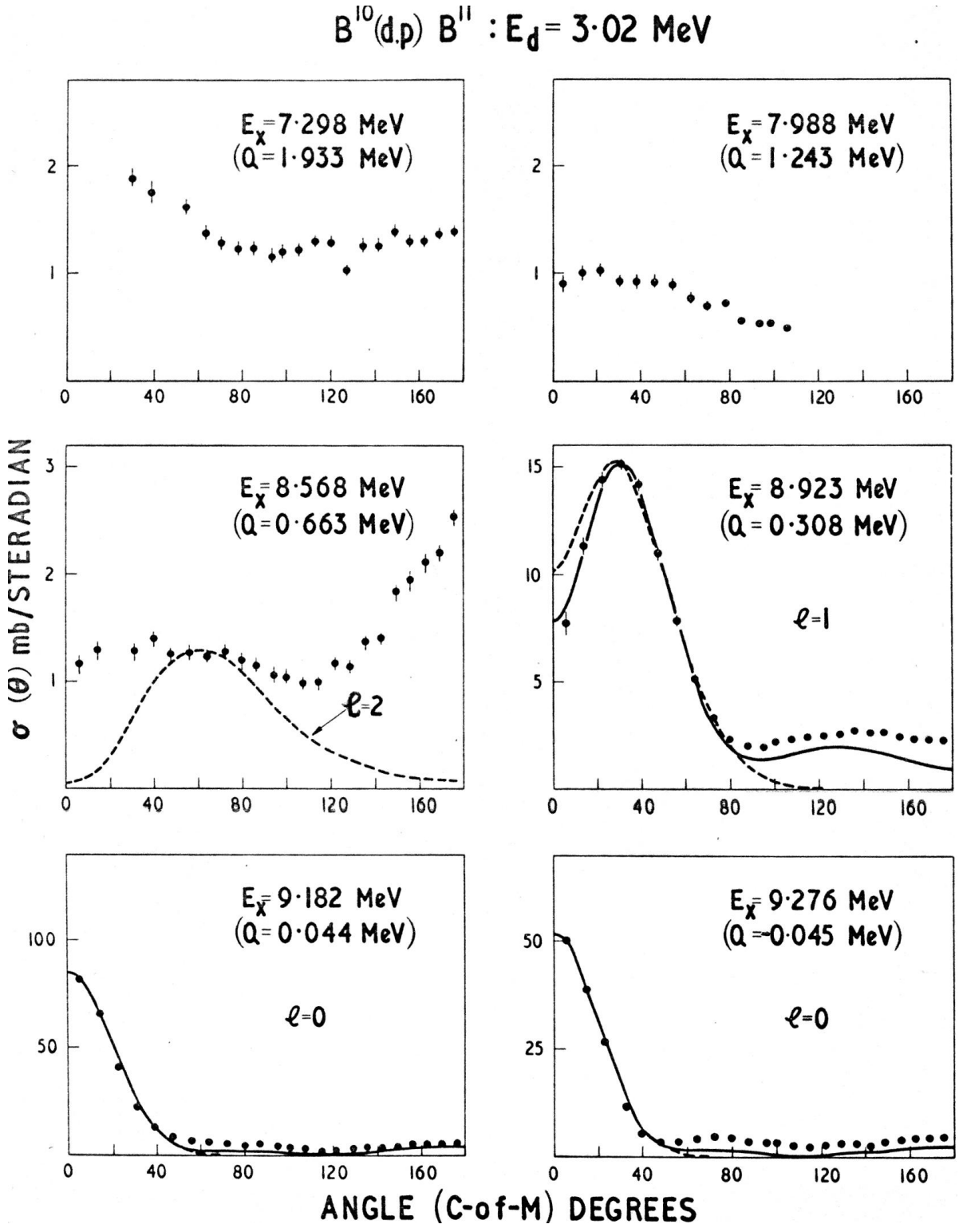

Fig. 3.3b *(See caption Fig. 3.3a)*

and -0.045 MeV, respectively, excellent agreement is obtained between the observed distributions and both plane wave and distorted wave theories. The 8.92 MeV level distribution shows a very well developed l = 1 stripping pattern and the agreement with Butler theory in the stripping peak is very satisfactory, although the experimental distribution is seen to dip slightly below the Butler curve at very small angles. The fit in detail is here improved with D.W.B.A. theory which is particularly successful in describing the distribution at large angles. Good agreement is also obtained with the Butler theory in the region of the stripping peak for the 6.76 MeV level. The differential cross-section at large angles relative to the peak value, however, is seen to be somewhat greater than in the previous case and the D.W.B.A. theory is again able to give a more satisfactory account of the distribution in this region.

The distributions for the high-Q transitions leading to the ground state (Q = 9.23 MeV) and 4.46 MeV level (Q = 4.77 MeV) differ considerably from the Butler curves. Although successful in giving the correct positions of the stripping peaks, the plane wave theory predicts them to be much sharper than observed. It is seen that for the 4.46 MeV distribution the observed backward peak is also predicted by the distorted wave theory and is therefore unlikely to be due to heavy particle stripping. However, the D.W.B.A. theory does not give very satisfactory overall agreement to this distribution, particularly at small angles where the calculated differential cross-section falls off too rapidly. In the case of the ground state, the angular distribution calculated from D.W.B.A. theory predicts a stripping peak at 85° in contrast with the observed peak at 25°. The calculated distribution here bears little resemblance to the experimental distribution and this somewhat anomalous behavior is discussed in more detail in section 3.5.

With the exception of the 8.92 MeV level the present l-value assignments are in agreement with the earlier measurements at 7.78 MeV by Bilaniuk and Hensel.[57] These authors interpreted their distribution for this level as comprising a mixture of l = 0 and l = 2 transitions, whereas the present measurement shows unmistakably l = 1. In view of this discrepancy, the distribution was measured at two further energies of 3.5 and 4.0 MeV and the results are shown in fig 3.4. These are again very well described by both plane wave and distorted wave theories (although at 4.0 MeV a slightly larger radius of 5.3 fm was necessary in the Butler theory to obtain agreement near the peak). The similarity in shape between the distributions measured at these three energies clearly rules out the possibility of resonances in the excitation function leading to rapid variations in the distributions. The assignment of l = 1 also agrees with the more recent measurement of Hinds and

Middleton [58] at 10.1 MeV deuteron energy, and is consistent with the L = 0 transition observed by the same authors [37] in the $Be^9(He^3,p)B^{11}$ reaction.

The stripping selection rules require all states formed by l = 1 transitions to have odd parity and spins 3/2, 5/2, 7/2 or 9/2. These are consistent with the known [51, 59, 60] spins and parities of $3/2^-$, $5/2^-$ and $(7/2^-)$ for the ground, 4.46 and 6.76 MeV levels, respectively. The $Be^9(He^3,p)B^{11}$ reaction limits the spin-parity values for the 8.92 MeV level to $1/2^-$, $3/2^-$ or $5/2^-$. Since the present work excludes $1/2^-$ this level must therefore be $3/2^-$ or $5/2^-$. The latter value is probably favoured since the excitation energy for this state is consistent with that of the second $B^{11}(5/2^-)$ state predicted by Kurath [6] from intermediate coupling shell model calculations.

The l = 0 transitions to the 9.19 and 9.28 MeV levels agree with the observations of Bilaniuk and Hensel [57] and of Hinds and Middleton [58] and these states must be $5/2^+$ or $7/2^+$. Bilaniuk and Hensel suggest that they may belong to a j-j doublet having the same reduced widths. The stripping intensities should therefore be in the ratio of the (2j+1) statistical factors, and since these authors observed a stronger transition to the 9.19 MeV state they assigned $7/2^+$ to this member and $5/2^+$ to the 9.28 MeV level. The ratio of intensities observed in the present study is fully in accord with these assignments.

The levels at 2.14, 5.04, 6.81, 7.30, 7.99 and 8.57 MeV are all only relatively weakly excited by this reaction and their angular distributions could not be fitted with any combination of l-values. At higher deuteron energies there is some evidence that the 8.57 MeV level may be formed by d-wave neutron capture [57,58]. There is little evidence for this in the present work, however, and the l = 2 Butler curve is shown in fig 3.3 for comparison.

The 2.14 MeV level is known [60] to be $1/2^-$ and if formed by a normal stripping process would require an l = 3 transition. Earlier work by Evans and Parkinson [61] at 7.7 MeV, however, indicated possible l = 1 and attempts have been made to explain this in terms of a spin-flip mechanism [62] and nucleon exchange stripping [21]. Neither l = 1 nor l = 3 can account for the present distribution which is essentially isotropic.

The l-values are summarised in Table 3.III together with the maximum observed differential cross-sections. The spins and parities J^π are the most probable values taken from the work of Donovan et al [60] and Ferguson et al [59] (from measurements of the de-excitation gamma-rays), Hinds and Middleton [37] (from $Be^9(He^3,p)B^{11}$), Bilaniuk and Hensel [57] (from $B^{10}(d,p)B^{11}$) and the present work. In the fifth column are listed the Butler radii R required to give best agreement in

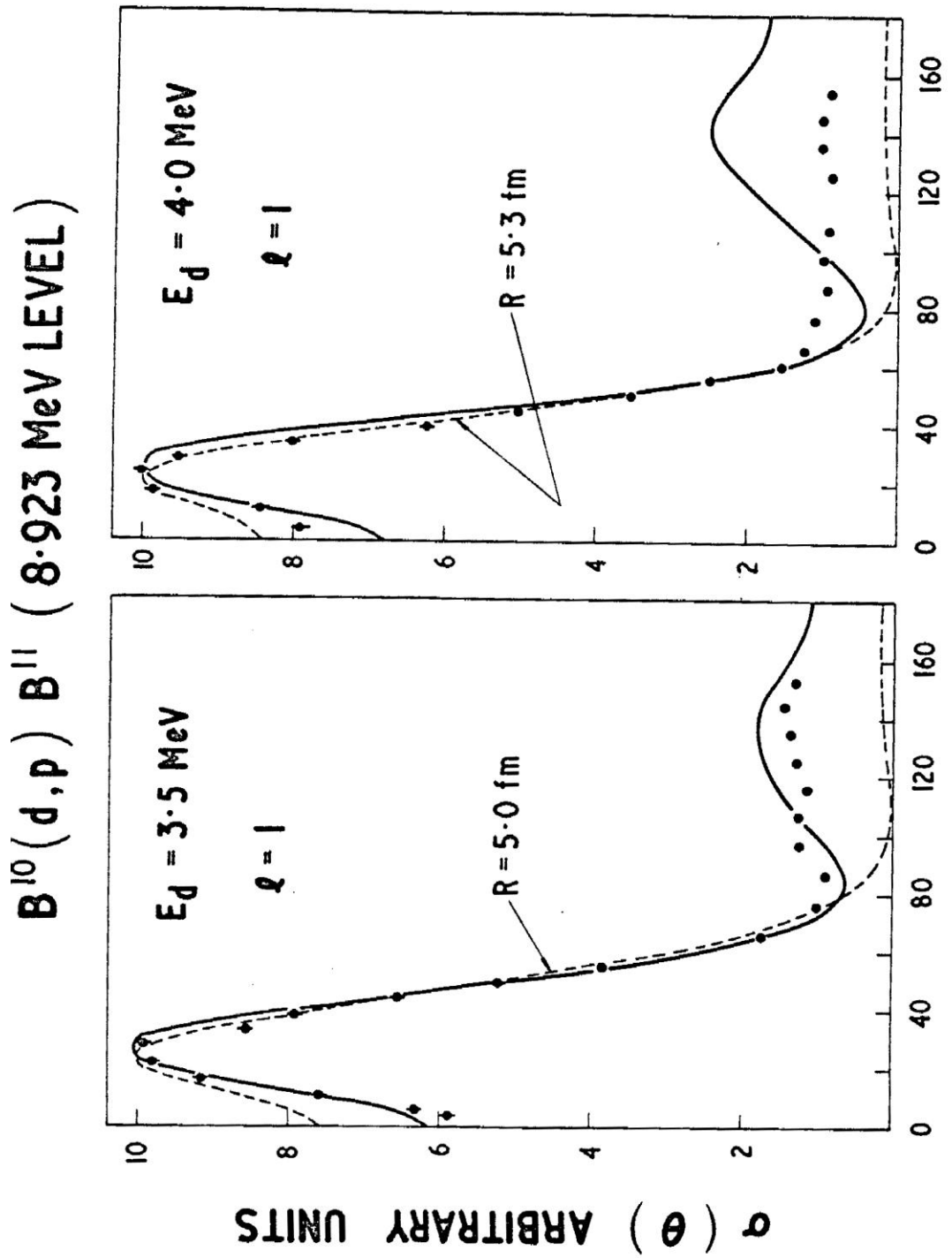

Fig. 3.4 *Proton distributions from* $B^{10}(d,p)B^{11}(Ex = 8.923\ MeV)$

each case and these values have been used to calculate the absolute reduced widths θ^2 given in the next column. In column seven are listed the empirical single particle reduced widths, $\theta_o^2(n,l)$, used to extract the relative values of the spectroscopic factors, S. Absolute and relative spectroscopic factors obtained from the distorted wave theory are given in the final two columns.

T A B L E 3.III

Summary of Results for $B^{10}(d,p)B^{11}$

Level Energy (MeV)	$\sigma(\theta)_{max}$ mb/ster)	ℓ	J^π	Butler Analysis				DWBA Analysis	
				R (fm	$\theta^2 = S\,\theta_o^2$			S	
					Absolute	$\theta_o^2(n,l)$	Relative (S/S_{gnd})	Absolute	Relative
0	4.0	1	$3/2^-$	5.0	0.027	(1p)0.04	1.0	1.9	1.00
2.138	0.5	1	$1/2^-$						
4.459	4.1	1	$5/2^-$	5.0	0.014	(1p)0.05	0.47	1.10	0.58
5.035	1.2		$(3/2)^-$						
6.756	11.8		$(7/2)^-$	5.6	0.021	(1p)0.06	0.56	1.03	0.54
6.807	0.6		(1/2,3/2)+						
7.298	1.9		$5/2^-$						
7.988	1.0								
8.568	2.5								
8.923	15.1	1	$3/2^-,5/2^-$	5.0	0.044, 0.029	(1p)0.06	1.08, 0.71	0.77, 0.51	0.41, 0.27
9.187	85	0	7/2+	5.0	0.022	(2s)0.17	0.19	0.24	0.12
9.276	52	0	5/2+	5.0	0.019	(2s)0.17	0.16	0.20	0.10

Since at this low bombarding energy the outgoing proton waves suffer very different distortions over the Q-value range of 9.2 MeV, the relative reduced widths obtained from the plane wave and distorted wave treatments are in surprisingly close agreement. However, the value of S obtained for the ground state from D.W.B.A. theory must be regarded as rather doubtful since the observed distribution is not well fitted by this theory and, as mentioned in section 3.5, the differential cross-section is very sensitive to the choice of distorting parameters. Such sensitivity is not observed in the case of the higher excited state distributions.

(b) $B^{11}(d,p)B^{12}$

Proton angular distributions for the ground, 0.95 and 1.67 MeV states of B^{12} are shown in fig 3.5. The first two are seen to be characterised by l = 1 transitions and the third by l = 0. In all cases excellent agreement is had with the Butler theory (broken curves) in the region of the forward stripping peaks. These curves were calculated with a radius of 6.3 fm for the ground state and 6.0 fm for the two excited states.

For the two l = 1 distributions, rather large cross-sections relative to the peak values are observed in the backward direction. These are well accounted for by the D.W.B.A. theory, although the fits obtained near the stripping peaks are rather less satisfactory. These peaks are predicted to be at about 30° which is some 8° beyond their measured positions. A somewhat broader l = 0 stripping peak is also suggested by the distorted wave theory than that observed experimentally for the 1.67 MeV distribution.

The present l-value assignments are in accord with the earlier measurements of Holt and Marsham [63]. The l = 1 transitions require final state spins and parities $\leq 3^+$. Since the ground state is known to decay by an allowed β^--ray transition to C^{12} (O^+) then this must be 1^+, and the spin-parity for the 0.95 MeV level is probably [64] 2^+ or 3^+. The l = 0 transition requires 1^- or 2^- for the l.67 MeV level. The results are summarised, together with the calculated reduced widths, in Table 3.IV. The relative spectroscopic factors extracted from the plane wave and distorted wave analyses are seen to agree reasonably well.

T A B L E 3.IV

Summary of Results for $B^{11}(d,p)B^{12}$

Level Energy (MeV)	$\sigma(\theta)_{max}$ mb/ster)	ℓ	J^π	Butler Analysis				DWBA Analysis	
				R (fm)	$\theta^2 = S\,\theta_o^2$			S	
					Absolute	θ_o^2(n,l)	Relative (S/S_{gnd})	Absolute	Relative
0	14.0	1	1+	6.3	0.028	(1p)0.06	1.0	1.05	1.00
0.950	22.0	1	2+, 3+	6.0	0.023, 0.015	(1p)0.06	0.75, 0.49	0.57, 0.41	0.54, 0.39
1.673	125	0	1^-, 2^-	6.0	0.080, 0.050	(2s)0.17	0.92, 0.57	0.61, 0.37	0.58, 0.35

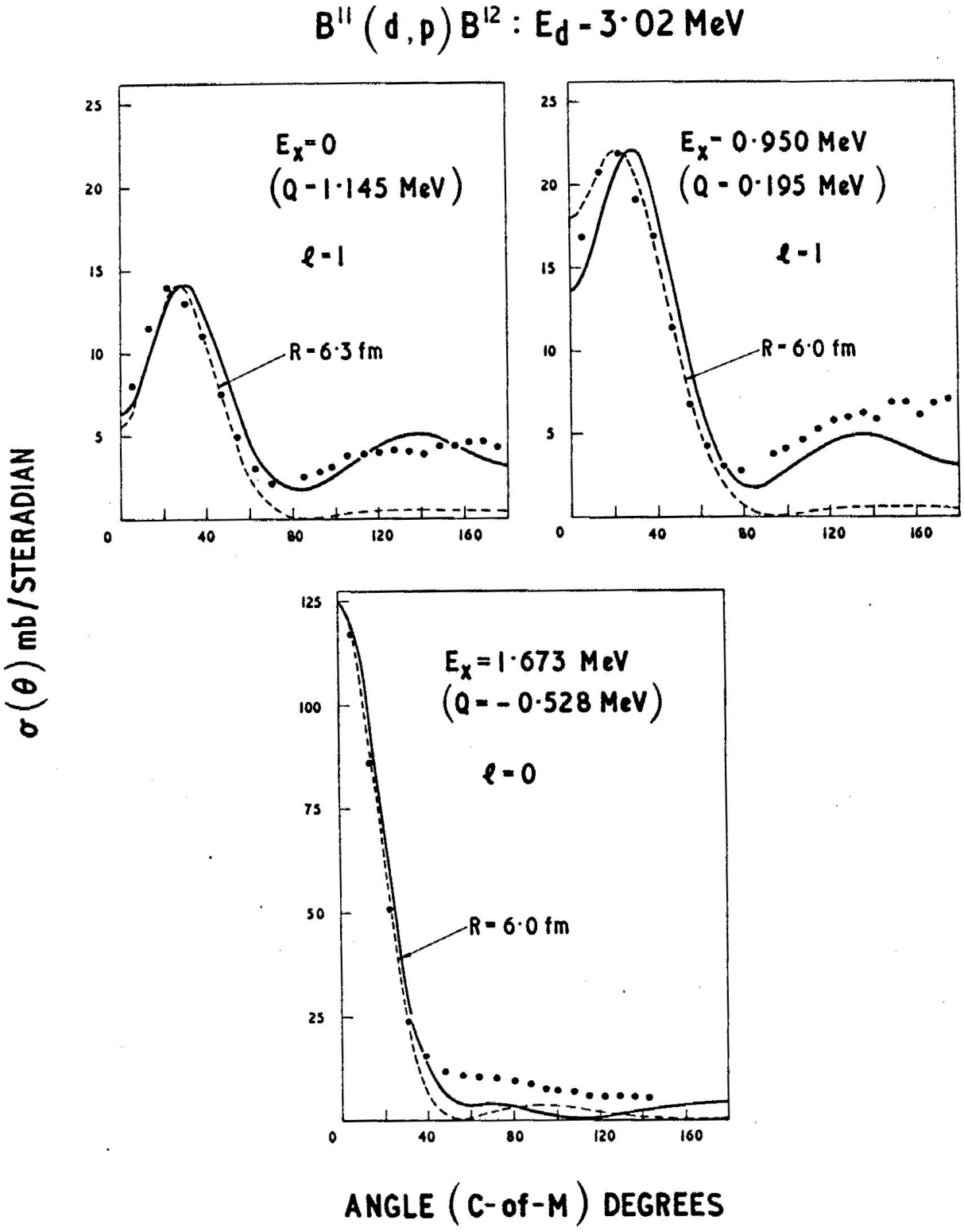

Fig. 3.5 *Proton distributions from the $B^{11}(d,p)B^{12}$ reaction.*

(c) $C^{12}(d,p)C^{13}$

Proton distributions for the ground, 3.09 and 3.68 MeV states of C^{13} are shown in fig. 3.6. The proton group corresponding to the 3.68 MeV state was not recorded on the nuclear plates beyond 100° owing to its excessively low energy at large angles. A radius of 5.0 fm was used in the Butler theory except for the ground state for which a larger radius of 6.0 fm was necessary to obtain a fit near the stripping peak. The l-values of 1, 0 and 1 are in accord with the known [54] spins and parities of, respectively, $1/2^-$ (ground), $1/2^+$ (3.09 MeV level) and $3/2^-$ (3.68 MeV level). For the ground state distribution the Butler theory predicts a somewhat sharper peak than that observed experimentally. This theory nevertheless agrees well with the stripping patterns observed for the two excited states. It is noted that the 3.68 MeV, l = 1 distribution peaks at 0° which is a consequence of the very low Q-value (-0.958 MeV) for this transition.

The full line curves were again calculated from distorted wave theory using the measured deuteron parameters. These give good agreement for the l = 0 distribution but are much less satisfactory in the case of the two l = 1 transitions. In particular the forward maxima are predicted at larger angles than observed experimentally. Several preliminary calculations were therefore carried out in an attempt to improve these fits. The distributions were found to be relatively insensitive to the proton parameters, providing these were maintained within the range of values normally required to fit elastic scattering data for this region of mass values and bombarding energies. These were therefore kept equal to the previously employed values. Improved agreement to the ground state distribution could be obtained if the deuteron real and imaginary potentials were increased to 50 MeV and 15 MeV, respectively. As seen in the figure this parameter set also predicts the rather large backward peak which is observed experimentally. Little change, however, is effected by these new parameters for the 3.09 and 3.68 MeV distributions, and in the latter case no reasonable optical model parameters were found which gave a maximum at 0°.

The results and reduced widths are summarised in Table 3.V. In view of the negative Q-values for the two excited state transitions, the energies of the outgoing protons are well below the coulomb barrier and the protons can be expected to suffer very different distortions compared with the ground state protons. This probably accounts for the rather large differences between the relative reduced widths extracted from the plane wave and distorted wave theories.

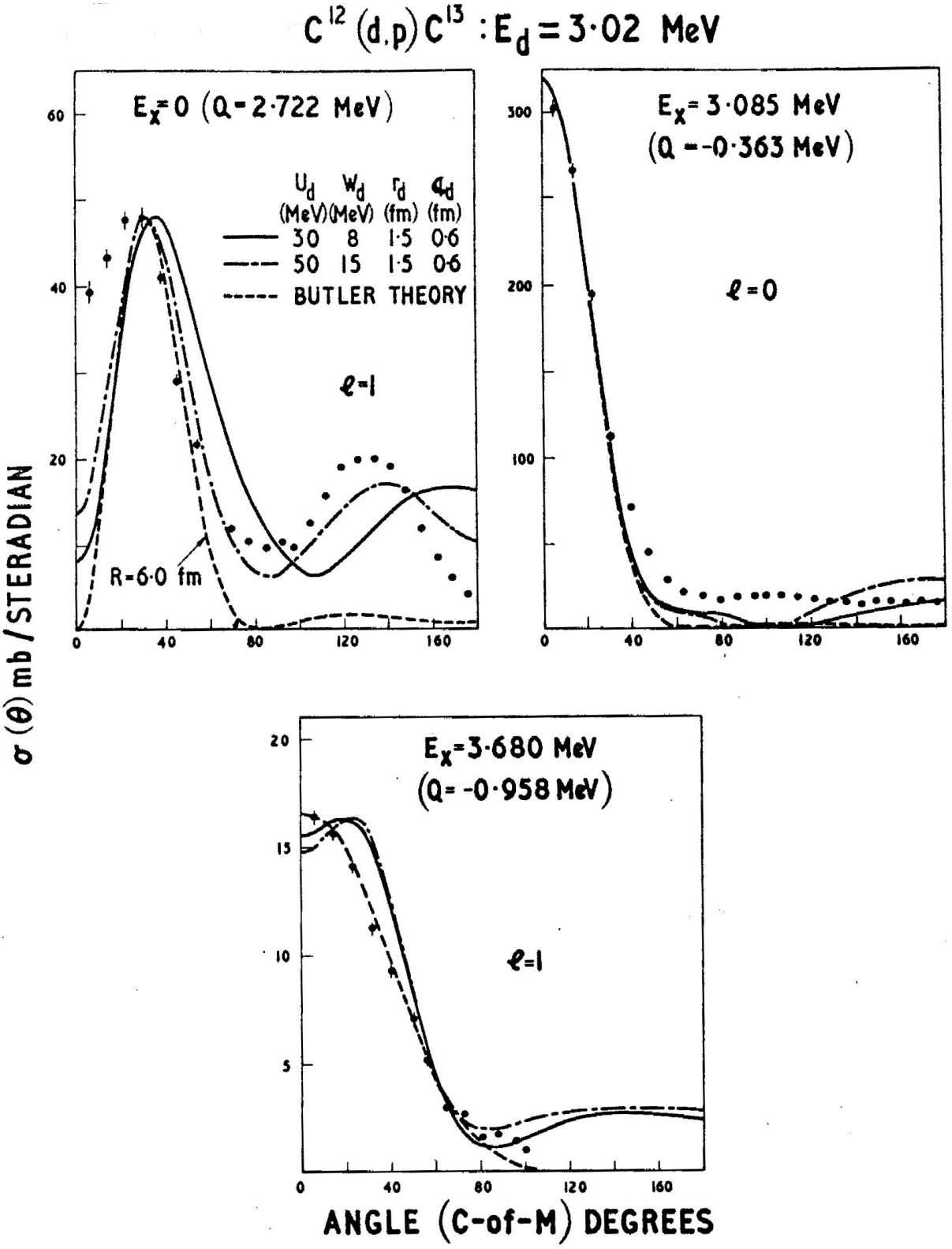

Fig. 3.6 *Proton distributions from the $C^{12}(d,p)C^{13}$ reaction*

T A B L E 3.V

Summary of Results for $C^{12}(d,p)C^{13}$

Level Energy (MeV)	$\sigma(\theta)_{max}$ mb/ster)	ℓ	J^{π}	Butler Analysis				DWBA Analysis	
				R (fm)	$\theta^2 = S\,\theta_o^2$			S	
					Absolute	θ_o^2(n,l)	Relative (S/S_{gnd})	Absolute	Relative
0	48.0	1	$1/2^-$	6.0	0.047	(1p) 0.05	1.0	2.5	1.00
3.085	335	0	1/2+	5.0	0.067	(2s) 0.17	0.42	0.69	0.28
3.680	16.5	1	$3/2^-$	5.0	0.005	(1p) 0.06	0.09	0.13	0.05

(d) $C^{14}(d,p)C^{15}$

Measurements were only made for the ground state transition in this reaction and the proton distribution, measured at 3.0 MeV, is shown in fig 3.7. The l = 0 Butler curve was calculated with a radius of 5.0 fm.

Earlier work by Moore and McGruer,[65] at a bombarding energy of 14.9 MeV, showed that equally good agreement could be obtained with the Butler theory for both l = 0 and l = 1 with radii of 4.1 and 6.5 fm, respectively. Since both values of the radius are reasonably acceptable the results were thus rather ambiguous. As mentioned in section 1.3, at high bombarding energies and for low Q-values (in this case Q = -1.007 MeV) the angular distributions for different l-values are very similar and only become clearly distinguishable at low bombarding energies. In the present work the ambiguity is completely removed, and excellent agreement is obtained with both plane wave and distorted wave theories assuming l = 0. To obtain a fit with the Butler theory and l = 1 requires an unphysically large radius of 8.5 fm.

The l = 0 assignment gives an unambiguous spin-parity of $1/2^+$ for C^{15}. This is in accord with the measured β^--decay of C^{15} [66] and also with the shell model calculations for T = 3/2 levels in A = 15 by Halbert and French.[67]

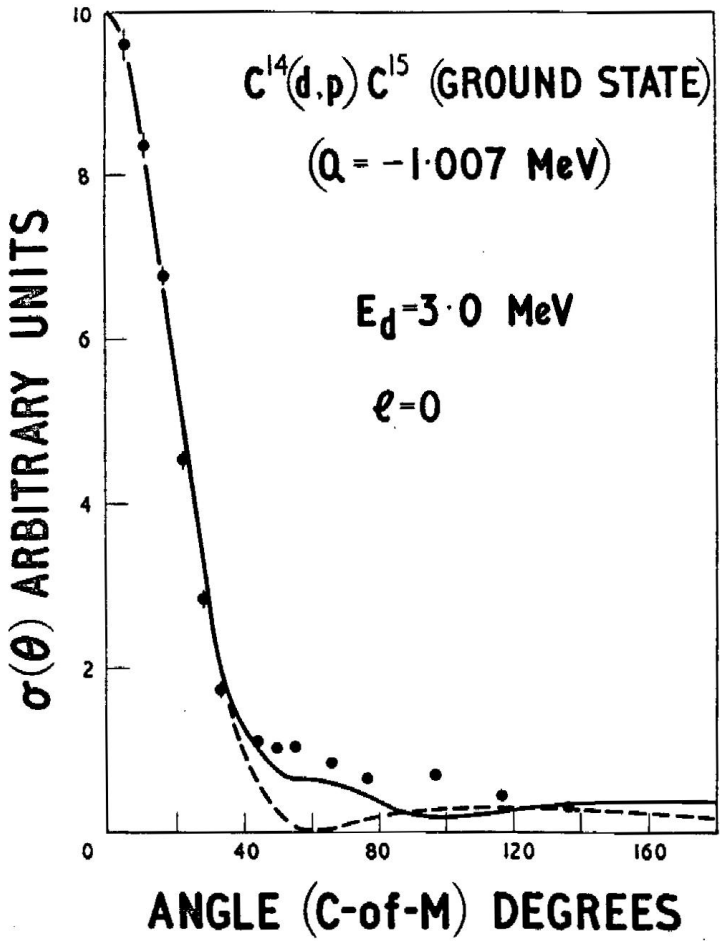

Fig. 3.7 *Proton distribution from the $C^{14}(d,p)C^{15}$ ground state transition*

(e) $O^{16}(d,p)O^{17}$

Angular distributions for the ground state and 0.87 MeV level of O^{17} are shown in fig 3.8. The observed l = 2 and l = 0 transitions are as required by the known spins and parities of $5/2^+$ (ground) and $1/2^+$ (0.87 MeV level).

Both distributions are seen to exhibit well formed stripping patterns and the Butler curves were calculated with R = 5.5 fm. This theory is seen to give the correct position for the maximum in the l = 2 distribution but predicts a rather sharper peak than that observed. Improved agreement is obtained with distorted wave theory, although in the backward direction the calculated distribution falls off more rapidly than experiment. Both theories give excellent agreement in the forward peak for the l = 0 distribution although neither is able to explain the rather large secondary maximum at 70°.

Reduced widths have been extracted and these are given in Table 3.VI. The ground and first excited states of O^{17} are expected to be good single-particle $1d_{5/2}$ and $2s_{1/2}$ levels (i.e. $S \approx 1$), so that the values of θ^2 determined from the Butler theory should give reasonable estimates of the single-particle reduced widths $\theta^2(1d)$ and $\theta^2(2s)$. In the present case, however, the values of θ^2 do not agree well with the values θ^2 suggested by MacFarlane and French,[19] particularly for the 2s-state. However, these authors have noted a strong energy variation in θ^2 between 2.1 and 8 MeV, and also the excitation function at low energies show marked fluctuations for both the ground and first excited state proton groups,[68] suggestive of strong compound nucleus contributions. The present values of θ^2 are in good agreement with those determined by MacFarlane and French at similar energies.

T A B L E 3.VI

Summary of Results for $O^{16}(d,p)O^{17}$

Level Energy (MeV)	$\sigma(\theta)_{max}$ mb/ster)	ℓ	J^π	Butler Analysis				DWBA Analysis	
				R (fm)	$\theta^2 = S\,\theta_o^2$			S	
					Absolute	$\theta_o^2(n,l)$	Relative (S/S_{gnd})	Absolute	Relative
0	32.5	2	5/2+	5.5	0.036	(1d)0.06	1.0	o.76	1.00
0.871	180	0	1/2+	5.5	0.023	(2s)0.17	0.23	0.49	0.65

3.5 Discussion and Furthur D.W.B.A. Calculations.

It is evident from the results described in the foregoing section that, in nearly all cases where the cross-sections are large, the Butler theory with suitable cut-off radius gives a very adequate account of the observed stripping patterns, at least in the forward direction, for those transitions with Q-values of -1 to ≈2 MeV. Furthermore, in these cases the distributions predicted by the plane wave theory are generally very similar to those given by the distorted wave theory. However, the latter is usually more successful in describing the stripping patterns at large angles where the measured differential cross-sections tend to be larger than predicted by plane wave theory. This is understandable since the reaction products emitted at large angles correspond to smaller deuteron impact parameters for which distortion effects will be more important.

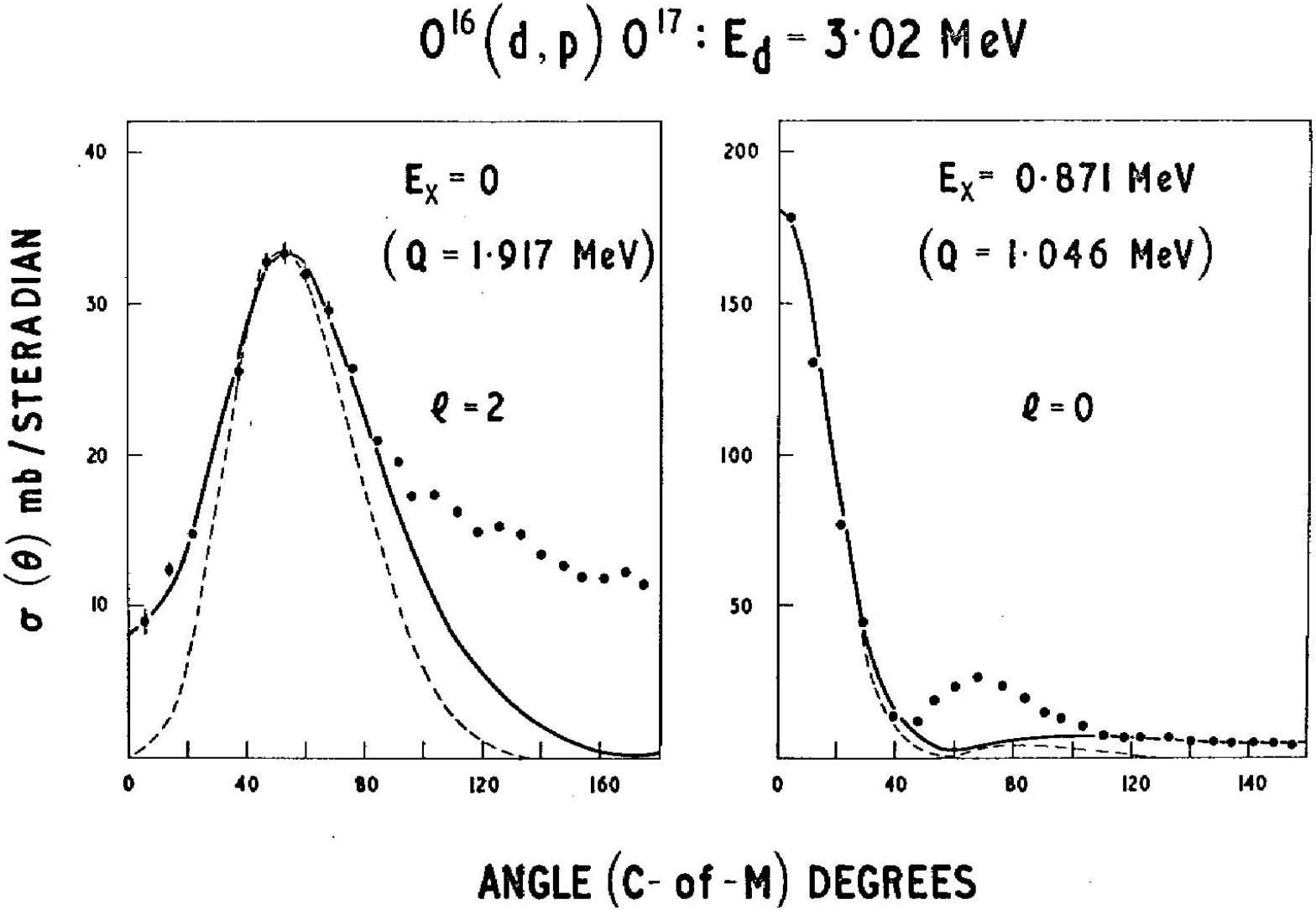

Fig. 3.8 *Proton distributions from the $O^{16}(d,p)O^{17}$ reaction*

In the case of the high-Q transitions, notably from the $B^{10}(d,p)B^{11}$ reaction leading to the ground and 4.46 MeV states of B^{11}, the situation is very different. The stripping patterns are now observed to be strongly distorted and no longer bear any close resemblance to the simple Butler form, even in the stripping peaks. The experimental evidence in support of Wilkinson's argument - that stripping patterns should retain their simple undistorted form at low energies providing the Q-value is low - is therefore clear.

That distortion effects are more important in stripping at 3 MeV, when the Q-value is high, than when the Q-value is low is clearly demonstrated in figs. 3.9 and 3.10. The distributions shown in the first of these figures correspond to the $B^{10}(d,p)B^{11}$ reaction leading to the ground state (Q = 9.231 MeV) and 8.923 MeV level (Q = 0.308 MeV) of B^{11}, and were calculated from D.W.B.A theory for various deuteron potentials U_d and W_d. The other optical model parameters were maintained equal to the values previously employed (Table 3.II) and the maximum differential cross-sections have all been normalized to the same (arbitrary) value. The distributions in fig. 3.10 were calculated for the same reasons, but with various proton potentials U_p and with U_d = 50 MeV, W_d = 15 MeV. It is evident that in the low-Q case the stripping pattern is relatively unaffected by the distortions for a wide range of distorting parameters, the only significant changes occurring at large angles. For the high-Q transition, however, the stripping pattern is extremely sensitive to the distortions and is far removed from the undistorted Butler form. Furthermore, the differential cross-sections measured at the first peak in the distributions for the various potentials used here varies by ± 42% in the high-Q reaction compared with only ±18% in the low-Q case. This throws considerable doubt on the reduced width extracted with D.W.B.A. theory for the ground state of B^{11}, since no agreement is had with the measured distribution.

It is apparent from these calculations that the distorted wave theory in its present form is totally inadequate in describing the B^{11} ground state distribution. Significant improvement may be had, however, if a cut-off radius is introduced, thereby removing any contributions to the stripping process which arise from within the nuclear interior. The results obtained with various (sharp) cut-off radii for the same two levels of B^{11} are shown in fig. 3.11, together with the experimental results. The optical model parameters are those given in Table 3.II. The low-Q distribution is seen to be little affected by a cut-off radius, whereas a very marked change occurs for the high-Q distribution. In the latter case, the predicted position of the main stripping peak agrees well with the measured position if a cut-off radius of 2.8 fm or more is employed, although the calculated peak is

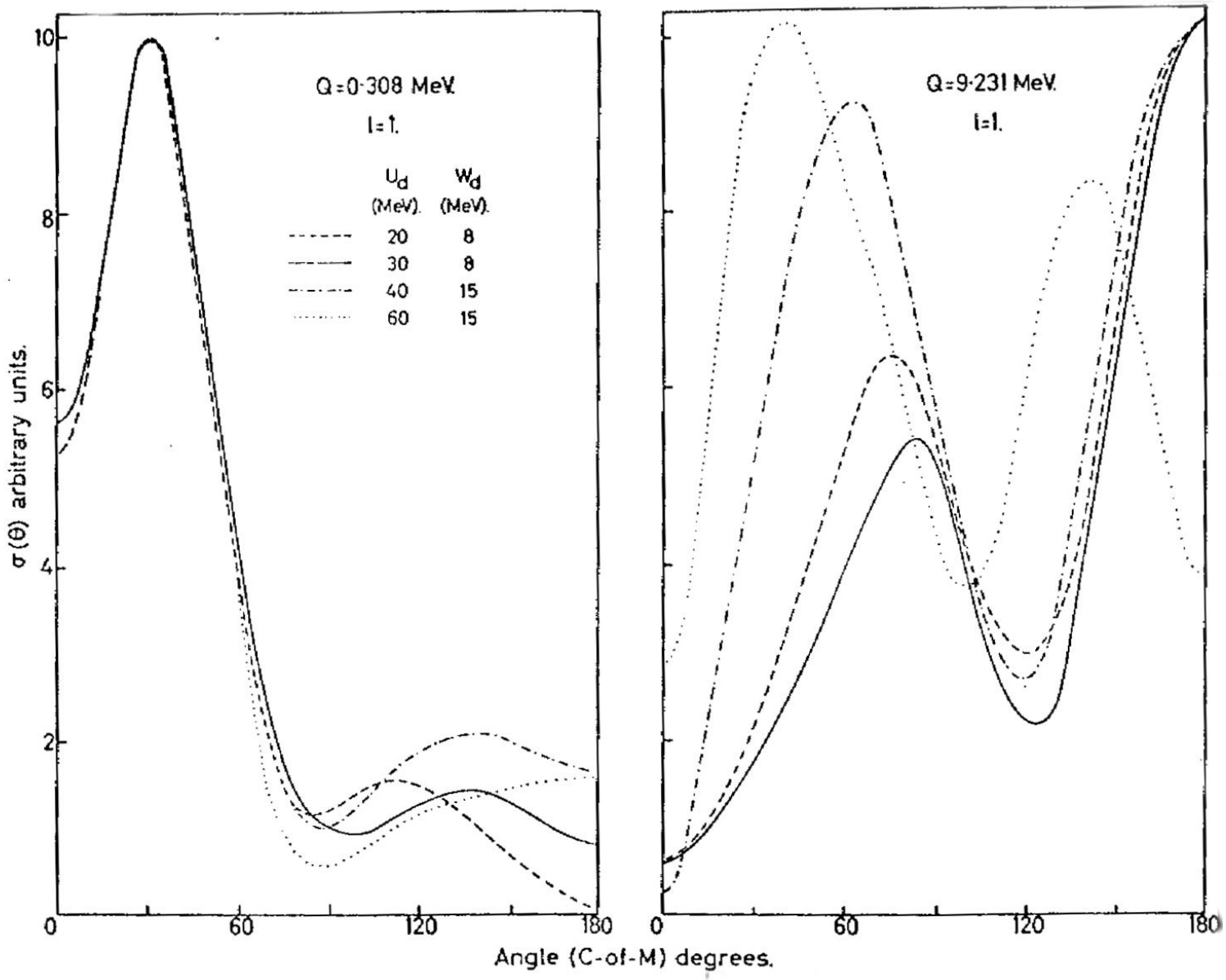

Fig. 3.9 *D.W.B.A. angular distributions from $B^{10}(d,p)B^{11}$ for various deuteron potentials*

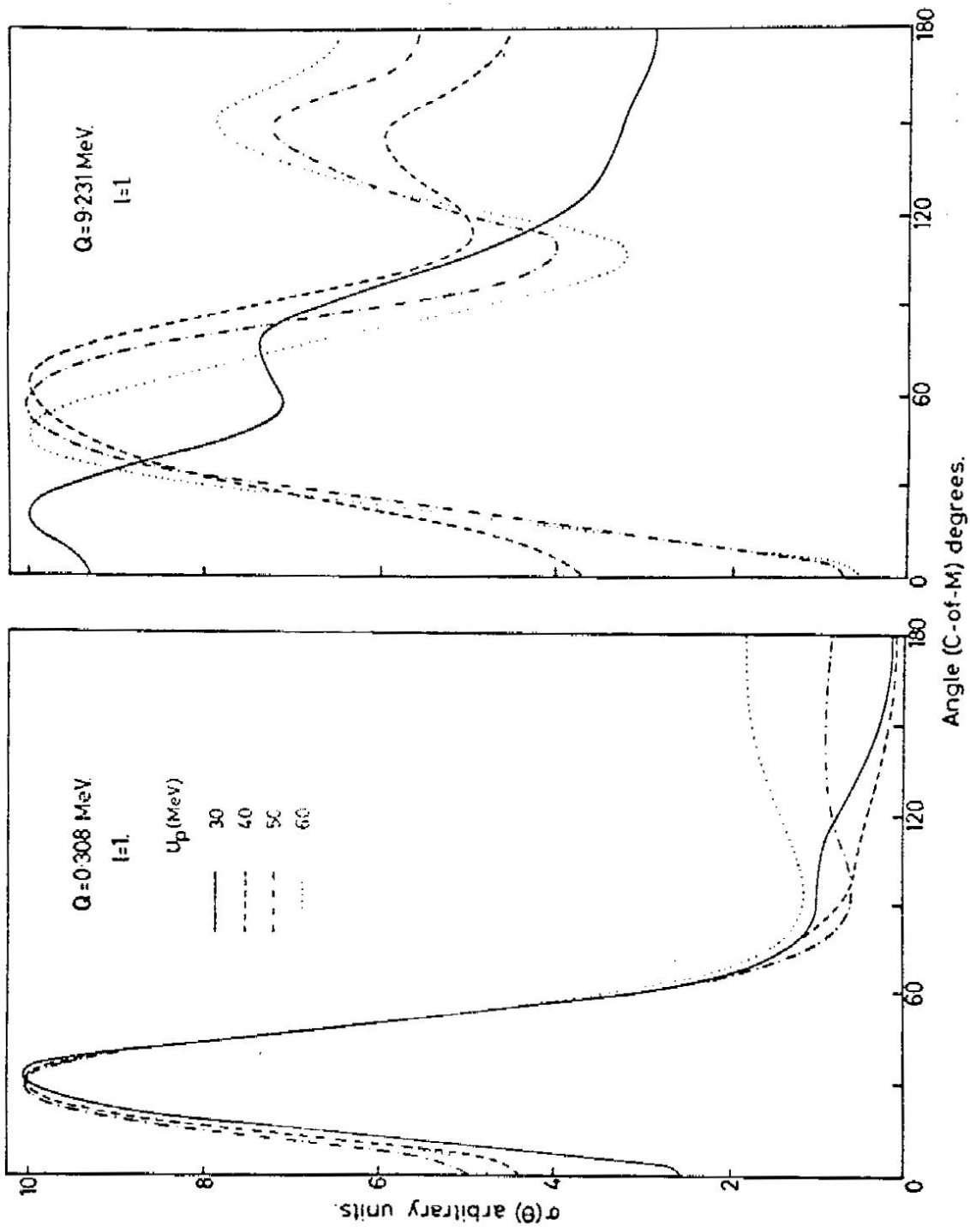

Fig. 3.10 *D.W.B.A. angular distributions from $B^{10}(d,p)B^{11}$ for various proton potentials*

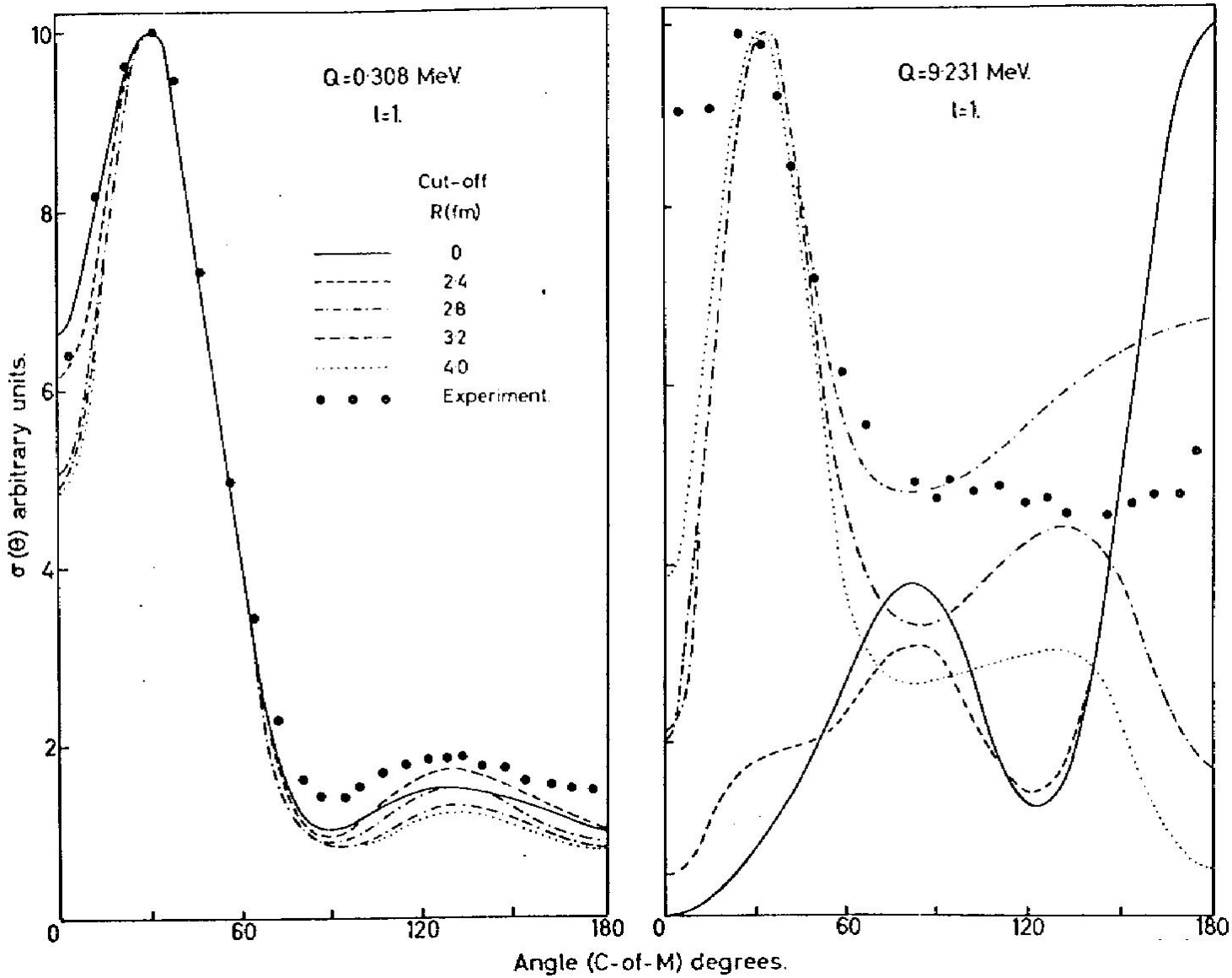

Fig. 3.11 *Measured angular distributions from $B^{10}(d,p)B^{11}$ compared with D.W.B.A. calculations with various cut-off radii to remove contributions to stripping from the nuclear interior.*

somewhat sharper than that observed. Also the large backward peak is very much reduced, thus giving improved agreement at very large angles. Indeed, a very close fit can be obtained in the backward direction if a cut-off radius of 2.9 fm is chosen. This effectively removes all the volume interaction and the reaction is confined to the nuclear surface region.

It is interesting to note that in the recent analysis by Rook and Mitra [30] of the $Ca^{40}(t,p)Ca^{42}$ double stripping reaction (see Appendix C), satisfactory agreement could also only be obtained if a cut-off radius was employed. Furthermore, it has been shown by Rook (ref. 30 and private communication) and Satchler [69] that introducing a finite range for the neutron-proton interaction in the D.W.B.A. theory results in a considerable reduction in the contribution to the stripping process from the nuclear volume, and this may be simulated by using a cut-off radius. Thus the need for a cut-off in the present case may reflect inadequacy of the 'zero-range' approximation.

In conclusion, the results of this investigation may be summarised as follows:

(1) The experimental measurements show that, even at low bombarding energies, the deuteron stripping patterns can be well described over a large angular range by the plane wave Butler theory providing the Q-value is low (say $\leq$ 2 MeV). Distorted wave calculations also show that under these conditions, the stripping patterns are close to the undistorted forms and relatively insensitive to the nuclear interactions.

(2) When the Q-value is high the stripping patterns bear little resemblance to the simple Butler forms and are very sensitive to the nuclear interactions. Together with (1) this therefore provides strong evidence in support of Wilkinson's hypothesis.

(3) The B^{11} ground state distribution can only be accounted for by distorted wave theory if a cut-off radius is used, which effectively confines the interaction to the nuclear surface region. This may indicate the need for including a finite range for the V_{np} interaction in the D.W.B.A. theory.

CHAPTER IV

A STUDY OF THE $Se^{76}(d,p)Se^{77}$ REACTION

4.1 Introduction

The assumption made in the distorted wave theory of (d,p) stripping, that the deuteron and proton waves are distorted only by elastic scattering interactions with the nuclear and coulomb fields of the target and residual nuclei, has already been referred to in previous sections. The main purpose of the investigation described in this chapter was to provide an experimental test of the validity of this assumption.

The optical model potentials used to describe the interactions may be obtained from analysis of the deuteron and proton elastic scattering, measured at the appropriate energies, from the target and residual nuclei, respectively. Thus, if the (d,p) and (d,d) measurements are carried out at any incident energy E_d, then the proton elastic scattering should be measured from the residual nucleus at an energy

$$E_p = \frac{m_f + m_p}{m_f}\left(\frac{m_i}{m_i + m_d}E_d + Q\right)$$

where m_d, m_p, m_i, and m_f are the masses of the deuteron, proton, initial nucleus and final nucleus, respectively, and Q is the (d,p) reaction Q-value. No such precise measurements had previously been made and the optical parameters had instead generally been obtained by interpolation from known elastic scattering data. These parameters were then frequently treated as freely adjustable parameters in the D.W.B.A. analyses in order to improve agreement with experiment. In the present more rigorous test of the theory, a specific (d,p) reaction has been studied together with the deuteron and proton elastic scattering to determine precisely these optical model parameters. The choice of a suitable (d,p) reaction was influenced by the following considerations.

(1) The target nucleus should be sufficiently heavy that the optical model is a good approximation,
(2) The initial and final nuclei must be stable, and
(3) The Q-value for the (d,p) reaction must not be too large in order that the proton energy required for the elastic scattering measurement was attainable from the Aldermaston Tandem accelerator.

Final consideration had also to be given to the current availability of separated stable isotopes, and the reaction finally chosen compatible with these requirements was $Se^{76}(d,p)Se^{77}$ (Q = 5.19 MeV).

4.2 Procedure

Thin self-supporting targets of Se^{76} and Se^{77} were prepared by evaporation of the separated isotopes, enriched to about 90% in each case. Total target thicknesses were estimated to be about 70 μgm cm^{-2} by direct weighing.

The measurements were made using the multi-channel spectrograph. An incident deuteron energy of 7.8 MeV was used for the (d,p) and (d,d) studies on Se^{76} and the elastic proton scattering from Se^{77} was measured at 13.0 MeV.

In view of the low melting point of selenium (≈180°C), it was found necessary to use beam currents of less than one microampère to minimise the loss of target material due to over-heating the beam spot area. Even so, the general instability of these targets under bombardment prevented absolute cross-sections from being measured for the (d,p) reaction.

4.3 $Se^{76}(d,d)Se^{76}$ and $Se^{77}(p,p)Se^{77}$: Results and Analysis

The deuteron and proton elastic scattering results are presented in fig. 4.1 (the arbitrary units of cross-section are not related). The differential cross-sections have been analyzed using the same optical model parameter search programme as described in section 3.3, and the full line curves in the figure are the best fits so obtained. The corresponding optical model parameters are given in the first two rows of Table 4.I together with the respective values of χ^2.

To test the 'uniqueness' of the present parameters, the calculations were repeated with several different sets of initial parameters and in both cases they were found to converge close to the earlier 'best-fit' values. However, the convergence was found to be rather less rapid for the elastic deuteron scattering than for the proton scattering. The former was found to be relatively insensitive to the choice of deuteron parameters whereas the latter was very sensitive to the proton parameters.

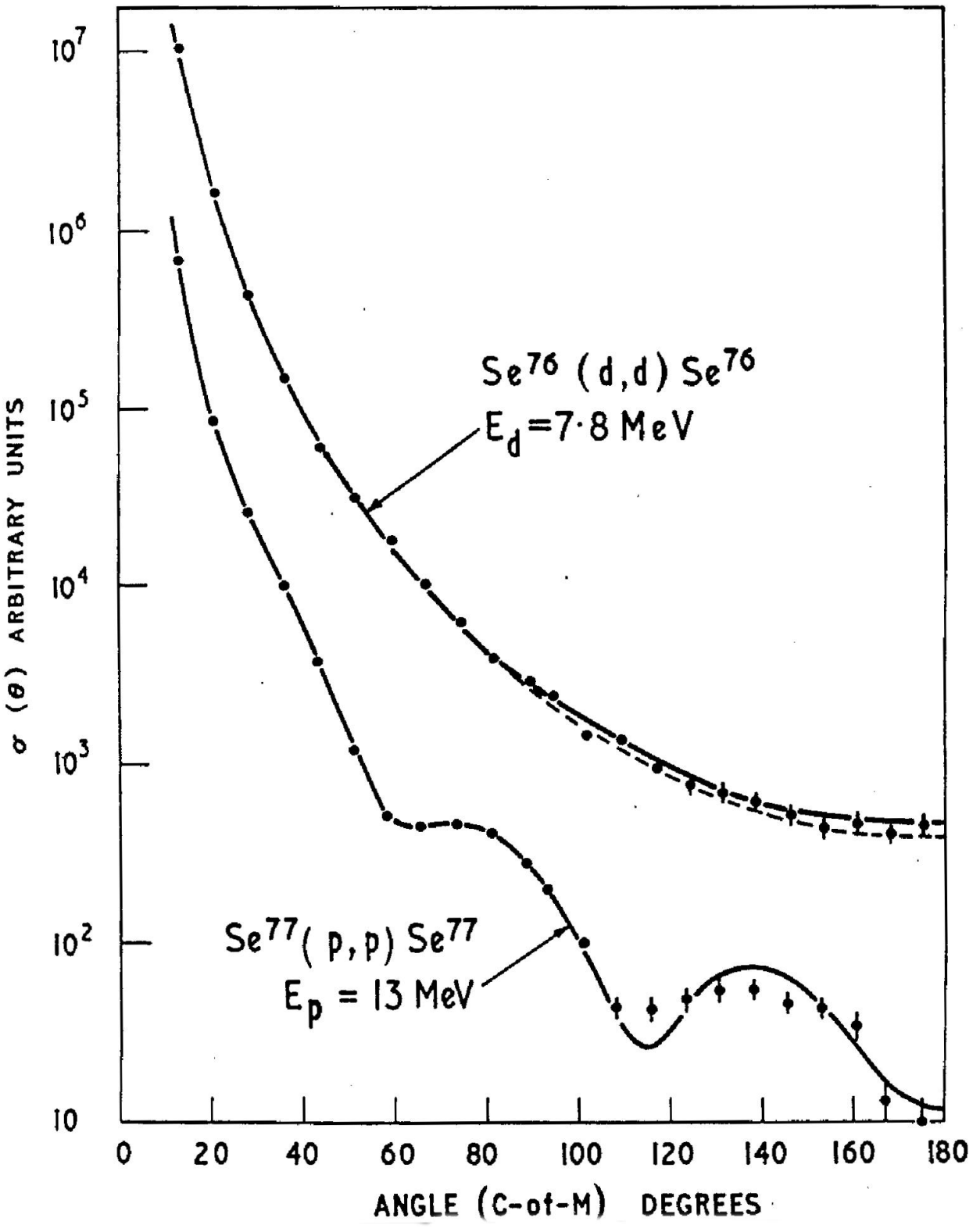

Fig. 4.1 *Deuteron and proton elastic scattering distributions from Se^{76} and Se^{77}*

T A B L E 4.I

Deuteron and Proton Optical Model Parameters

Parameter	U (MeV)	W (MeV)	r_o (fm)	a (fm)	χ^2
Proton	51.4	10.0	1.27	0.55	30
Deuteron (I)	75.8	16.0	1.48	0.55	35
Deuteron (II)	65	16	1.35	0.60	54

4.4 The $Se^{76}(d,p)Se^{77}$ Reaction

4.4.1 Level Excitations

A proton energy spectrum from this reaction, measured at an angle of 35^o, is shown in fig. 4.2. The various groups have been labeled according to the levels in the final nucleus. In all, seventeen groups have been examined and their angular distributions analysed. The unlabelled groups beyond group 16 probably correspond to high excited states in Se^{77}, but these were not measured at other angles. An unidentified light-mass impurity group is seen to the left of group-3.

A small amount of C^{12} impurity was present in the target and by observing at several angles the ground state proton group from the $C^{12}(d,p)C^{13}$ reaction (Q = 2.722 MeV), the mean of six measurements for the incident deuteron energy was determined to be 7.836 ± 0.010 MeV. From this value for the beam energy the ground state Q-value for the $Se^{76}(d,p)Se^{77}$ reaction was calculated to be 5.192 ± 0.012 MeV, in good agreement with that determined from the most recent masses of Everling et al [70] as 5.191 ± 0.060 Mev.

The excitations in Se^{77} attributed to the groups numbered in fig. 4.2 are listed in column 1 of Table 4.II. In most cases these are again the means of six determinations at different angles. The groups labeled 4, 8, 11 and 15 were only weakly excited by this reaction, however, and since their positions could not be accurately located in the proton energy spectrum their excitation energies have a somewhat larger associated error than have the other states. For purpose of comparison, the excitation energies of previously known states are listed in column 2 of the table. These values were taken from Landolt-Bornstein [71].

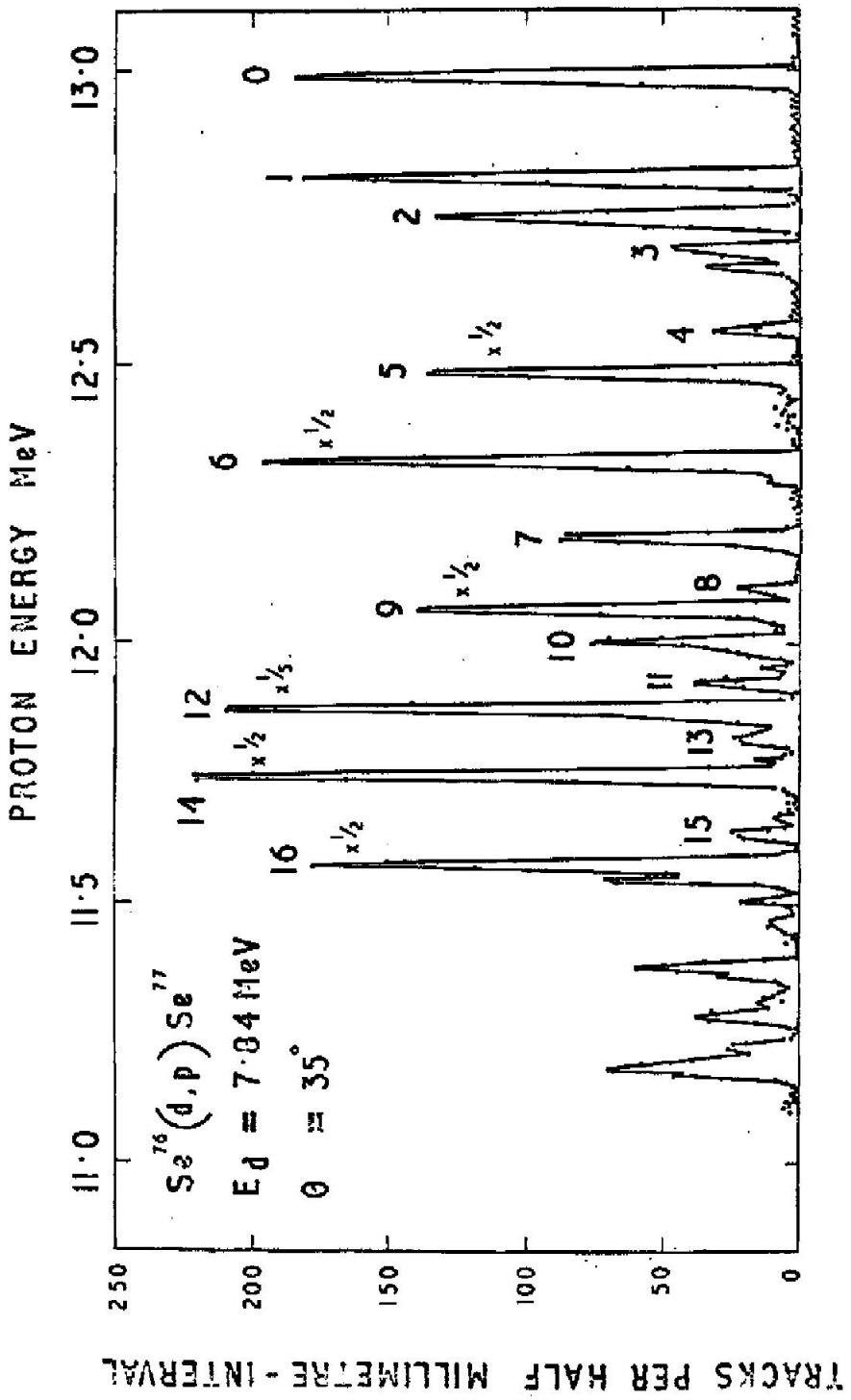

Fig. 4.2 *Proton energy spectrum from $Se^{76}(d,p)Se^{77}$*

T A B L E 4.II

Level Properties of Se^{77}

Group	1	2		ℓ	J^{π}	(2J+1)S
	E_x (MeV ± keV)	E_x (MeV)	J^{π}			
0	0	0	1/2⁻	1	1/2⁻, 3/2⁻	1.0
1	0.177±3	0.161	7/2+	3 or 4	5/2⁻, 7/2⁻, 9/2+	3.8 or 8.0
2	0.254±5	0.246	3/2⁻	1	1/2⁻, 3/2⁻	0.27
			5/2⁻	3	5/2⁻, 7/2⁻	1.7
3	0.306±5					
4	0.440±20	0.457	5/2⁻			
5	0.522±5	0.524	1/2⁻, 3/2⁻	1	1/2⁻, 3/2⁻	0.82
6	0.682±5			2	3/2+, 5/2+	1.3
7	0.826±5	0.82	3/2⁻	1	1/2⁻, 3/2⁻	0.33
8	0.92±20					
9	0.956±10			0	1/2+	0.18
10	1.013±10	1.00	1/2⁻, 3/2⁻	1	1/2⁻, 3/2⁻	0.20
11	1.09±20					
12	1.134±10			0	1/2+	0.71
13	1.191±10					
14	1.258±10			2	3/2+, 5/2+	1.1
15	1.37±20					
16	1.424±10			2	3/2+, 5/2+	0.79

4.4.2 Angular Distributions: Results and Analyses

(a) Ground State Transition.

The proton distribution corresponding to the ground state transition in Se^{76} is shown in fig. 4.3. The marked forward peaking is clearly indicative of a direct reaction mechanism and the various curves have been calculated from stripping theories assuming an orbital angular momentum transfer of l = 1, as required by the known spins and parities of 0^+ (Se^{76}) and $1/2^-$ (Se^{77}).

Curve I in the figure illustrates the best fit which could be obtained with the Butler plane wave theory and was calculated for a radius of 5.0 fm. This is considerably less than the Gamow-Critchfield value (6.9 fm) and reflects the strong coulomb deflection of the charged particles at this rather low deuteron energy. Curve II was calculated from D.W.B.A theory without a cut-off radius and using the optical model parameters derived from the elastic scattering measurements (Table 4.I). Although the fit to the detailed structure away from the main stripping peak is not very good it is nevertheless a considerable improvement on the plane wave theory.

To further improve the fit the sensitivity of the distorted wave theory on the various optical model parameters was investigated. The stripping pattern was found to be relatively insensitive to changes in the proton parameters and these were subsequently maintained equal to the measured values. It was, however, found to be very sensitive to the choice of deuteron parameters (with the exception of the imaginary potential, W_d), and by adjusting these the much improved fit shown by curve III in fig. 4.3 was obtained. The parameters used to calculate this curve are listed in the third row in Table 4.I. (deuteron II).

These new parameters have been used to recalculate the elastic deuteron differential cross-section and the result is shown by the broken line curve in fig. 4.1. It is evident that agreement with the observed scattering is still good, and the corresponding value for X^2 of 54 (Table 4.I) is not statistically very different from the previous value of 30.

(b) Excited State Transitions

Proton distributions corresponding to transitions to excited states in Se^{77} are shown in figs. 4.4 and 4.5. Those shown in the first of these figures correspond to the more intense transitions while those in fig. 4.5 correspond to only the weakly excited states. The distributions are labeled according to the group numbering in the spectrum of fig. 4.2 and for comparison the ground state distribution is also included. The second excited state distribution is presented later.

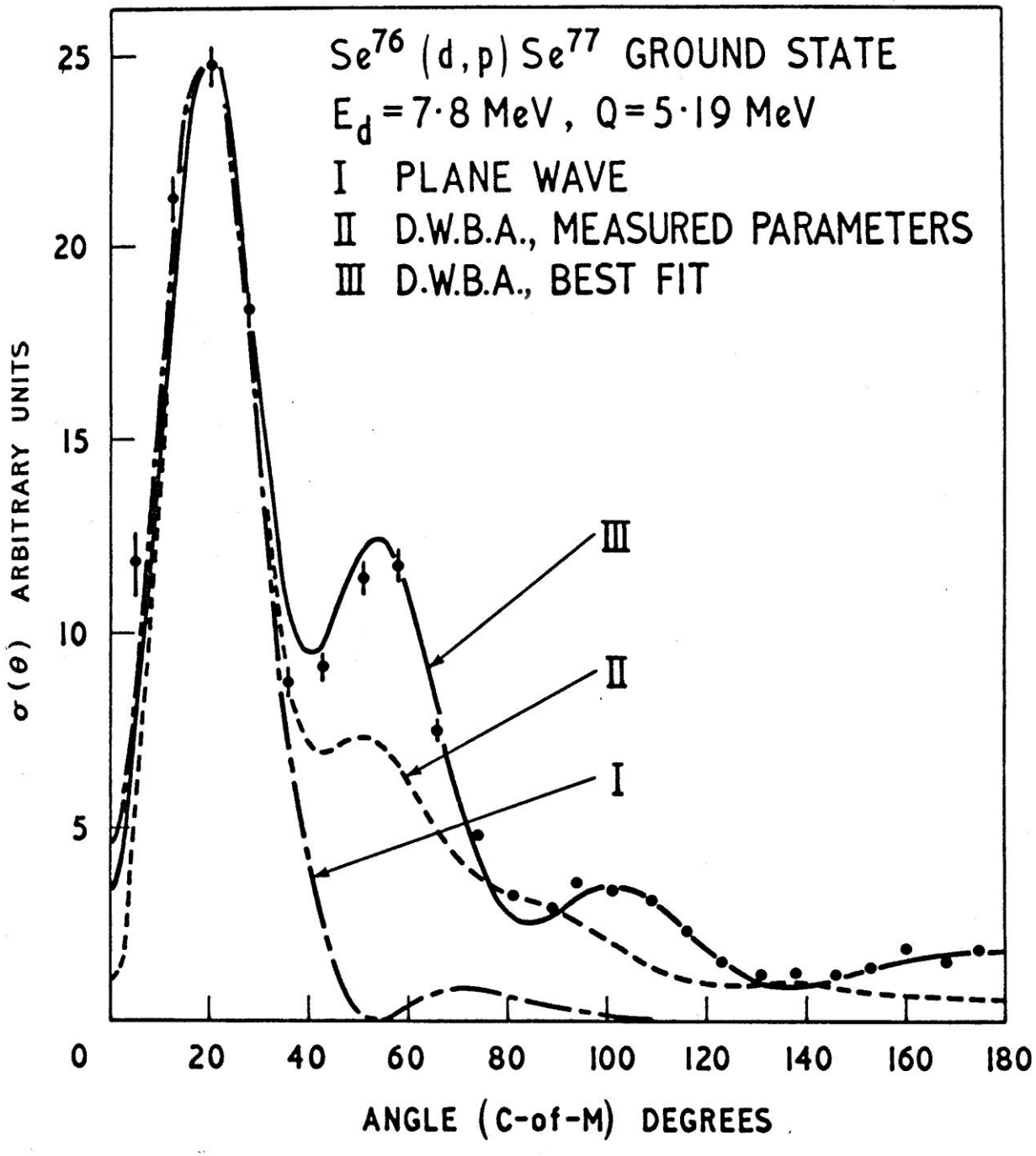

Fig. 4.3 *Proton distribution for the ground state transition in* $Se^{76}(d,p)Se^{77}$

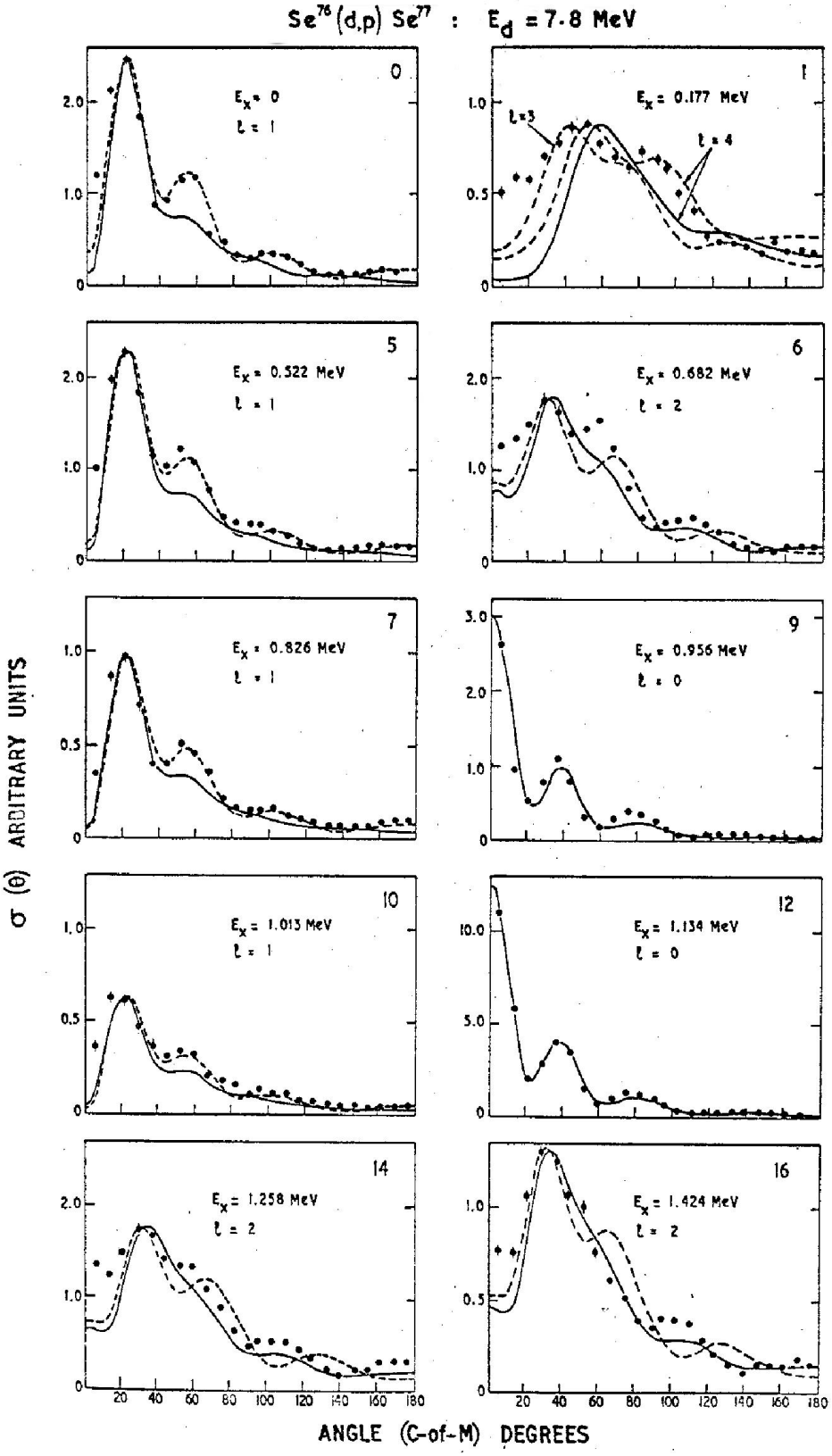

Fig. 4.4 *Proton distributions from $Se^{76}(d,p)Se^{77}$*

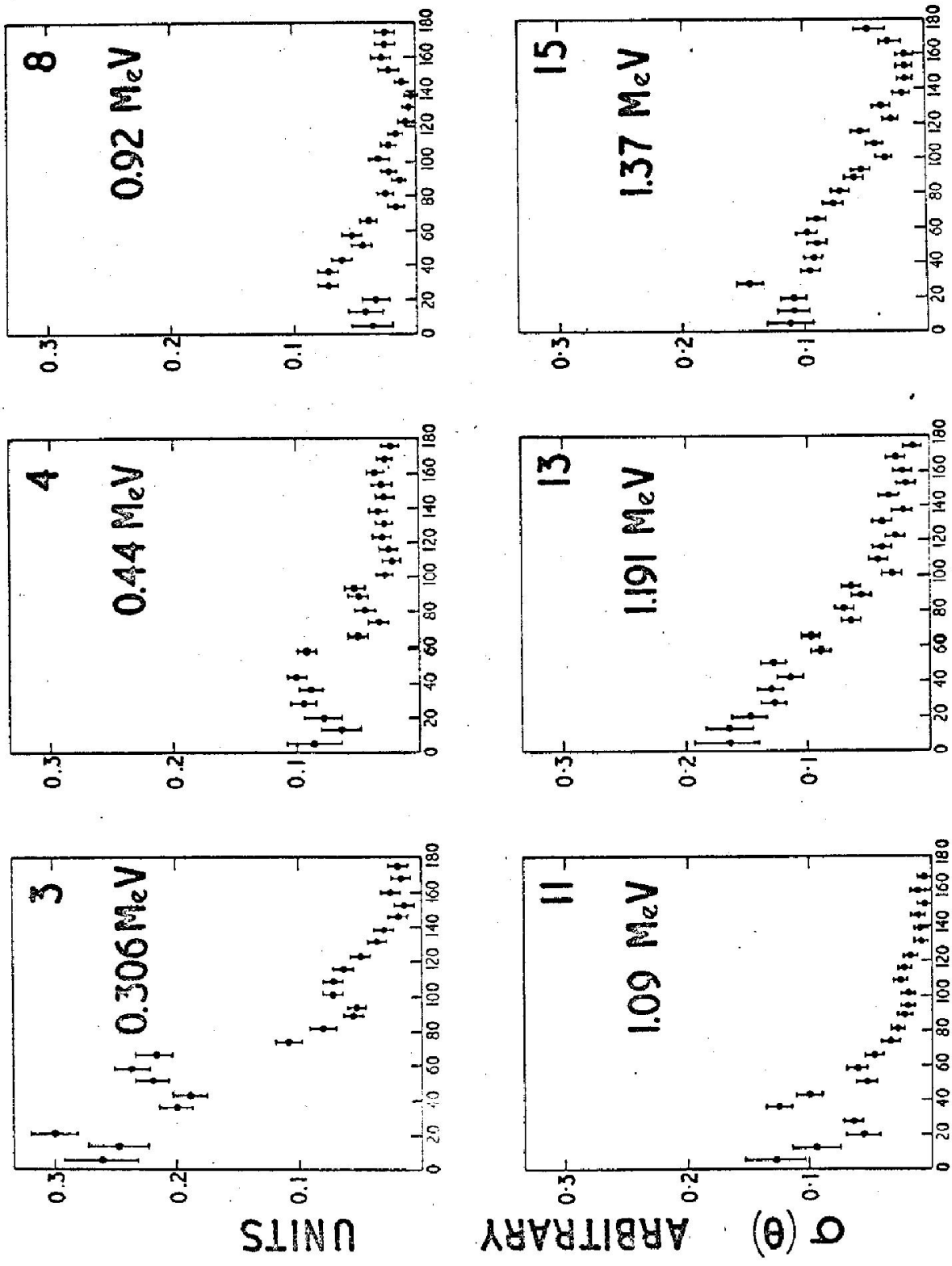

Fig. 4.5 *Proton distributions from $Se^{76}(d,p)Se^{77}$*

The curves shown were calculated from distorted wave theory with the proton optical model parameters equal to their measured values. The full line curves correspond to the measured deuteron parameters (Deuteron I) and the broken curves to the deuteron parameters which give best agreement with the ground state distribution (Deuteron II). The assumed *l*- values are indicated in the figure and are also summarised in Table 4.II.

The angular distribution for the 0.245 MeV state is shown in fig. 4.6. The broken curves were calculated with 'set II' deuteron parameters assuming $l = 1$ and $l = 3$ transitions. It is clear that neither alone is able to account for the observed distribution, but reasonable agreement can be obtained if a mixture of these two transitions is assumed with peak amplitudes in the ratio 1.9:1, respectively. The combined distribution is given by the full curve.

Since Se^{76} has zero spin the stripping selection rules require the spins of the final states to be $l \pm 1/2$. Considerable restriction is therefore place on the possible spin-values and in the special case of $l = 0$ transitions these are uniquely determined to be 1/2. The spin-parity values determined in this investigation are listed in Table 4.II together with the values obtained from previous measurements [71].

Since the absolute cross-sections could not be determined it was only possible to obtain the relative reduced widths for the various states. Values of (2J+1)S are given in the final column of table 4.II, with the ground state value taken to be unity.

4.5 Discussion

4.5.1 Level Properties

From Table 4.II it is seen that excitation energies of the states in Se^{77} obtained in the present work are in good agreement with previously measured values, with but one exception. The first excited state observed in this investigation is at 0.177 ± 0.003 MeV whereas earlier work [72] placed the first state at 0.1616 ± 0.0005 MeV. This was determined by Rutledge et al. [72] by measuring the energy of the conversion electrons emitted following the decay of the 17.5 sec. isomeric state of Se^{77}. Since the other level determinations are in agreement (within their quoted limits) with previous measurements, it would appear at first that there exist two states at approximately the same energy. However, there is no evidence in this work of any other state in the region of 170 keV excitation other than that already observed. Appreciable broadening of the proton group would have been seen for a separation in excess of 10 keV with an intensity of about ten per cent of the main peak.

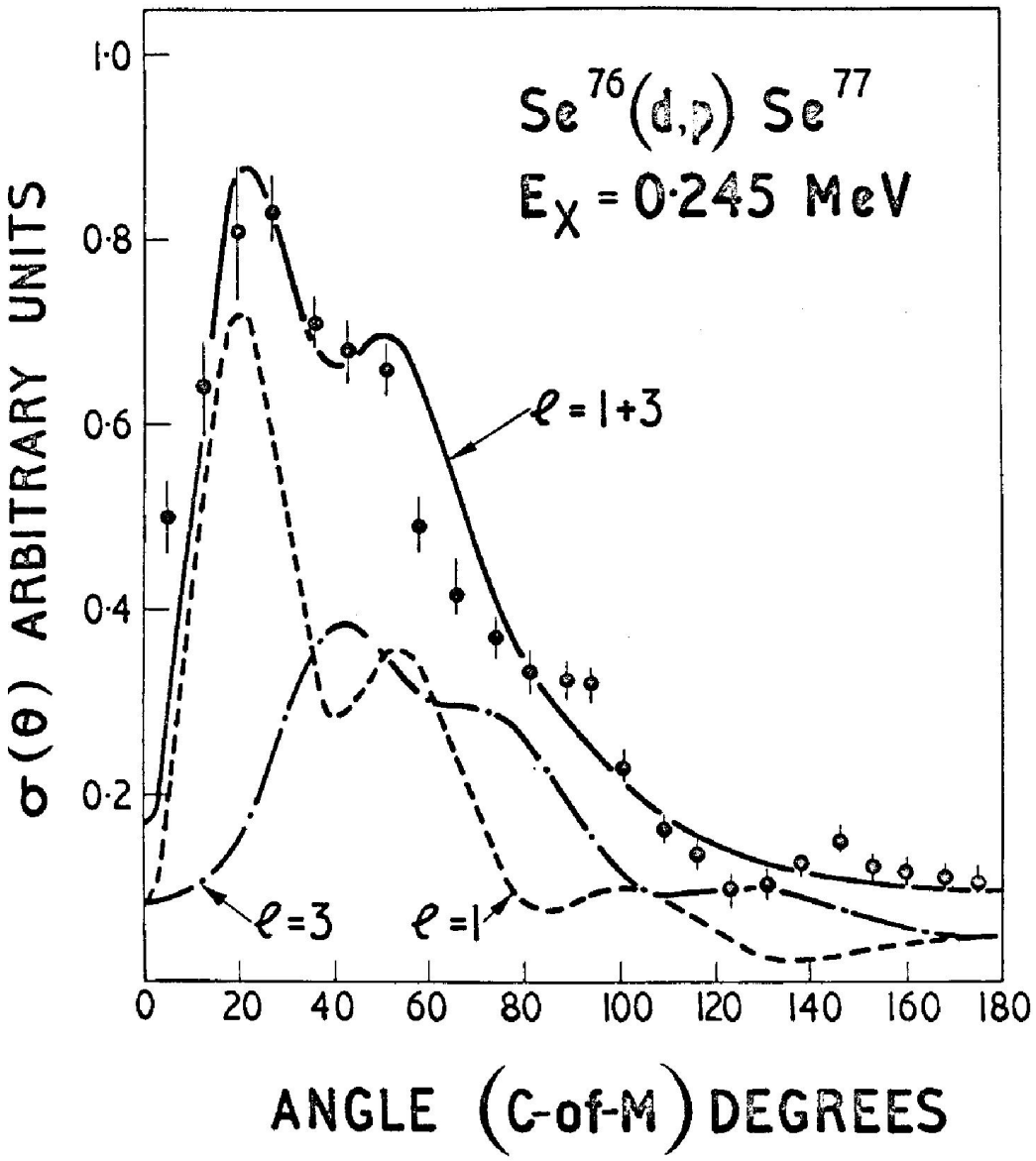

Fig. 4.6 *Proton distribution from the second excited state of* Se^{77}

Previous information on the Se^{77} level scheme has come from studies of the β-decay of Br^{77} [73] and As^{77} [74], (n,γ) capture measurements [72] and coulomb excitation studies [75]. The spins and parities obtained from these investigations are compared with the present results in Table 4.II. Agreement is had in all cases although in the present work there is some ambiguity in the assignment to the 0.177 MeV state. It is evident from fig. 4.4 that the distribution for this level could correspond to either an $l = 3$ or $l = 4$ transition, although the latter is probably preferred. If $l = 4$ is assumed then a spin-parity of $7/2^+$ or $9/2^+$ is required which is consistent with the earlier $7/2^+$ assignment.

The level at 0.245 MeV has previously been reported as a possible doublet [71, 73]. Strong evidence in support of this is obtained from the present distribution for this state, which can only be fitted if a combination of $l = 1$ and $l = 3$ transitions is assumed. These would require spins and parties of $1/2^-$ or $3/2^-$ and $5/2^-$ or $7/2^-$, respectively, which are compatible with the previous $3/2^-$ and $5/2^-$ assignments.[71] No broadening of the proton group from this doublet could be observed and an upper limit of 10 keV may be placed on the separation of the member states.

On comparing the relative values of (2J + 1)S for transitions to the different states, the strength of the (assumed) $l = 4$ transition (to the 0.177 MeV state) and $l = 3$ transition (to the 0.245 MeV state) suggest reasonably pure single particle excitations in the 1g and 1f shells. The appearance of several low-lying states with $l = 1$ and $l = 2$ orbitals may, however, indicate considerable residual state interactions between these states which distributes the single particle widths over several levels.

4.5.2 Angular Distributions

It is evident from fig. 4.4 that, in most cases, best agreement with the measured proton distributions is obtained with 'set II' deuteron parameters. These parameters also give a good account of the observed deuteron elastic scattering from Se^{76}. In the case of the two $l = 0$ transitions (0.956 and 1.134 MeV states), only the full curves which correspond to the measured parameters have been shown, since for these the two sets of deuteron parameters give nearly identical results.

With only a relatively small variation of Q-value between the states there is a considerable range of angular momentum transfer in the reaction. Furthermore, with increasing *l*-value the fit to the observed proton distributions deteriorates and their shapes become more sensitive to the distorting parameters. This latter effect is more evident in fig. 4.7 where a comparison is made

between the calculations for l = 1, for the ground state transition, and l = 3, corresponding to the 0.177 Mev state, with various deuteron parameters. The curves have been normalised to the same peak cross section.

Although the position of the main stripping peak for the l = 1 case is more or less unaffected by the changes in distorting parameters, it can be shifted by several degrees by the same changes for l = 3. It may also be noted that, in both cases, increasing either U or r_o causes the diffraction maxima in the distributions to move to smaller angles, the extent of the movement depending on the angular position. Even with these trends it has nevertheless been possible to assign unambiguous l-values to all but the distribution for the 0.177 MeV state.

There are several interesting features concerning the three l = 2 transitions to the levels at 0.682, 1.258 and 1.424 MeV. Firstly, the two higher excited state distributions both exhibit a small peak at 0^o which might at first seem to suggest a small admixture of l = 0. However, the distorted wave calculations show that such a rise can be associated with l = 2 alone and it is unnecessary to assume mixed transitions. Bethe and Butler [76] have suggested that in a case where, for example, l = 2 is favoured by a shell model configuration and l = 0 and 2 are allowed by the stripping selection rules, a study of the stripping reaction could provide information on the purity of the configuration. These examples clearly show the care necessary in interpreting such stripping patterns and that forward peaking with l = 2 distributions need not necessarily imply mixed configurations.

Secondly, although the distributions for the 0.682 and 1.258 MeV states are very similar, they differ markedly in shape from that for the 1.424 MeV state. Specifically, the latter is much more sharply peaked and has a less prominent secondary maximum at about 50^o than the two others. It seems reasonable to suppose that, if these states differ in spin, the different distributions could be due to spin dependence of the distorting potentials.

Using a fully spin-dependent programme for stripping, Macefield [35] has investigate the sensitivity of the l = 2 distributions to spin orbit forces in the deuteron and proton distortions. The spin-orbit potential was assumed to be real and of the Thomas-Fermi form, i.e.

$$-\frac{V_{so}}{r}\frac{df(r)}{dr}\bar{l}.\bar{\sigma}$$

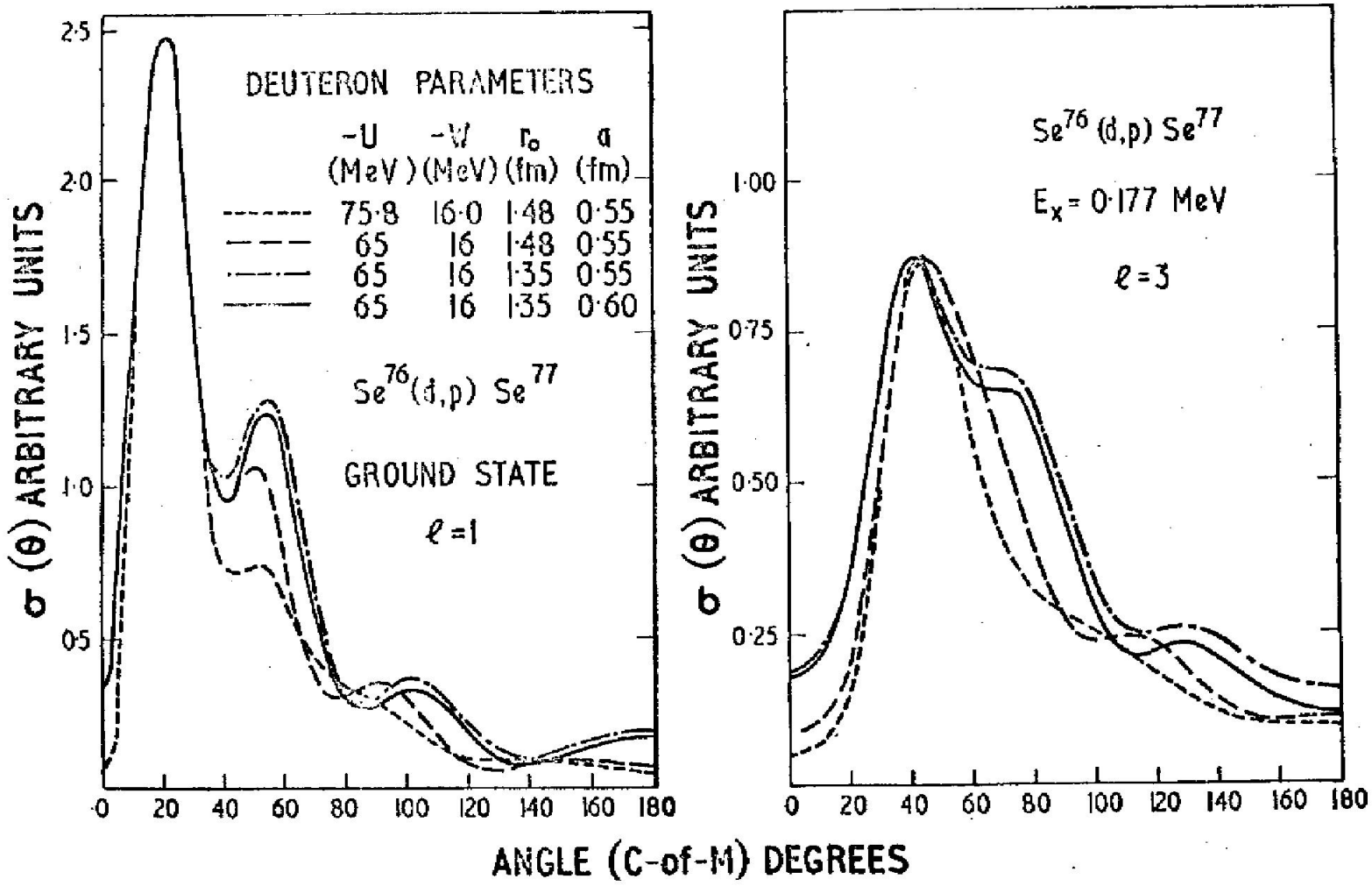

Fig. 4.7 *Effect of deuteron parameters on l=1 and l=3 distribution shapes*

where f(r) is the Saxon-Woods radial form for the central potential. The inclusion of such a term in the proton potential was found to have little effect on the distributions. Deuteron spin-orbit forces, however, were found to have a more marked effect. Figure 4.8 shows the effect on the 1.258 MeV distribution of including a deuteron spin-orbit potential of strength 4 MeV. It is evident that the cross sections at 0° for J = 3/2 and J = 5/2 now differ by some 30% and this is just the difference observed experimentally between the 1.258 and 1.424-MeV level distributions. The difference in excitation of these states is sufficiently small that kinematical differences in the distributions are negligible. Unfortunately, there are no data yet available from which the strength of the spin-orbit force in this reaction may be determined.

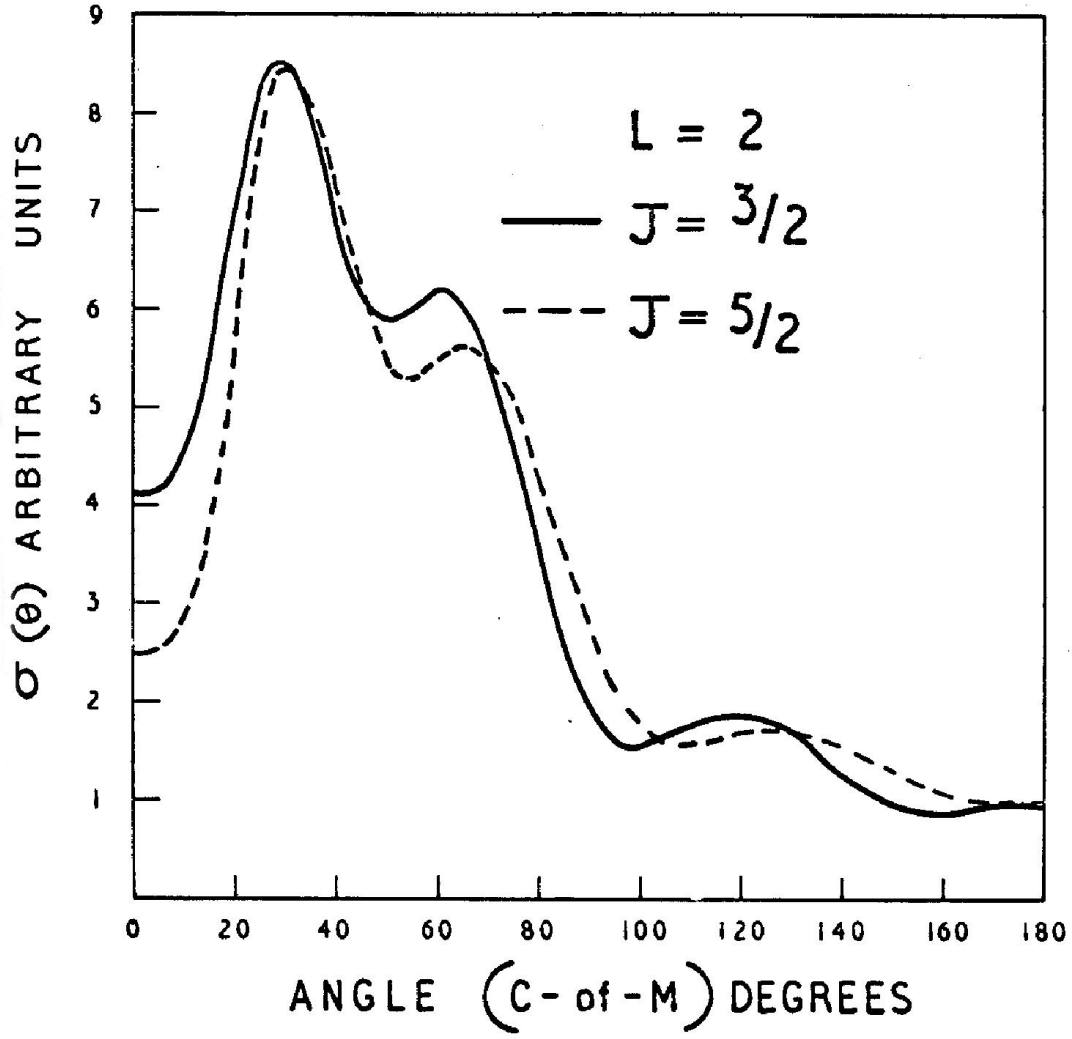

Fig. 4.8 *Effect of including a deuteron spin-orbit potential for the 1.258 MeV distribution*

No attempts have been made to fit the angular distributions of the weak states with distorted wave theory, since these are of low intensity and not strongly anisotropic. There is a possibility that some may be due to other selenium isotopes in the target since owing to the small proportional differences in masses these cannot be distinguished from the Se^{77} groups. However, this is considered unlikely since only the strong groups from impurity isotopes would be seen and these would be expected to show typical stripping distributions. It is therefore concluded that these weak groups do arise from the $Se^{76}(d,p)Se^{77}$ reaction, and probably correspond to states having relatively complex configurations not easily excited by stripping.

4.6 Conclusion

Excellent agreement has in general been obtained between distorted wave theory and the measured distributions for the intense transitions in $Se^{76}(d,p)Se^{77}$. The deuteron and proton optical model parameters used in these calculations are also found to be entirely consistent with those required to describe the deuteron and proton elastic scattering data. However, since at this energy the deuteron scattering is less sensitive to the nuclear distortions than stripping this restricts any quantitative estimates of the equality or otherwise of these distortions in the two processes. It would be interesting to carry out a similar investigation at a higher deuteron energy or with a lighter mass target where greater sensitivity of the elastic scattering to the distortions may be expected. It also seems not essential to measure the proton elastic scattering at precisely the energy appropriate to the (d,p) study, since the stripping distributions are not strongly dependent on the proton distorting parameters.

The agreement between D.W.B.A. theory and the measured distributions becomes progressively worse as the orbital angular momentum exchange in the reaction increases. This is probably attributable in part to the increased sensitivity of the higher *l*-value distributions to the optical parameters.

Finally, there is some evidence that spin-dependent interactions can have an observable effect on the shape of the angular distributions, particularly at small angles.

C H A P T E R V

A STUDY OF (t,p) REACTIONS IN LIGHT NUCLEI

5.1 Introduction

Considerable interest has recently centred on reactions involving the transfer of two nucleons. Theoretical treatments of the double stripping reaction mechanism have been given by a number of authors [24, 30, 40, 41] and the plane wave formalism and double stripping selection rules have already been referred to in Section 1.5.

Most early experimental investigations of two-nucleon stripping were carried out with (He^3,p) reactions, usually at energies less than 5 MeV [77-79]. As pointed out by Bromley and Almqvist [80], at these energies the reaction mechanism is usually a mixture of compound and direct processes having comparable amplitudes. Interference between these amplitudes then makes detailed analysis of the angular distribution data extremely difficult. More recently, however, considerable experimental data have accumulated (e.g. refs 36-38) which strongly suggest that at energies between 5 and 10 MeV the direct reaction mode begins to dominate, and in several cases the angular distributions have been well accounted for by plane wave double stripping theory.

Very few experimental studies have been reported on the (t,p) reaction although some have been made, notably by Holmgren and Wolicki [81] at energies below 2.4 MeV, by Jaffe et al [82] at 5.5 MeV and by Pullen et al [42] at 10 MeV. From these few studies it is apparent that, as for (He^3,p), there is again considerable competition between compound nucleus and direct interaction processes at energies up to about 5 MeV, with the latter beginning to dominate at higher energies.

In many respects the (t,p) reaction is more interesting than (He^3,p). For example, the two neutrons must be captured with S = 0 in the (t,p) double-stripping process whereas in (He^3,p) S can be either 0 or 1. This results in more stringent selection rules for (t,p) double stripping and in the case of zero-spin target nuclei the spins and parities for the final nuclear states are uniquely defined. A second advantage of the (t,p) reaction over (He^3,p) is that coulomb distortion is less owing to the lower charge of the triton and therefore plane wave theory should be a better approximation. Also, since two neutrons are transferred in the reaction this results in the formation of highly neutron rich nuclei which are not easily accessible by other reactions. As for He^3, the large mass excess of the

triton generally gives rise to high (t,p) reaction Q-values, thus facilitating the study of highly excited states.

The paucity of experimental data on the (t,p) reaction and its advantages over other reactions clearly demanded a close study to be made of this process. In this chapter, the results of a systematic study of the reaction are presented for target nuclei B^{10}, B^{11}, C^{12}, C^{14}, O^{16}, O^{18}, Si^{28}, Si^{29} and Ca^{40}. In general, incident energies of about 10 MeV have been used although in some cases a wider energy range was employed.

The investigation was carried out using tritons from the Aldermaston Tandem accelerator and the proton distributions from the (t,p) reactions were measured with the multi-channel spectrograph. The plane wave double stripping theory of Newns [41] (section 1.5) has been used throughout in the analysis of the distributions.

5.2 Targets

The B^{10} and B^{11} targets were prepared by evaporation of the enriched metals 99.2% and 98.6% respectively) as previously described (Section 3.2). In the case of B^{11} a thin carbon backing film (approximately 10 μgm cm^{-2}) was used which also enabled measurements to be made of the higher excited states of C^{14} formed in the $C^{12}(t,p)C^{14}$ reaction. The targets were found by direct weighing to have surface densities of 54 ± 10 μgm cm^{-2} (B^{10}) and 48 ± 10 μgm cm^{-2} (B^{11}).

The method of fabrication of the C^{14} target is described in Appendix A. The total target thickness was estimated to be approximately 150 μgm cm^{-2}.

Targets of O^{18} were prepared by evaporating tungsten oxide enriched in O^{18} directly on to a thin carbon backing film, a procedure first described by Muggleton and Howe [(83)]. The final target contained approximately equal proportions of O^{16} and O^{18} and so served also as an O^{16} target. A precise mass analysis of the target was later made from measurements of the elastically scattered tritons and this yielded, for the O^{16} and O^{18} masses, the values 4.0 μgm cm^{-2} and 5.1 μgm cm^{-2}, respectively.

A self-supporting target containing approximately equal amounts of Si^{28} and Si^{29} was prepared by the evaporation of silicon dioxide enriched in the mass-29 isotope. The total target surface density was estimated to be about 60 μgm cm^{-2}.

In the case of Ca^{40} it was required to measure separately the (t,p) reaction and the elastic triton scattering using the same target. In this case it was not possible to use a metallic calcium target in view of its rapid oxidation and subsequent deterioration when exposed to the atmosphere

between the two measurements. A more suitable material for this study was found to be calcium fluoride, and a target of this compound was prepared by evaporating the material on to a thin carbon backing film. The Ca^{40} mass was determined from the triton scattering measurements to be 56 ± 5 μgm cm^{-2}.

5.3 The reactions $B^{10}(t,p)\ B^{12}$ and $B^{11}(t,p)\ B^{13}$

5.3.1 Results

(a) $B^{10}(t,p)B^{12}$: This reaction has previously been studied at 5.5 MeV by Jaffe et al [82] who obtained a value of 6.346 MeV for the Q-value. The present investigation was carried out at 10.0 MeV and a typical proton energy spectrum, measured at 27.50°, is shown in fig. 5.1. Proton groups corresponding to states in B^{12} are labeled numerically and were identified by their characteristic energy variation with angle. The principal contaminant groups are seen to be due to the presence of O^{16} in the target. The proton continuum observed at energies below 12.2 MeV may be attributed to the three-body break-up process $B^{10}(t,pn)B^{11}$ (Q = 2.98 MeV), B^{12} being unstable with respect to neutron emission at excitations above 3.37 MeV.

No new states of B^{12} were observed in the present work. The widths of most of the proton groups corresponding to the virtual states were in general found to be greater than the instrumental width of 15 keV. Thus measurements of these widths were made directly from the spectra at five angles between 20° and 50° and the mean values are given in Table 5.I, together with the most recently published values from Ajzenberg-Selove and Laurtisen [54]. Agreement is had within the quoted limits for all except the 5.00 MeV level. However this was only relatively weakly excited in the $B^{10}(t,p)B^{12}$ reaction and the present value is rather uncertain. Jaffe et al [82] observed a width of 50 keV for the 4.51 MeV level which conflicts both with the present value and that observed by Bockelman et al [84] from neutron resonance scattering measurements on B^{11}.

Angular distributions were measured for all proton groups and these are shown in fig. 5.2. The absolute differential cross-sections are accurate to ±25%. In general these are very low and only significantly exceed 1mb/steradian for the 5.61 MeV level. With the exception of the levels at 4.30 and 5.00 MeV, the distributions are all predominantly forward peaked and double stripping plane wave fits to these are shown by the curves in the figure. In all cases these were calculated for a radius of interaction of 5.0 fm which was found to give best overall agreement to the measured distributions. The L-values and corresponding spin-parity assignments are summarised in Table 5.I. Also listed for comparison are the spins and parities obtained from previous work [54].

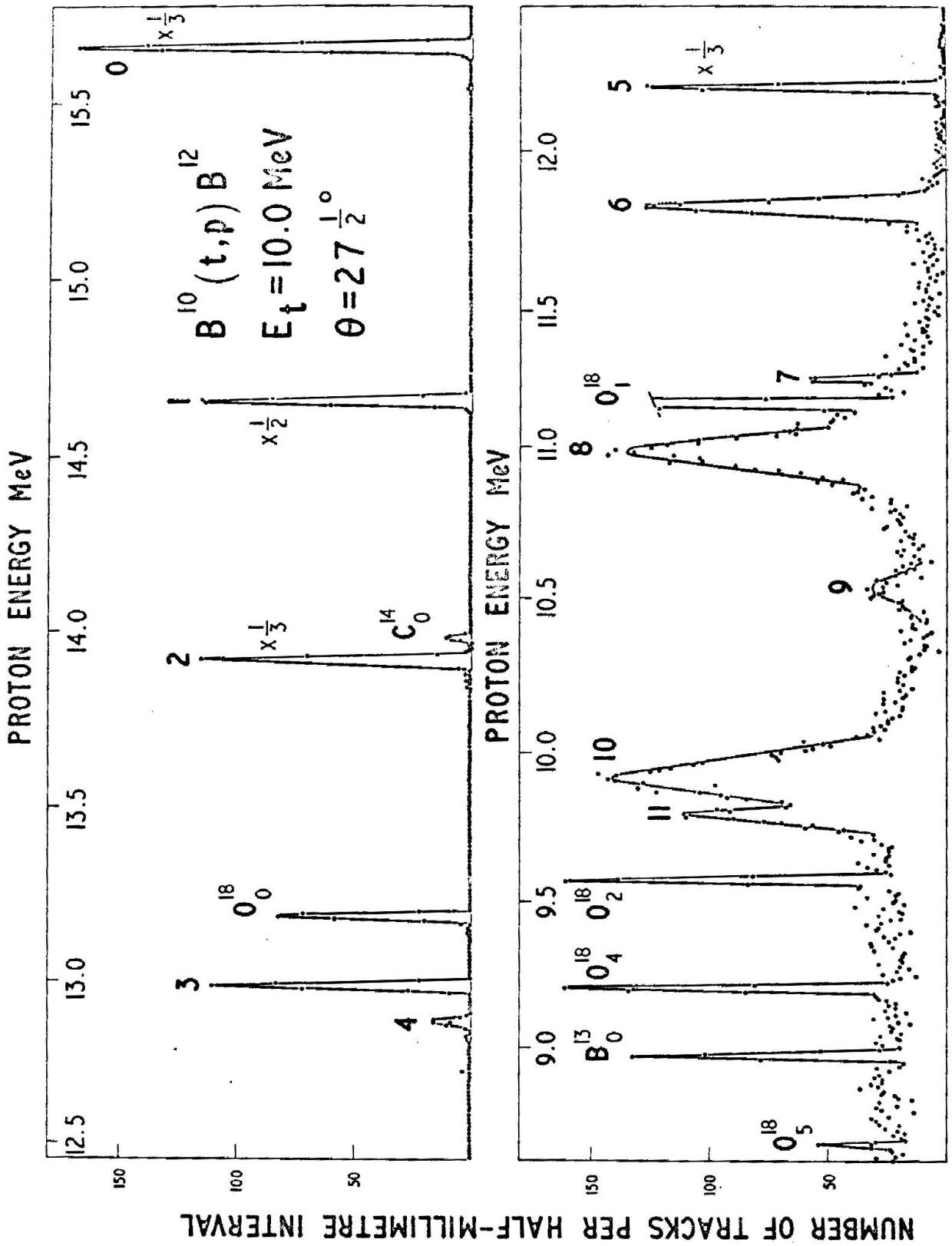

Fig. 5.1 *Proton spectrum from $B^{10}(t,p)B^{12}$*

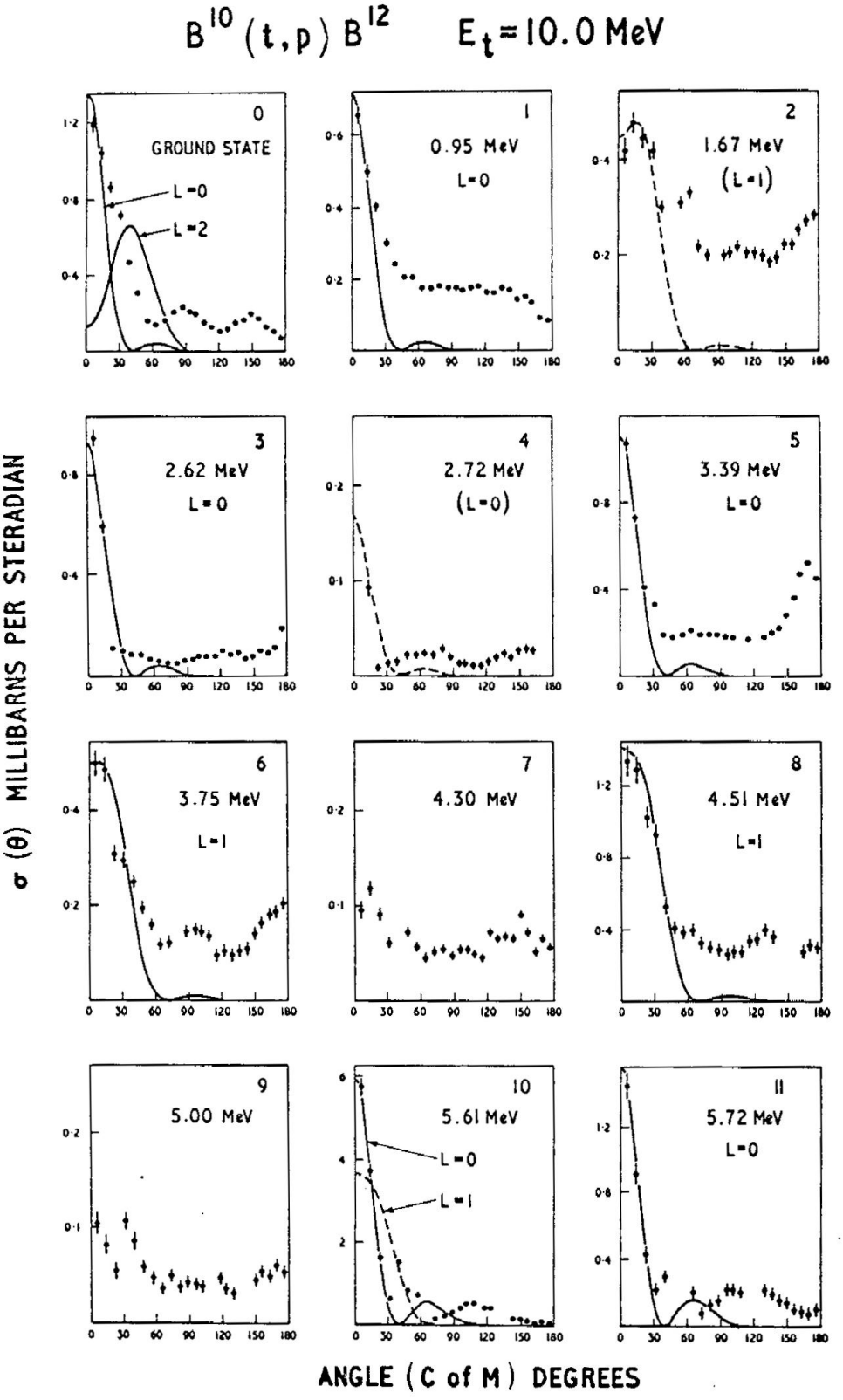

Fig. 5.2 *Proton angular distributions from $B^{10}(t,p)B^{12}$*

T A B L E 5.I

L-values and Level Properties for B^{12} from $B^{10}(t,p)B^{12}$

Group	Excitation Energy (MeV) (a)	Γ		L	J^{π}	
		(b)	(a)		(b)	(a)
0	0					1^+
1	0.95			0	3^+	$(2^+,3^+)$
2	1.67			(1)	$2^-,3^-,4^-$	$1^-,2^-$
3	2.62			0	3^+	
4	2.72			(0)	(3^+)	
5	3.39			0	3^+	$\leq 3^+$
6	3.75	42 ± 5	40 ± 5	1	$2^-,3^-,4^-$	2^+
7	4.30	<15	10 ± 4	weak		1^-
8	4.51	100 ± 15	~100	1	$2^-,3^-,4^-$	3^-
9	5.00	130 ± 40	60 ± 20	weak		1
10	5.61	120 ± 20	120 ± 40	0	3^+	2
11	5.72	70 ± 20	60 ± 20	0	3^+	3

(a) Ajzenberg-Selove and Lauritsen [54]

(b) Present work

Since the spins and parities of B^{10} and B^{12} are respectively, 3^+ and 1^+ the double stripping selection rules require the ground state transition to proceed with orbital angular momentum transfer L = 2. (L = 4 is also allowed by the selection rules but the expected shell model configuration for B^{12} prohibits this since both neutrons would have to be captured into the 1d-orbit). However, the predicted maximum in the L = 2 distribution occurs at 40° whereas the observed distribution peaks at 0°. Agreement with L = 2 could only be obtained if an unphysically large value of 8.0 fm were assumed for the interaction radius. Also shown in the figure for comparison is the calculated L = 0 distribution.

The first excited state distribution is best fitted assuming L = 0 capture of the neutron pair but agreement is again not very satisfactory. This transition would require a spin-parity of 3^+ for this state, however, which is consistent with the previous assignment [54] of 2^+ or 3^+. The distribution for the 1.67 MeV level does not exhibit a well developed stripping pattern. The known spin-parity of 1^- or 2^- would require L = 3 or L = 1, respectively, and the latter is shown by the broken line curve in the figure. This gives reasonable agreement only out to 30° and the L = 1 assignment must be regarded as very tentative.

The distributions for the states at 2.62, 3.39, 5.61 and 5.72 MeV can all be well accounted for in the region of the forward peaks with L = 0. This results in an unambiguous assignment of 3^+ for these states which only conflicts with previous values in the case of the 5.61 MeV level. There is also some evidence that the 2.72 MeV level is formed by L = 0. However, this is rather uncertain since the important measurement at 5° could not be obtained owing to interference at this angle with the proton group from the $0^{16}(t,p)0^{18}$ ground state transition. Also, the differential cross-section is unusually small for an L = 0 transition.

The 3.75 and 4.51 MeV distributions are both formed by L = 1 which requires 2^-, 3^- or 4^- for these states. This is consistent with the previous 3^- assignment for the higher excited state but conflicts with the reported spin-parity of 2^+ [84] for the 3.75 MeV level.

(b) $B^{11}(t,p)B^{13}$ Muto, Barros and Jaffe [85] have previously studied this reaction at 5.5 MeV but owing to the relatively high excitation of the first excited state of B^{13}, and also the low reaction Q-value, measurements were confined to the ground state. Their value for the Q-value was determined to be -0.233 MeV. In the present investigation 11.0 MeV tritons were used which enabled several excited states to be observed in addition to the ground state. Fig. 5.3 shows a typical proton energy spectrum measured at an angle of 35^o and groups corresponding to states in B^{13} are labeled numerically. A number of groups corresponding to states in C^{14} were also identified. These arose due to the use of carbon as a target backing material. The proton continuum, which extends over the entire spectrum, can be attributed to the reactions $B^{11}(t,pn)B^{12}$ (Q = -5.12 MeV) and $C^{12}(t,pn)C^{13}$ (Q = 3.54 MeV). For convenience of presentation, the B^{13} ground state group is not shown in the spectrum owing to the rather large energy separation from the first excited state group.

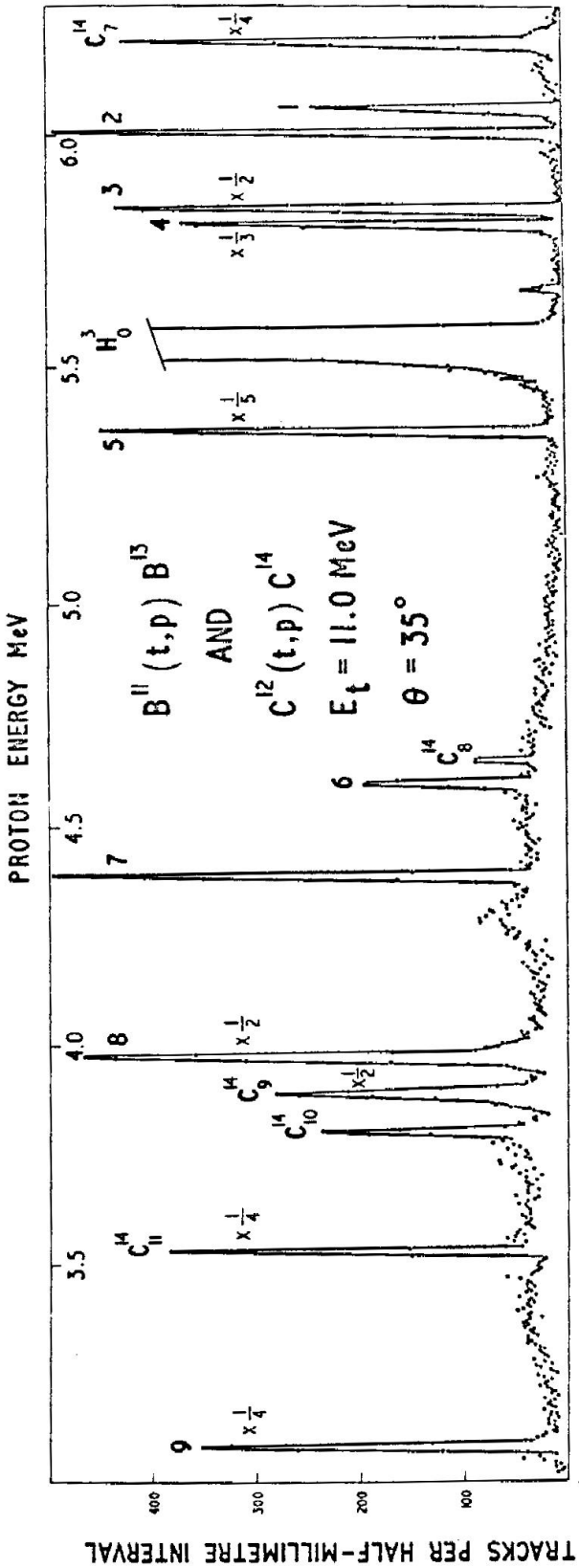

Fig. 5.3 *Proton spectrum from $B^{11}(t,p)B^{13}$*

Listed in Table 5.II are the excitation energies of the first nine excited states of B^{13}. These are the mean values of at least five determinations made at different angles, except for group-9 which was observed at only the first three angles. Also listed are the level energies obtained by Morrison and Galey [86] using the $Li^7(Li^7,p)B^{13}$ reaction. Although the states in B^{13} above 4.88 MeV are unstable with respect to neutron emission, only the 5.38 MeV level was observed to have any appreciable excess width and this was estimated to be 15 ± 5 keV. It is concluded that the remaining virtual states all have widths less than 10 keV.

T A B L E 5.II

L-values and Level Properties for B^{12} from $B^{10}(t,p)B^{12}$

Group	Excitation Energy (MeV)		L	J^{π}
	(a)	(b)		
0	0	0	0	3/2-
1	3.483±0.005		1	$1/2^+,3/2^+,5/2^+$
2	3.533±0.005		2	$1/2^-,5/2^-,7/2^-$
3	3.681±0.005		1	$1/2^+,3/2^+,5/2^+$
4	3.712±0.005	3.70±0.05	2	$1/2^-,5/2^-,7/2^-$
5	4.13±0.01	4.16±0.05	2	$1/2^-,5/2^-,7/2^-$
6	4.82±0.01		weak	
7	5.01±0.01	5.05±0.08	1	$1/2^+,3/2^+,5/2^+$
8	5.38±0.01	5.5 ±0.1		
9	6.17±0.02			

(a) Present work

(b) From Morrison and Galey [86]

Angular distributions of the ground and first seven excited states, except the sixth, are shown in fig. 5.4. No distribution was measured for this state since it was consistently observed to be only weakly excited and superimposed on a large continuous background. The higher excited state groups could not be recorded at large angles owing to their rapid energy variation with angle and the eighth and ninth excited states were only observed out to 50°.

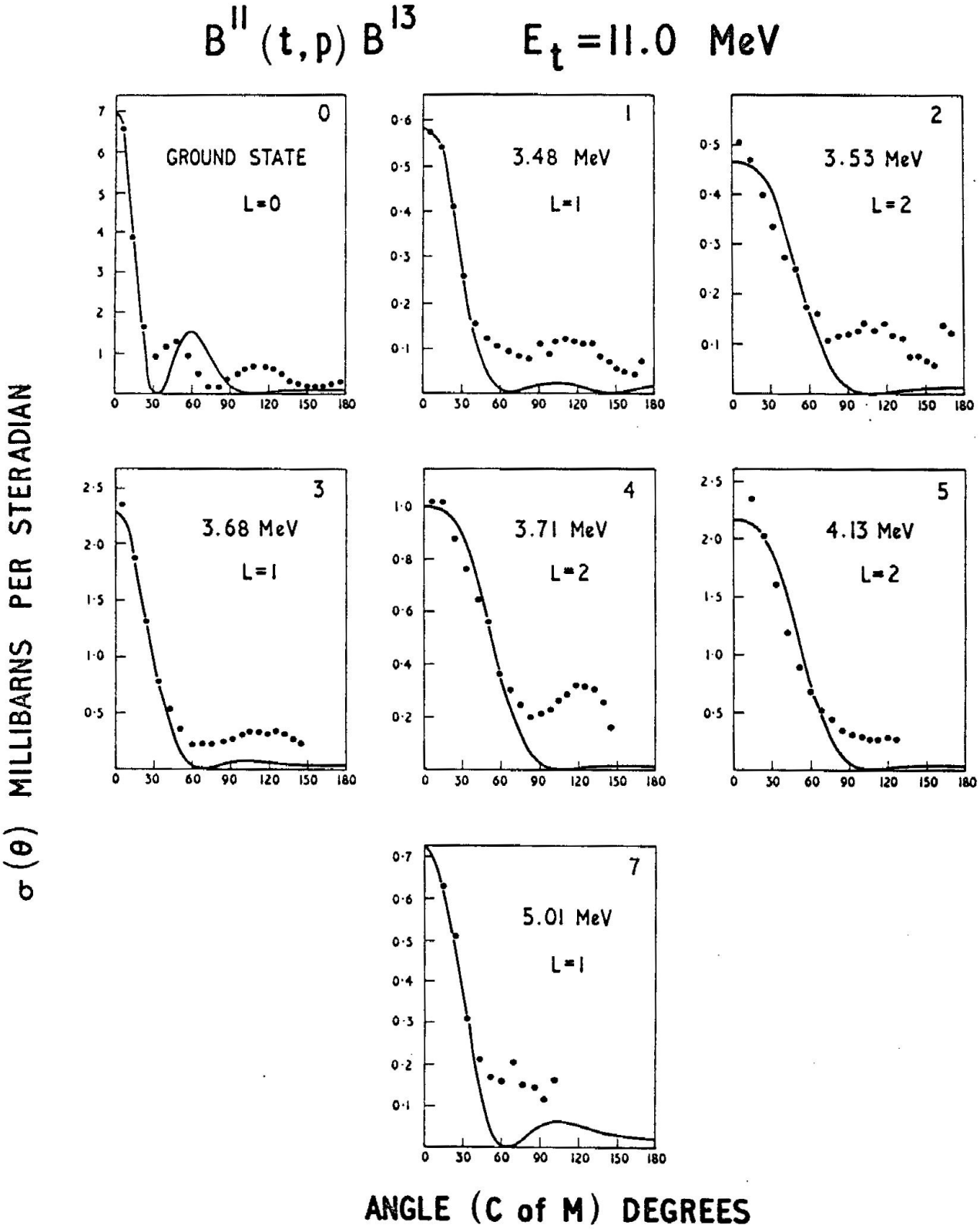

Fig. 5.4 *Proton angular distributions from $B^{11}(t,p)B^{13}$*

The curves shown in fig. 5.4 were again calculated from plane wave theory for an interaction radius a = 5.0 fm. Both L = 1 and L = 2 distributions are observed to peak at 0° owing to the negative Q-values for all transitions and the rather high bombarding energy. In most cases agreement is good in the region of the stripping peaks and the required L-values are summarized in Table 5.II, together with the corresponding spin-parity assignments. Although the 3.53, 3.71 and 4.13 MeV states are all formed by L = 2 transitions, and the double stripping selection rules allow final spins $1/2^-$, $3/2^-$, $5/2^-$, or $7/2^-$, the $3/2^-$ assignment has not been included. This is thought reasonable since a $3/2^-$ state should be preferentially excited by an L = 0 transition and no evidence for this was observed.

5.3.2 Discussion

In the case of the $B^{10}(t,p)B^{12}$ reaction, the agreement obtained with plane wave double stripping theory is generally rather unsatisfactory. This is particularly so for the ground state transition which should proceed with L = 2 capture of the two neutrons. In view of this, and also the rather low cross-sections observed, it appears that the double stripping process is not the predominant reaction mechanism. This may result from the relatively complex configuration of B^{10} which may not be simply related to these states in B^{12}.

An exception to this however is the L = 0 transition to the 5.61 MeV level which is much more strongly excited than any other, with a peak differential cross-section of 6 mb/steradian. It is probable that this state can be well described by a B^{10} ground state core with two extra-core neutrons. However, neutron resonance scattering measurements from B^{11} [84] suggest J = 2 for this state and this would require at least L = 1 (L = 2 if no parity change) in the present measurement. It is evident from fig. 5.2 that this gives no agreement with the observed distribution. Jaffe et al [82], in their study of the $B^{10}(t,p)B^{12}$ reaction, were only able to obtain agreement with L = 1 by using an unusually large radius of 7.0 fm, and it is likely that equally good agreement could have been obtained with L = 0 using a smaller radius.

In contrast to the $B^{10}(t,p)B^{12}$ reaction, proton angular distributions measured from $B^{11}(t,p)B^{13}$ are very well described by plane wave theory in the region of the stripping peaks, and spins and parities have been obtained for the ground and six excited states. No previous measurements of these level properties have been made, however, with which to compare the the present values. Only four excited states were previously known and these were observed by Morrison and Galey [86] using the $Li^7(Li^7,p)B^{13}$ reaction.

The β^- decay of B^{13} has recently been studied by Marques et al [87] who observed an allowed transition to the ground state of C^{13}. This is in accord with a spin-parity of $3/2^-$ for B^{13} as expected from the shell model, and also with the present work and that of Muto, Barros and Jaffe [85].

5.4 The Reactions $C^{12}(t,p)C^{14}$ and $C^{14}(t,p)C^{16}$

5.4.1 Results

(a) $C^{12}(t,p)C^{14}$: The use of carbon as a backing material for the B^{11} target enabled the excited states of C^{14} to be studied simultaneously with the $B^{11}(t,p)B^{13}$ reaction. One new level in C^{14} was observed (C_{11}^{14} in fig. 5.3) at 10.74 ± 0.02 MeV excitation. The proton group observed by Pullen et al. during a study of the $Be^9(t,p)Be^{11}$ reaction (Chapter 6), which was then thought to arise from the $C^{12}(t,p)C^{14}$ reaction can be attributed to this level.

Proton distributions corresponding to the ground state transition (Q = 4.641 MeV) were measured at 1 MeV intervals between 8 and 13 MeV using a self-supporting carbon target. The 6.09 Mev energy interval between the ground and first excited states of C^{14} enabled all exposures to be made on one set of nuclear plates. In this technique the spectrograph magnetic field was maintained constant throughout and successive exposures made at the various incident energies. The ground state distributions are shown in fig. 5.5. These are all strongly forward peaked, exhibiting no strong energy dependence, and are generally characteristic of a direct reaction mechanism. For clarity no theoretical curves are shown but the distributions can all be well described in the region of the forward peaks if zero orbital angular momentum transfer is assumed. This is consistent with the known spin-parity of 0^+ for C^{14}.

Angular distributions for the first seven excited states, measured at a triton energy of 11.0 MeV, are shown in fig. 5.6. The curves were calculated for a radius of interaction a = 5.5 fm and the full line curves correspond to the L-values required assuming the spin-parity values from previous measurements [54]. Since C^{12} has spin O^+, the spins and parities for the final states are uniquely determined by L.

In general the agreement is rather unsatisfactory and only in the case of the second excited state at 6.58 MeV is the L-value (L = 1) consistent with the previous spin-parity assignment [54, 82] of 1^-. The first excited state at 6.09 MeV is known to be 1^- from its observed γ-decay [88] and from the $C^{13}(d,p)C^{14}$ stripping reaction.[54] The $C^{12}(t,p)C^{14}$ reaction should therefore proceed with L = 1 to this state. It is evident from fig. 5.6, however, that this gives no agreement with the measured distribution which is best fitted with L = 2, as illustrated by the broken curve. This would imply 2^+

for this state in conflict with the accepted 1^- assignment. Agreement with L = 1 can only be obtained if an unacceptably small interaction radius of 3.0 fm is assumed.

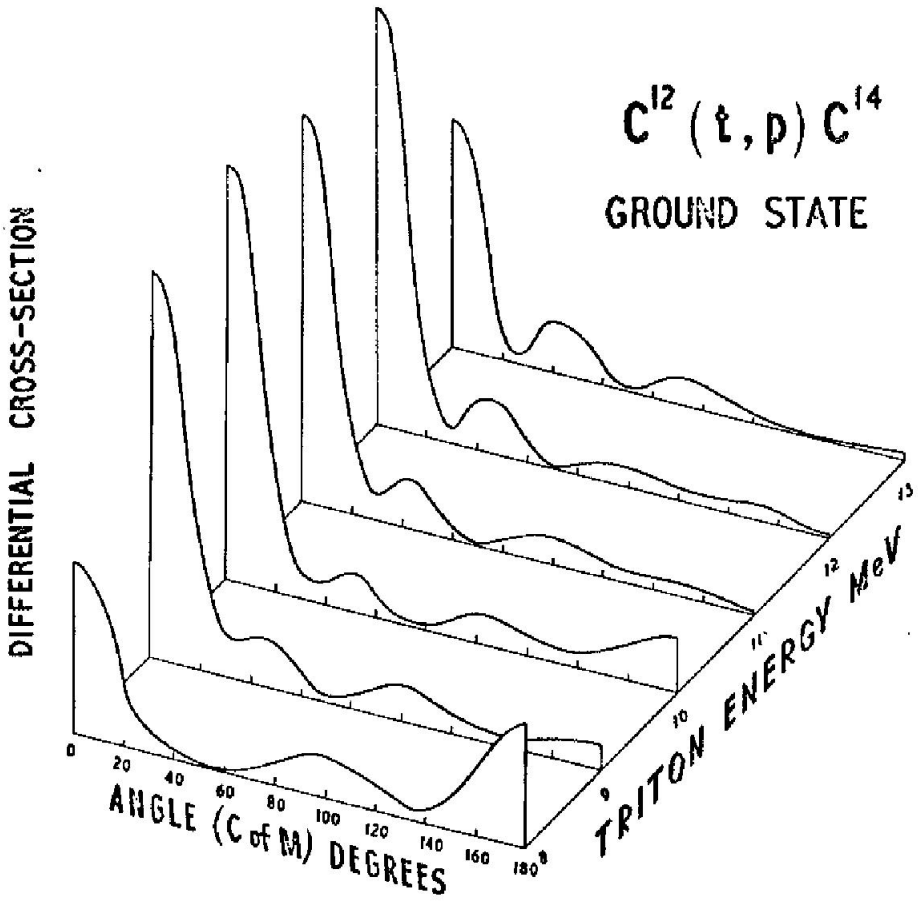

Fig. 5.5 *Proton distributions for ground state transition in $C^{12}(t,p)C^{14}$*

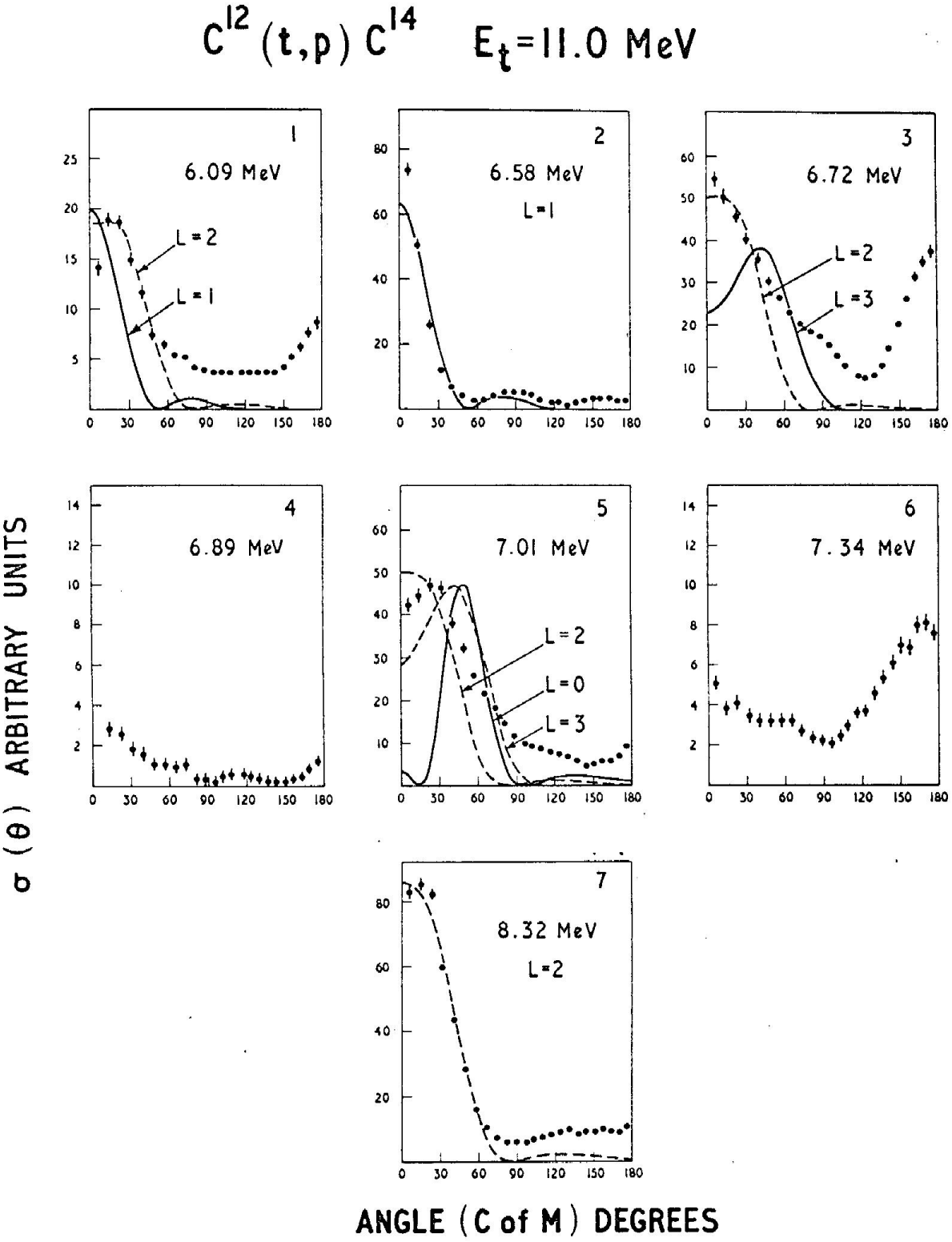

Fig. 5.6 *Proton angular distributions from $C^{12}(t,p)C^{14}$*

In Table 5.III the L-values giving best agreement with the present data are compared with those obtained by Jaffe et al [82] who studied this reaction at 5.5 MeV. Besides the first excited state there is also disagreement in the assignments to the 6.72 and 7.01 MeV levels. Jaffe et al observed these to be formed by L = 3 and L = 0 transitions, respectively, but as can be seen from fig. 5.6 very poor agreement is obtained with these L-values. Possible best agreement with the present results is had with L = 2 in both cases. However, agreement is still far from satisfactory and these L-values are regarded as very tentative.

T A B L E 5.III

L-values and Level Properties for C^{14} from $C^{12}(t,p)C^{14}$

Group	Excitation Energy (MeV) (a)	J^{π}	L	
			(b)	(c)
0	0	0^+	0	0
1	6.09	1^-	1	(2)
2	6.58	1^-	1	1
3	6.72	(3^-)	(3)	(2)
4	6.89	$0(^-)$	weak	weak
5	7.01	0^+	0	(2)
6	7.34	(2^-)	weak	weak
7	8.32			2

(a) Ajzenberg-Selove and Lauritsen [54]

(b) Jaffe et al. [82]

(c) Present work

The states at 6.89 and 7.34 MeV are only weakly excited and their angular distributions cannot be interpreted in terms of a direct reaction process. A possible explanation is that they have spins and parities according to the sequence 0^-, 1^+, 2^-, 3^+ etc which cannot be formed by double stripping since the required spin and parity selection rules cannot be simultaneously satisfied. Thus, the present observations are consistent with the reported [54] tentative assignments of 0^- and 2^-, respectively, for these states.

Recent neutron resonance scattering measurements from C^{13} by Cohn, Blair and Willard [89] suggest the 8.32 MeV level in C^{14} to be 1^+ which should, therefore, again not be excited by double stripping. However, in the present study this transition is observed to proceed strongly and excellent agreement with double stripping theory is obtained with L = 2. This would require a spin-parity of 2^+ for this state in conflict with the previous assignment.

(b) $C^{14}(t,p)C^{16}$: This reaction was first observed by Hinds, Middleton, Litherland and Pullen [90] using the Aldermaston single-channel spectrograph. The published account of this investigation is given in Appendix B. Only the ground state of C^{16} was observed in this work, and in view of the low reaction Q-value (-3.014 MeV) and the energy limitation of the accelerator it was not possible to measure its angular distribution. In the present investigation 12-MeV tritons were used, which enabled angular distributions to be measured for both the ground and first excited states.

A proton energy spectrum from this reaction, measured at 57.5°, is shown in fig. 5.7. The two groups corresponding to states in C^{16} are labeled numerically. Since the target was enriched to only about 40% in C^{14} several intense groups were also observed arising from C^{12}. The proton continuum which extends over the entire spectrum may be attributed to reactions with the gold target backing and also, for proton energies below about 6.4 MeV, to the $C^{12}(t,pn)C^{13}$ reaction.

The excitation energy for the first excited state, which was readily identified by its energy variation with angle, was measured at six angles and the mean value found to be 1.753 ± 0.012 MeV. The very small peaks observed in the background between the ground and the first excited C^{16} states in fig. 5.7 were not similarly observed at other angles. These probably arise from statistical fluctuations in the background. No other groups corresponding to states in C^{16} were observed up to an excitation of 3.8 MeV with peak intensities greater than 8% that of the ground state.

Angular distributions for the ground and first excited states are shown in fig. 5.8 together with the results of double stripping calculations. Two curves are shown for the ground state distribution, both calculated for L = 0 as expected from the shell model. The broken line curve, calculated with a = 5.5 fm which is the interaction radius normally required for this mass region, gives no agreement at all. This curve is seen to exhibit only the second maximun of the spherical Bessel function of zero order whereas the observed distribution is strongly forward peaked. This behaviour is discussed later and probably arises from an inadequacy of the plane wave theory for L = 0 transitions proceeding with very negative Q-values. By reducing the radius to 4.0 fm the

primary peak of the spherical Bessel function is suitably restored, as illustrated by the full line curve.

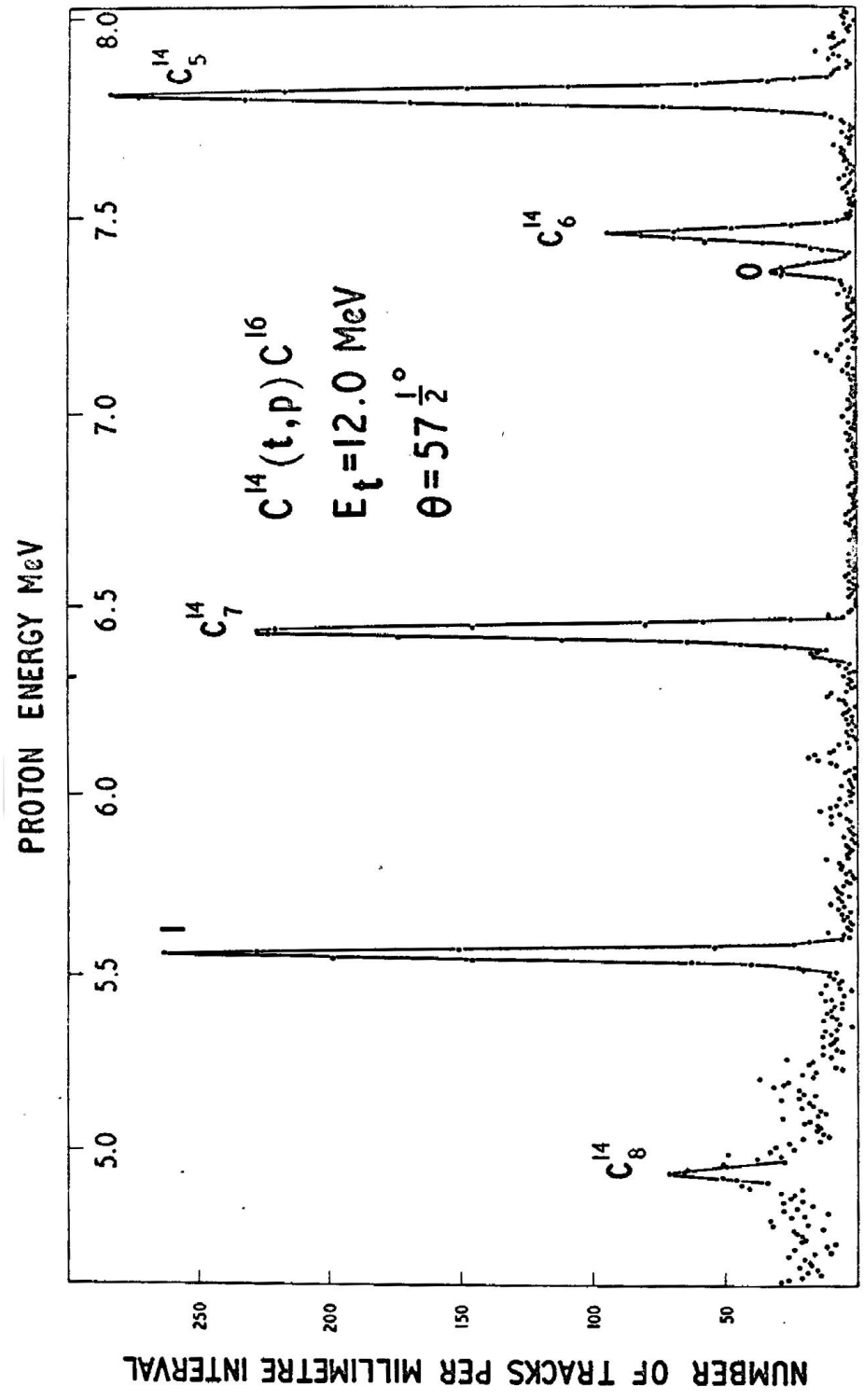

Fig. 5.7 *Proton spectrum from $C^{14}(t,p)C^{16}$*

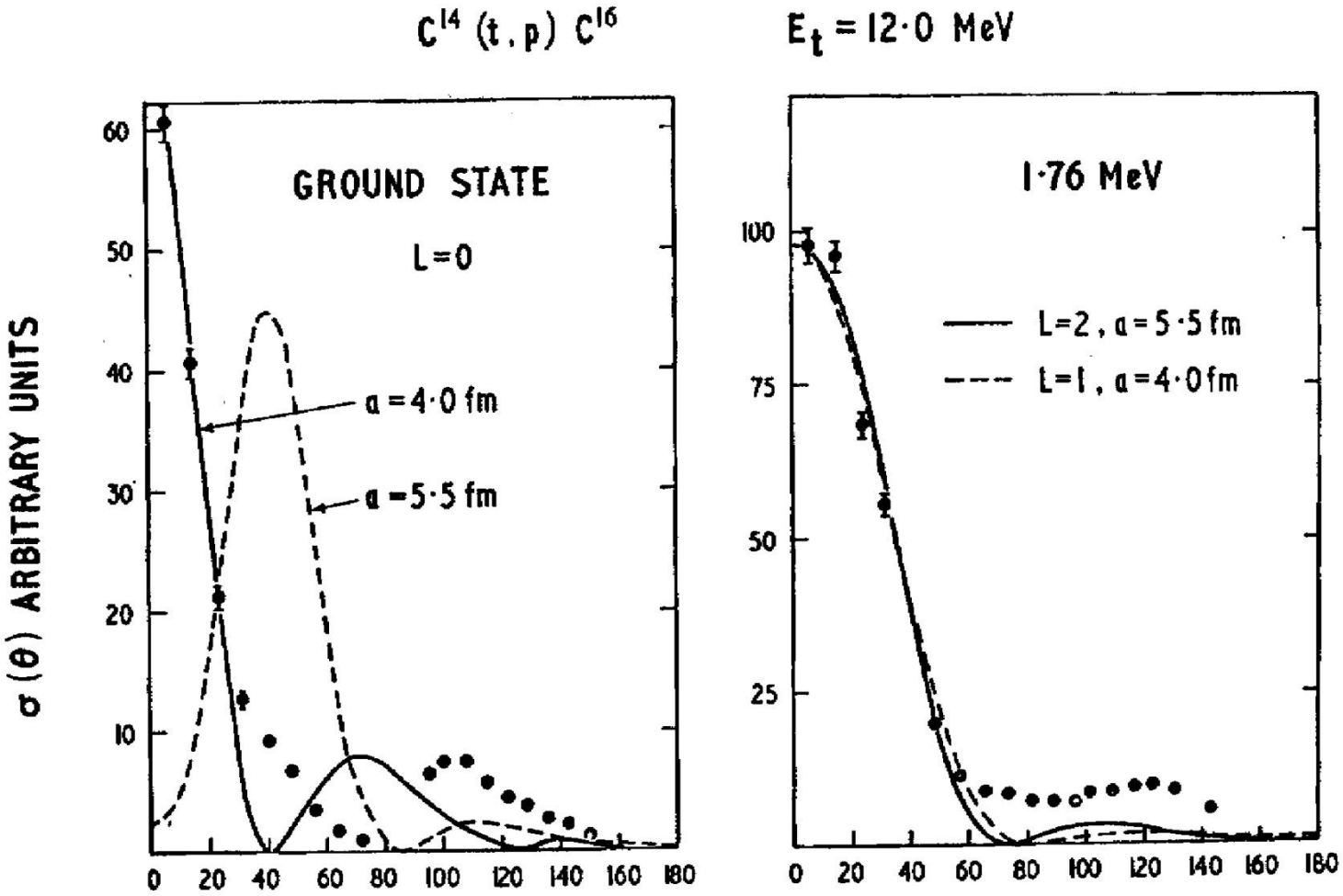

Fig. 5.8 *Proton angular distributions from $C^{14}(t,p)C^{16}$ for the ground and first excited states.*

In the case of the first excited state equally good agreement can be obtained with either L = 1 or L = 2 if radii of 4.0 fm and 5.5 fm, respectively, are assumed. However, the inadequacy of the plane wave theory observed for the ground state distribution should not effect the higher L-value transitions which may be satisfactorily described with the normal radius of 5.5 fm. Thus, the choice of L = 1 in this case is considered unlikely and the L = 2 assignment is most probably correct. This requires a spin-parity of 2^+ for this state as expected for the first excited state of an even-even nucleus.

5.4.2 Discussion

It is interesting to compare the present results for the $C^{12}(t,p)C^{14}$ reaction with those of Hinds and Middleton [91] for $C^{12}(He^3,p)N^{14}$. They observed equally unsatisfactory agreement with double stripping theory with but one exception. This was for the transition to the T = 1 first excited state of N^{14} which is the analogue of the C^{14} ground state. As in the present work, several angular distributions were measured for this state up to 10.1 MeV and in all cases good agreement was had with stripping theory assuming L = 0. The other states, however, all exhibited a strong energy dependence and were generally inconsistent with stripping theory.

It may be seen from fig. 5.6 that several excited state distributions show features which suggest a significant compound nucleus contribution to the reaction mechanism. In particular, the yield at large angles is higher than that usually encountered in a predominantly stripping process and some transitions, notably to the 6.09 and 6.72 MeV states, exhibit pronounced backward peaks. Although some of these features may be due to distortion effects, it is possible that the distributions have a marked energy dependence similar to that observed in the $C^{12}(He^3,p)N^{14}$ reaction and which results from interference between the double stripping and compound nucleus reaction amplitudes. This may then account for the erroneous L-value assignments in the present study.

Only the transitions to the 6.58 and 8.32 MeV states appear to proceed predominantly by double stripping. These are more intense than any other excited state transitions and in both cases good agreement is had with plane wave theory. However, the assignment of $J = 2^+$ for the 8.32 MeV state conflicts with the earlier 1^+ assignment [89] and an independent determination of this level property is desirable.

The 7.01 MeV level in C^{14} was first observed by Jaffe et al [82]. They suggested that this may be an anomalous L = 0 transition in which, owing to the negative Q- value, only the secondary maximum of the spherical Bessel function appears in the distribution. However, to obtain

agreement it was necessary to use a radius of interaction of 7.5 fm compared with 6.0 fm which gave best agreement with the ground state distribution. At the present energy of 11 MeV plane wave theory again predicts only the secondary maximum as illustrated by the full line curve in fig. 5.6. This type of distribution is probably of little physical significance and arises from inadequacies in the plane wave theory for negative Q-value transitions. Similar anomalies have been encountered [19] in deuteron stripping but have usually been removed by distorted wave theory. The present result for the 7.01 MeV level cannot be satisfactorily fitted with any L-value unless the interaction radius is adjusted, but L = 0 is definitely considered unlikely.

Another example of the anomalous behaviour of plane wave theory for negative-Q, L = 0 transitions is observed for the ground state of C^{16}. Agreement in this case can only be obtained with L = 0 if the interaction radius is reduced to 4.0 fm. This reduction is not usually necessary to obtain agreement for the higher L-values [92], however, and in the case of the first excited state of C^{16} the normal radius of 5.5 fm with L = 2 is strongly preferred.

It is apparent in the case of negative-Q transitions that, as for deuteron stripping, equally good agreement can frequently be had from plane wave double stripping theory with different L-values if slightly different radii are assumed. Thus, in general, level properties extracted from these measurements are always to some extent uncertain and must be regarded as tentative. In the case of positive Q-values, the radii required to obtain agreement with different L-values are usually sufficiently different as to exclude the possibilities of all but one of them.

5.5 The Reactons $O^{16}(t,p)O^{18}$ and $O^{18}(t,p)O^{20}$

5.5.1 Results

(a) $O^{16}(t,p)O^{18}$: This reaction was studied at an incident energy of 10.0 MeV and proton angular distributions were measured corresponding to the ground and first nine excited states of O^{18}. In fig. 5.9 is shown a proton energy spectrum measured at 35° to the incident beam direction. Since the target contained both O^{16} and O^{18}, groups arise corresponding to states in both O^{18} and O^{20}. The former are labeled numerically.

The proton distributions are shown in fig. 5.10 and the absolute differential cross-sections are accurate to ±10%. Most distributions are seen to be strongly characteristic of a double stripping mechanism and the theoretical curves shown were calculated with a = 5.5 fm, except for the 5.33 MeV distribution for which a radius of 5.0 fm was found necessary.

The L-values are summarised in table 5.IV and are compared with those obtained by Jaffe et al [82] for the ground and first five excited states. The excitation energies are the values measured by Hinds, Marchant and Middleton [93]. Also given in the final column are the spins and parities obtained from the present work which are uniquely determined by L.

The present L-values agree with those of Jaffe et al except for the transition to the 4.45 MeV state. This is seen to have a very small cross-section at 10.0 MeV incident energy and the distribution cannot be interpreted in terms of double stripping. At 5.5 MeV bombarding energy Jaffe et al. tentatively assigned L = 3 to this transition.

The 3.55 MeV level distribution can be equally well described with L = 3 and L = 4, the latter being favored by its known spin-parity of 4^+. Both the 3.63 and 5.33 MeV states are well fitted with L = 0 in the region of the stripping peaks. However, the former has an unusually small cross-section for such a transition and also exhibits a strong and sharp backward peak, suggestive of an exchange contribution in the stripping process. The reduced interaction radius required to fit the distribution for the 5.33 MeV state (Q = -1.62 MeV) can again be attributed to the anomalous behaviour of plane wave theory noted previously.

The states at 3.92 , 5.25 and 5.37 MeV are all formed with L = 2 which requires a spin-parity of 2^+ for these states. The 5.09 MeV level is best accounted for by an L = 3 and 3^- assignment. The broken line curve, calculated for L = 2, is shown for comparison.

(b) O^{18}(t,p)O^{20}: O^{20} has previously been studied with this reaction by Jarmie and Silbert [94] and by Hinds, Marchant and Middleton [93]. In both cases excitation energies only were measured and no determinations were made of other level properties. In the present work at an incident energy of 10.0 MeV, no new levels were observed and the excitation energies listed in table 5.V are from ref. (93). A proton energy spectrum has already been shown (fig. 5.9).

Angular distributions for the ground and first four excited states are shown in fig. 5.11. These are again strongly characteristic of a double stripping mechanism and the curves were calculated with a = 5.5 fm, except for the negative-Q transition to the 4.45 MeV state which required a radius of 5.0 fm. The general agreement is seen to be very good and has enabled unambiguous spin-parity assignments to be extracted in all cases. These are summarised in Table 5.V.

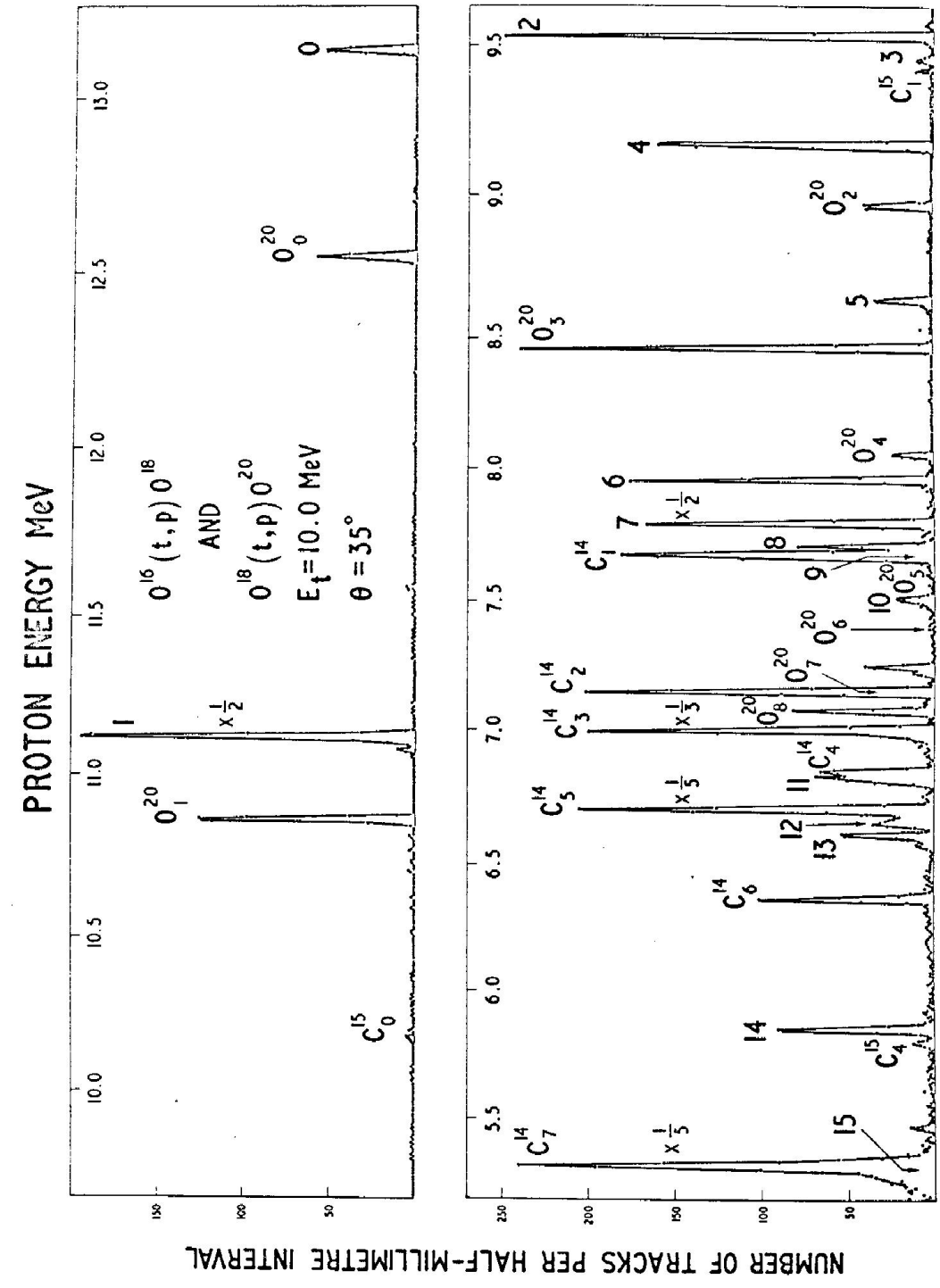

Fig. 5.9 *Proton spectrum from $O^{16}(t,p)O^{18}$ and $O^{18}(t,p)O^{20}$*

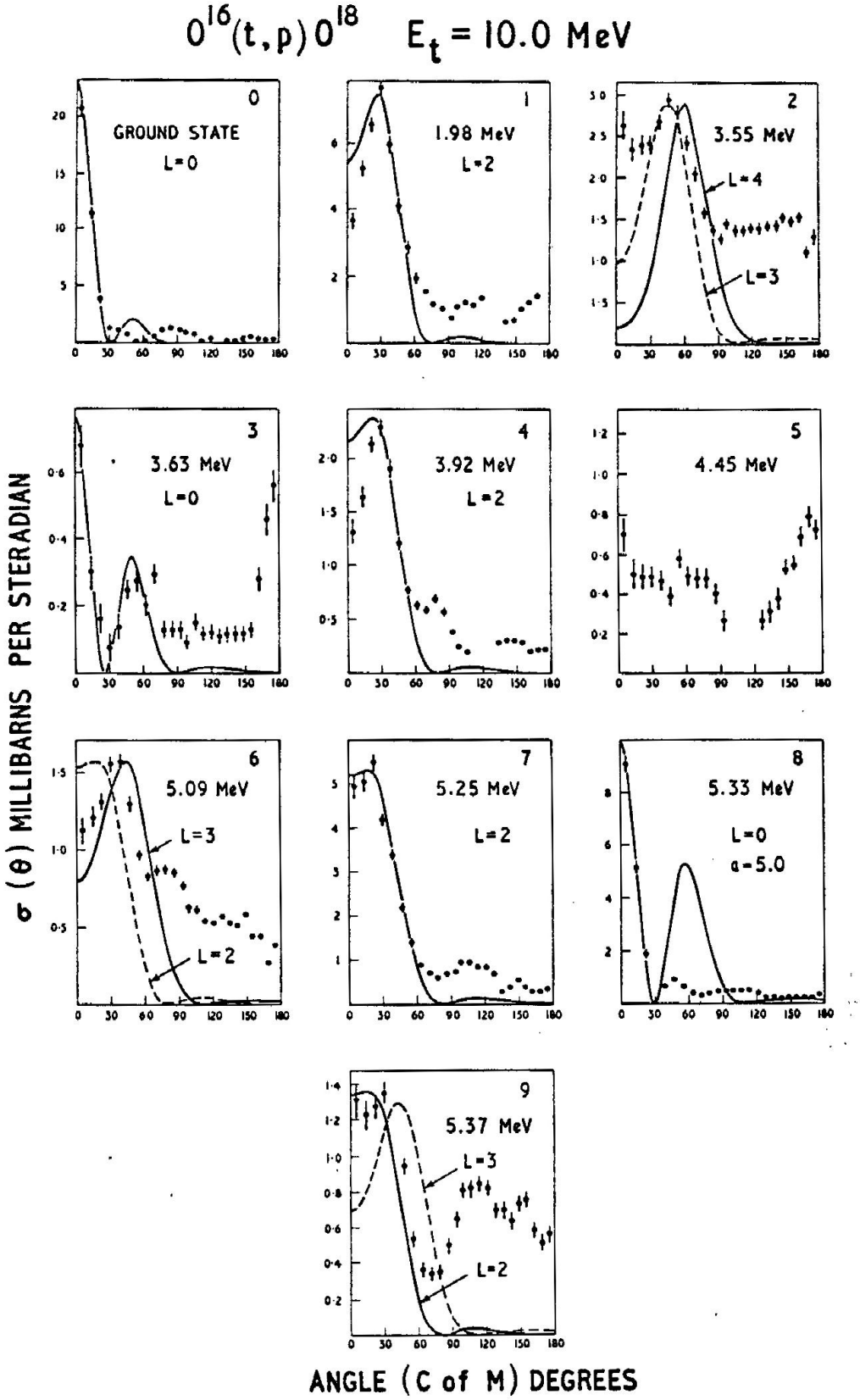

Fig. 5.10 *Proton angular distributions from $O^{16}(t,p)O^{18}$*

T A B L E 5.IV

L-values and Level Properties for O^{18} from $O^{16}(t,p)O^{18}$

Group	Excitation Energy (MeV) (a)	L		J^π (b)
		(a)	(b)	
0	0	0	0	0^+
1	1.98	2	2	2^+
2	3.55		3 or 4	3^- or 4^+
3	3.63	0	0	0^+
4	3.92	2	2	2^+
5	4.45	(3)	weak	
6	5.09		3	3^-
7	5.25		2	2^+
8	5.33		0	0^+
9	5.37		(2)	(2^+)

(a) Jaffe et al. [82]

(b) Present work

T A B L E 5.V

L-values and Level Properties for O^{20} from $O^{18}(t,p)O^{20}$

Group	Excitation Energy (MeV)	L	J^π
0	0	0	0^+
1	1.67	2	2^+
2	3.57	4	4^+
3	4.06	2	2^+
4	4.45	0	0^+

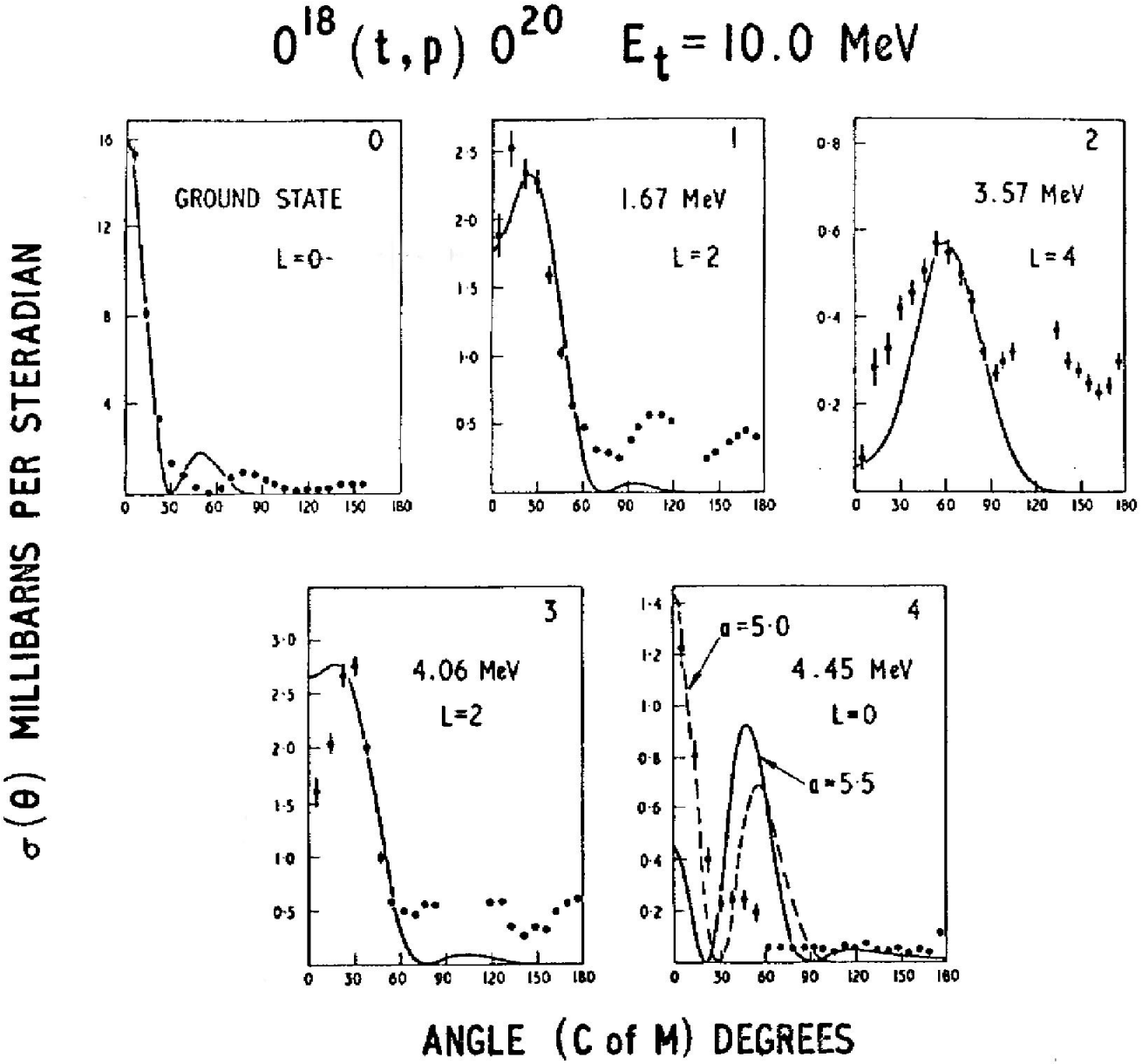

Fig. 5.11 *Proton angular distributions from $O^{18}(t,p)O^{20}$*

5.5.2 Discussion

The generally good agreement obtained between plane wave double stripping theory and the measured distributions for most states in O^{18} and O^{20} has enabled their spins and parities to be uniquely determined. Only the 4.45 MeV level in O^{18} could not be accounted for by a stripping mechanism. This transition may, however, be forbidden by the double stripping selection rules, or the state may have a relatively complex configuration not easily excited by double stripping.

A number of shell model calculations have recently been carried out for the low-lying states in these nuclei. In particular, the even parity states arising from the $d_{5/2}$ and $s_{1/2}$ configurations have been considered by Talmi and Unna [95] who neglected in their treatment the effect of configuration interaction. In O^{18}, six states can be formed with the configurations of $d^2_{5/2}$ ($J = 0^+, 2^+, 4^+$), $s^2_{1/2}$ ($J = 0+$) and $d_{5/2}s_{1/2}$ ($J = 2^+, 3^+$). The ground and first four excited states can account for all but the 3^+ state and this was predicted to lie between 4.5 and 5.8 MeV excitation. Calculations have also been carried out by Wilmore [96] who included in his treatment the $d_{3/2}$ configuration and configuration mixing. The predicted position of the 3^+ state in this case was between 4.0 and 5.5 MeV.

Since the formation of a 3^+ state by (t,p) double stripping is forbidden by the selection rules it is expected to be only very weakly excited by this reaction. This is seen to be the case for the 4.45 MeV level which lies within the limits of excitation quoted above and which may, therefore, qualify for the 3^+ level. More positive evidence could be obtained with the O^{17}(d,p)O^{18} reaction which should proceed with an $l = 0$ transition to a 3^+ state.

As mentioned above this weak transition may alternatively be due to a relatively complex configuration such as that resulting from core excitation. Harvey [97] has suggested that the first odd-parity state in O^{18} should be 1^- arising from the $(1p)^{-1}(2s,1d)^3$ configuration. Its excitation is predicted to be between 4 and 5 MeV. Although the double stripping selection rules permit $L = 1$ to such a state it is unlikely to proceed by simple stripping since a 1p-nucleon must be excited from the O^{16}-core. This is again consistent with the observed 4.45 MeV level distribution (see also ref. (117).

The first level in O^{18} which can be assigned odd-parity with reasonable certainty is the 3^- level at 5.04 MeV and this is probably formed by the capture of one of the neutrons into the $1f_{7/2}$ orbit. The remaining states at 5.25, 5.33 and 5.37 MeV all have even-parity and are probably formed by capture of one or both neutrons into the $d_{3/2}$ orbits.

In O^{20}, a 4^+-2^+-0^+ level sequence was predicted by Talmi and Unna [95] at 3.90, 4.36 and 4.60 MeV excitations, respectively. This sequence can be identified with the observed levels at 3.57, 4.06 and 4.45 MeV which therefore probably have the principal configurations $d^4_{5/2}$, $d^3_{5/2}s_{1/2}$ and $d^2_{5/2}s^2_{1/2}$, respectively.

5.6 The Reactions $Si^{28}(t,p)Si^{30}$ and $Si^{29}(t,p)Si^{31}$

Since the Q-values for the $Si^{28}(t,p)Si^{30}$ and $Si^{29}(t,p)Si^{31}$ reactions are similar [98] (10.607 MeV and 8.724 MeV, respectively) it was possible to study both reactions simultaneously. In fig. 5.12 are shown the proton distributions corresponding to the ground and first excited state transitions measured at an incident energy of 10.0 MeV. The arbitrary units of cross-section are not the same for both reactions although the relative intensities for the ground and first excited states have been preserved. The curves were calculated with a = 6.0 fm. Within the limitations of the plane wave theory the agreement is very satisfactory and in all cases the L-values are consistent with the known spins and parities for the final states [98].

The ground state transition for the $Si^{29}(t,p)Si^{31}$ reaction is of particular interest in view of the initial and final spins and parities ($1/2^+$ and $3/2^+$, respectively). According to the usual double stripping selection rules this transition should only proceed with L = 2. However, if it is possible in double stripping for the neutron pair to be captured with total spin S = 1, or if some other mechanism, such as knock-out, is taking part for which S = 1 is allowed, then the transition could proceed with L = 0. Thus, since an L = 0 transition is intrinsically more intense than L = 2 this appears to provide a sensitive test as to whether double stripping with S = 0 really is the predominant mechanism. Indeed, from fig. 5.12 there is no evidence for an L = 0 contribution to this transition. Unfortunately, however, the probable shell model configuration for Si^{31} in the (s,d)-shell ($s^2_{1/2}d_{3/2}$) also forbids L = 0. This arises since the two neutrons must be captured with $l_1 = 0$ and $l_2 = 2$ which can only couple to give L = 2. Thus, no definite conclusion can be reached in this case on the predominance or otherwise of double stripping with S = 0.

5.7 The Reaction $Ca^{40}(t,p)Ca^{42}$

The $Ca^{40}(t,p)Ca^{42}$ reaction was studied at an incident triton energy of 7.2 MeV. This comparatively low energy was chosen since measurements had been made of the triton elastic scattering from Ca^{40} at this energy (Chapter 7) to facilitate a full distorted wave analysis of the reaction [30].

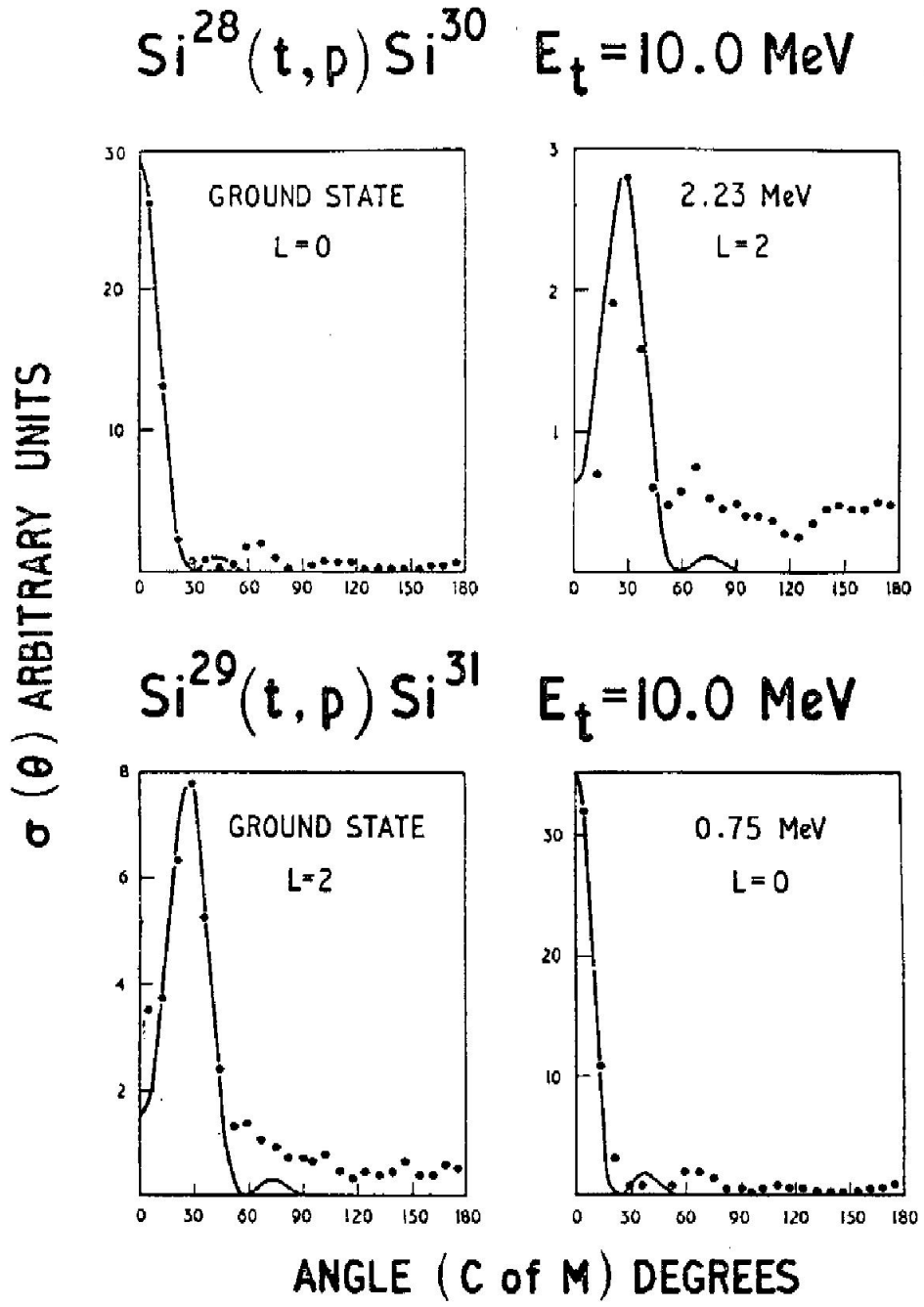

Fig. 5.12 *Proton angular distributions from $Si^{28}(t,p)Si^{30}$ and $Si^{29}(t,p)Si^{31}$.*

Proton angular distributions were measured for the ground and first four excited states of Ca^{42} and these are shown in fig. 5.13. The absolute cross-sections are accurate to ±10%. The characteristic forward peaking in the distributions is well accounted for by plane wave stripping theory as illustrated by the curves in the figure. These were calculated with a = 7.0 fm except for the 1.52 MeV state for which a radius of 7.5 fm was required. The detailed structure away from the stripping peaks, however, is not so well described by this simple theory. In view of the rather low incident energy used for this study the distortion effects are expected to be significant. Considerable improvement has been obtained with the D.W.B.A. double stripping theory of Rook and Mitra [30] and an account of this is given in Appendix C.

No accurate measurements of the excitation energies of the Ca^{42} states were made since these have been very precisely determined by Braams [99] and the values given in Table 5.VI were taken from his work. Also summarised in the table are the L-values and corresponding spin-parity assignments obtained from the present study. These are in agreement with the assignments obtained by Morinaga et al [100] from observations of the de-excitation γ-rays, and by McCullen and Kraushaar [101] who measured the β^--ray transitions from K^{42} to these states.

The measured spin sequence of $J = O^+, 2^+, 0^+, 2^+, 4^+$ for the lowest states of Ca^{42} indicates considerable rearrangement of the simple shell model states. On the basis of simple theory the two $f_{7/2}$ neutrons outside the doubly-magic Ca^{40} core are expected to couple to give $J = 0^+, 2^+, 4^+, 6^+$ for the lowest states. The recent shell model calculations by Mitler,[102] which include configuration mixing, also fail to explain the observed level scheme. In particular, the 0+ state at 1.84 MeV cannot be accounted for and the 2.42 MeV state, which is observed to be 2^+, is predicted to be 4^+.

TABLE 5.VI

L-values and Level Properties for Ca^{42} from $Ca^{40}(t,p)Ca^{42}$

Group	Excitation Energy (MeV)	L	J^π
0	0	0	0+
1	1.52	2	2+
2	1.84	0	0+
3	2.42	2	2+
4	2.75	4	4+

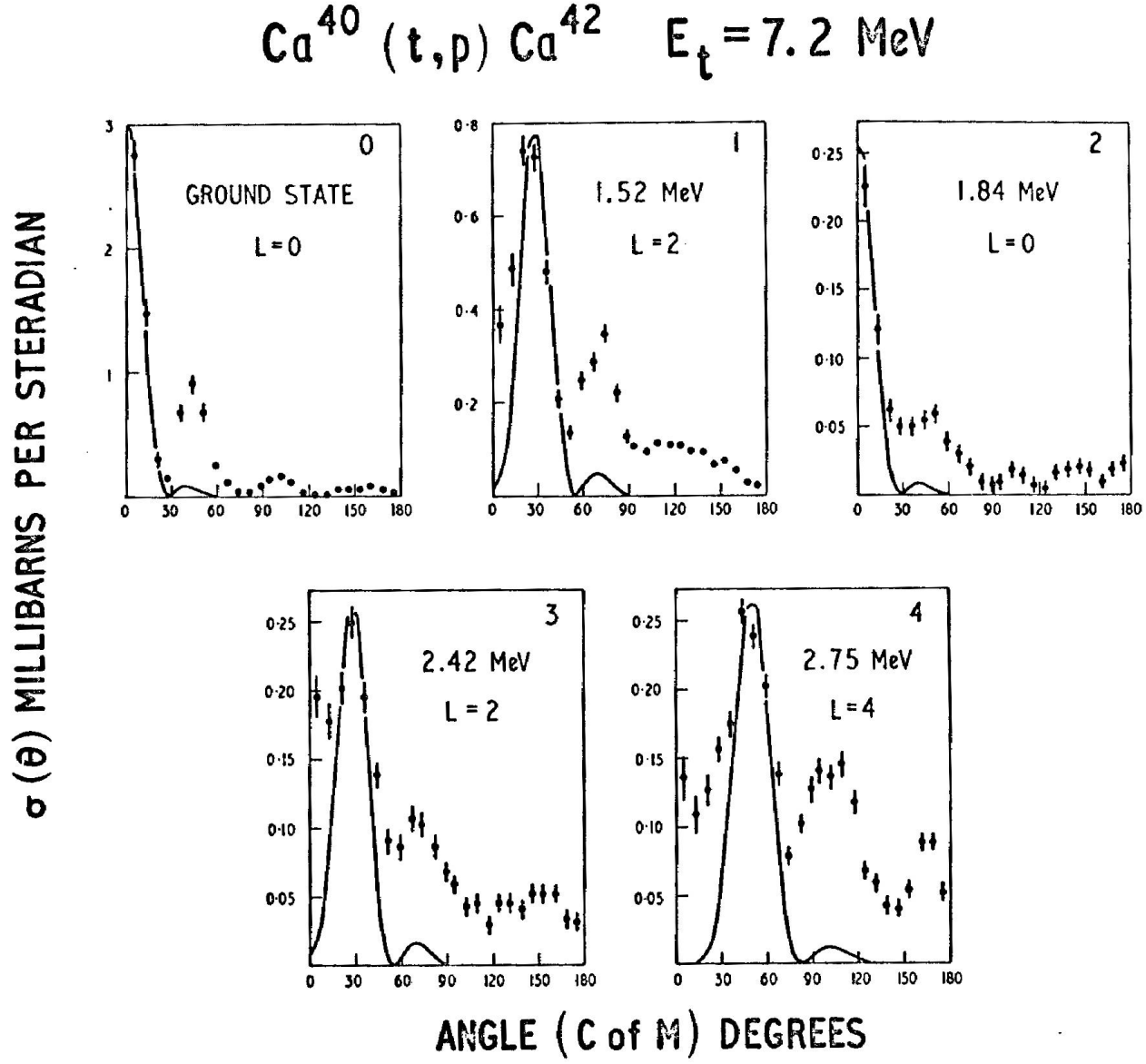

Fig. 5.13 *Proton angular distributions from $Ca^{40}(t,p)Ca^{42}$*

5.8 Conclusions

In most cases studied in this investigation, surprisingly good agreement has been obtained between the observed proton distributions and the plane wave double stripping theory of Newns. With very few exceptions the interaction radius has not been treated as a freely adjustable parameter but has been maintained close to the value normally required by the plane wave Born approximation treatments, namely, the Gamow-Crithfield radius plus 1 fm. In the case of L = 0 transitions which proceed with rather negative Q-values, however, the theory sometimes exhibits only the secondary maximum of the spherical Bessel function. Since the observed distributions are always peaked at 0° this would appear to be an inadequacy of the theory which can usually be removed only by reducing the radius. A particular case in point is the ground state transition for the $C^{14}(t,p)C^{16}$ reaction. More generally, the increased sensitivity of plane wave theory to the choice of radius for negative-Q transitions tends to throw some doubt on the L-value assignments. It is to be hoped that this uncertainty will be removed by the distorted wave theory as it has in the case of deuteron stripping [30].

The spins and parities obtained from this investigation are generally in excellent agreement with the known values, although some serious discrepancies are observed for the $B^{10}(t,p)B^{12}$ and $C^{12}(t,p)C^{14}$ reactions. In the former case not only is poor agreement had with double stripping theory but also the differential cross-sections for most transitions are usually small. It does not appear that double stripping is the dominant process in either of these cases.

The cross-sections observed for the (t,p) reactions generally appear to be about an order of magnitude less than those for the equivalent (d,p) reactions. It should therefore not to be too surprising if more exceptions are encountered in double stripping. Nevertheless, the present results suggest that in general (t,p) reactions do proceed predominantly via a double stripping process at energies of about 10 MeV. In the case of zero-spin target nuclei in particular, the L-values determine uniquely the spins and parities of the final states. This is perhaps one of the most important features of the reaction and deserves full exploitation.

CHAPTER VI

THE PARITY OF Be^{11}

6.1 Introduction

Recent experimental and theoretical studies of Be^{11} have aroused considerable interest in this nucleus. The simple shell model predicts its ground state spin and parity to be $\frac{1}{2}^-$ since the seventh neutron is expected to be in the $1p_{(1/2)}$ -shell. This is also predicted by the independent particle model in intermediate coupling [6]. However, in a study of the β^- -decay scheme of Be^{11}, Wilkinson and Alburger [43] measured log ft values of 6.77 and 6.63, respectively, for the β^- -ray 'transitions to the ground ($3/2^-$) and first excited ($1/2^-$) states of B^{11}. As pointed out by these authors these values are rather large for allowed transitions but would be consistent with first forbidden transitions and therefore with even parity for Be^{11}.

The detailed β^--decay scheme measured by Wilkinson and Alburger is shown in fig 6.1. In addition to the transitions to the ground and first excited states of Be^{11}, weak transitions were also observed to a member of the 6.756-6.807 MeV doublet and to the 7.987 MeV state with log ft

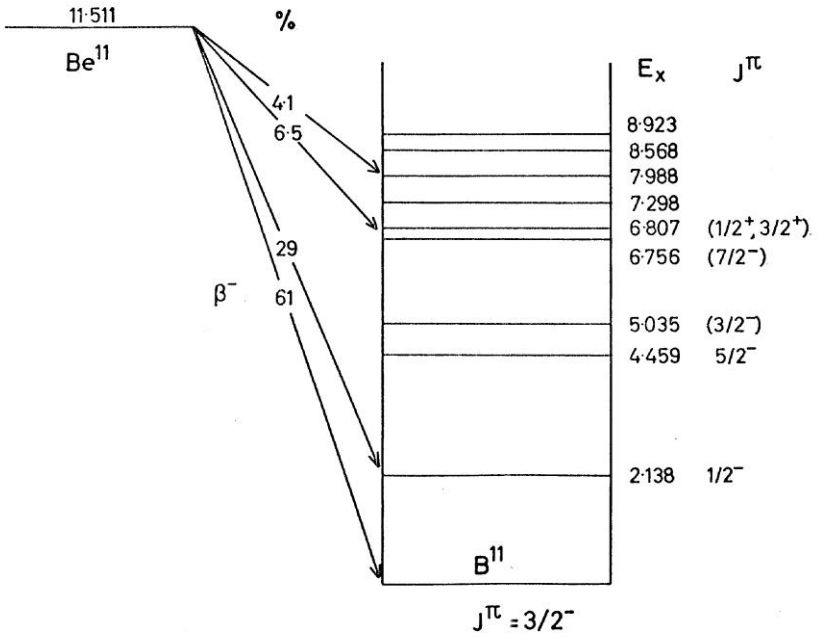

Fig. 6.1 *Beta decay scheme of Be^{11}* [43]

values of 5.93 and 5.33, respectively. Although these presumably correspond to allowed β^--ray transitions, and therefore to no parity changes, the spins and particles of the final states involved were not known. No definite conclusion could thus be reached concerning the parity of Be^{11}.

Measurements of the γ-decay of the 6.756 MeV state [59] suggest its most probable spin-parity to be $7/2^-$. An allowed β^--ray transition to this level would therefore require $5/2^-$, $7/2^-$, or $9/2^-$ for Be^{11} which is most improbable. On the other hand, the 6.807 MeV state has been shown to have even parity and probable spin 3/2 from its γ-decay [59] and also from the $Be^9(He^3,p)B^{11}$ reaction [36]. Furthermore, Donovan et al [104] have since pointed out that the β^--transition to this doublet is followed by γ-ray transitions [43] to both the ground and 2.138 MeV states of B^{11}, which is the known behavior of only the 6.807 MeV member.[59] The evidence therefore points to this state as being the level involved in the β^--decay of Be^{11}, and therefore again to even-parity for Be^{11}.

The low-lying levels of Be^{11} might be expected to resemble those of C^{13}, since this differs from Be^{11} only by two protons which can be considered to be coupled together to give zero total angular momentum. However, following the work of Wilkinson and Alburger, Talmi and Unna [103] showed that the residual two-body interactions can cause a profound change in the order of filling of the $2s_{1/2}$ and $1p_{1/2}$ orbits in Be^{11} compared with C^{13}. On the basis of the systematic variation in excitation energy of the $2s_{1/2}$ state in the neighboring nuclei, they predicted that the $1/2^+$ level in Be^{11} should lie about 210 keV below the $1/2^-$ level. This may be compared with the situation in C^{13} where the $1/2^+$ level lies 3.09 MeV above the $1/2^-$ ground state. Thus according to the predictions of Talmi and Unna there was good reason to suppose that Be^{11} has a $1/2^+$ ground state.

This somewhat anomalous position of Be^{11} in the 1p-shell clearly warranted further study and it was for this reason that the experiments to be described in this chapter were undertaken. The first was a direct study of Be^{11} by means of $Be^9(t,p)Be^{11}$ reaction. It was hoped that by measuring the ground state proton distribution from this reaction the parity of Be^{11} could be obtained together with limits on its spin. It was further hoped to obtain the energies of the excited states of Be^{11} which were hitherto unknown, and in particular to check the prediction of Talmi and Unna for the $2s_{1/2}$ and $1p_{1/2}$ level separation in the nucleus. An experiment on the $C^{12}(t,\alpha)B^{11}$ reaction was also carried out in the hope that the α-particle angular distributions would be interpretable in terms of a direct pick-up mechanism. Some success had been reported in the interpretation of the distributions from other pick-up reactions such as (He^3,α) [105], (d,t) [19], and (p,d).[19] Of particular interest was the transition to the 5.035 MeV state in Be^{11}. Wilkinson and Alberger had placed a lower limit of 8.2 on the log ft values for the β^--transitions to the 4.459 and 5.035 MeV states, and these values

safely precluded allowed transitions. The lower excited state was known to be $5/2^-$ which was therefore consistent with a forbidden transition whether Be^{11} has spin parity $1/2^+$ or $1/2^-$. However, the spin-parity of the 5.035 MeV state was rather uncertain, although measurements of its γ-decay[59] favoured $1/2^-$ or $3/2^-$. As pointed out by Wilkinson and Alburger, if the spin-parity of this level could be confirmed then this would provide important evidence on the parity of Be^{11}.

6.2 Procedure

The $Be^9(t,p)Be^{11}$ reaction was studied at incident energies of 5.96 and 10.08 MeV using self-supporting Be^9 targets prepared by evaporation. The lower energy investigation was carried out with tritons from the Aldermaston Van de Graaff generator and the proton groups were analysed with the single-channel spectrograph. Exposures were made at laboratory angles ranging from 6° to 120° and the exposure strengths were 350 microcoulombs.

The investigation at 10 MeV was carried out with the Tandem Accelerator and the multi-channel spectrograph was employed for analysis of the proton groups. The total exposure strength was 600 microcoulombs. A further measurement was also made at 10 MeV with a thin self-supporting carbon target to study the $C^{12}(t,\alpha)B^{11}$ reaction.

The Be^9 targets used in the 6 MeV and 10 MeV exposures were later weighed and found to have surface densities of 37 μgm cm^{-2} and 47 μgm cm^{-2}, respectively. From these values absolute cross-sections have been determined to within ±25% for the $Be^9(t,p)Be^{11}$ reaction at both energies.

6.3 Energy Levels of Be^{11}

Proton energy spectra from the $Be^9(t,p)Be^{11}$ reaction were measured at seven angles at 5.96 MeV incident energy and ten angles at 10.08 MeV. In fig. 6.2 (a) and (b), energy spectra are shown measured at angles of 12.5° and 72.5°, both obtained at the higher energy. The various groups were identified in the usual way by their characteristic energy variation with angle. In addition to the proton groups corresponding to states in Be^{11}, impurity groups arising from C^{12} and O^{16} are also observed.

At both angles a proton continuum is observed which has a cut-off energy close the to first excited state group of Be^{11}. This can be attributed to the $Be^9(t,pn)Be^{10}$ reaction since Be^{11} is neutron unstable at excitations above 0.53 MeV. The unidentified proton group which occurs at a proton energy of about 4.15 MeV in (b) was not observed at other angles and probably arises from statistical fluctuations. The group in (a) attributed to the eleventh exited state in C^{14} was only observed at five angles between 5° and 42.5°. It was apparent, however, that its energy variation

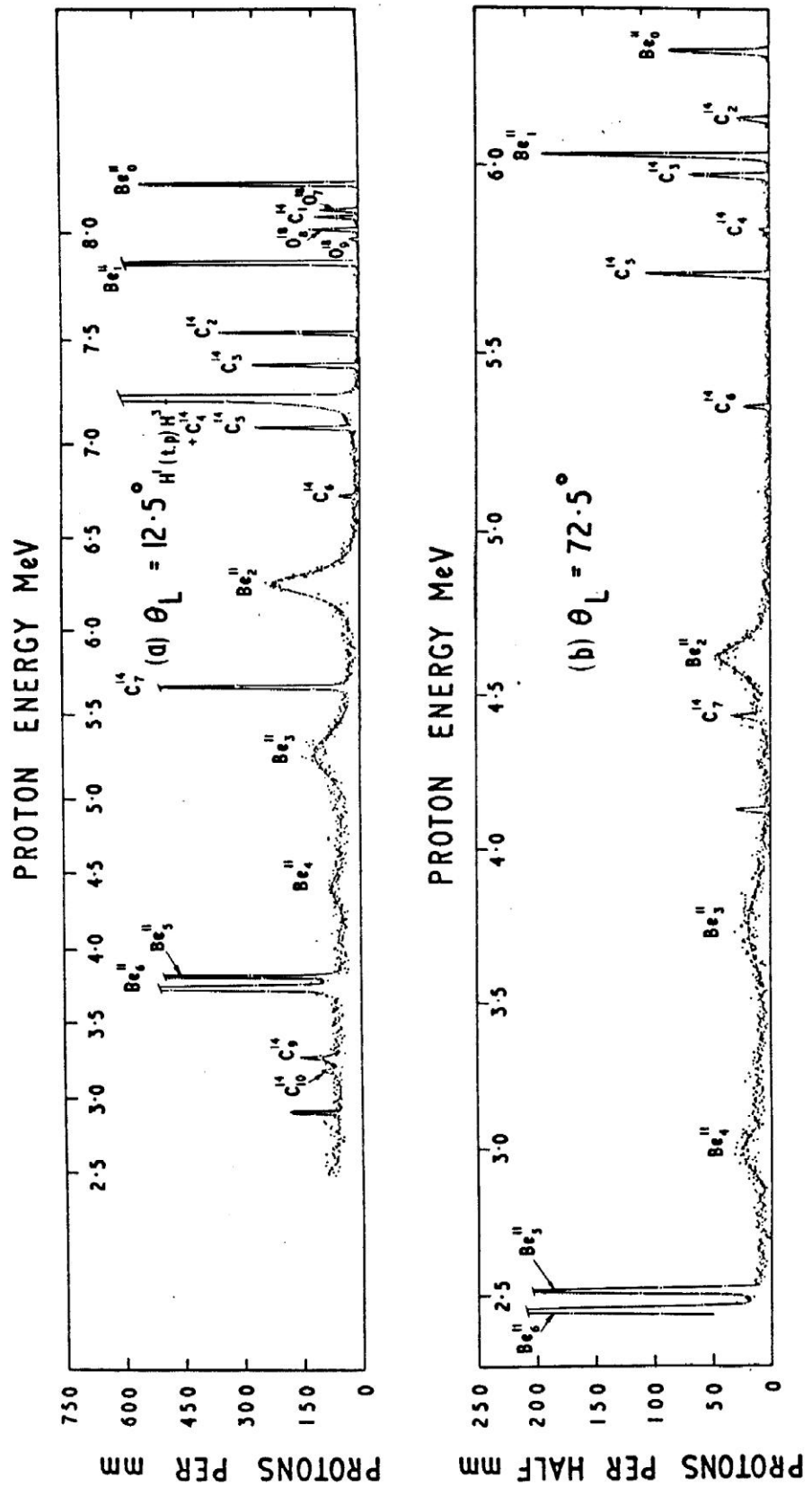

Fig. 6.2 *Proton spectra from* $Be^9(t,p)Be^{11}$

was characteristic of a mass-14 residual nucleus although at the time of this investigation it did not correspond to any known level in C^{14}. In a later investigation of the $C^{12}(t,p)C^{14}$ reaction (Section 5.4) it was confirmed that this group corresponds to a new level in C^{14} at 10.74 MeV excitation energy.

By taking the mean of nine measurements made at different angles of observation on the proton group from the $C^{12}(t,p)C^{14}$ (first excited state) reaction, the lower bombarding energy was determined to be 5.961 ± 0.012 MeV. The Q-value for this reaction was assumed to be 4.641 MeV from the mass excess data of Everling et al [70] and the first excited state of C^{14} was taken to be at 6.091 ± 0.010 MeV [54]. With this value for the beam energy the ground state Q-value for the $Be^9(t,p)Be^{11}$ reaction was calculated and the mean of twelve values found to be at -1.164 ± 0.015 MeV. This is consistent with a mass excess of 20.175 ± 0.015 MeV for Be^{11} (referred to the scale in which the mass excess of C^{12} is zero) and a Be^{11}-B^{11} mass difference of 11.510 ± 0.015 MeV. The latter is in good agreement with the earlier value of 11.48 ± 0.15 MeV determined by Wilkinson and Alburger.[43]

Two excited states of Be^{11} were observed at the lower bombarding energy and six at 10.08 MeV. These levels are identified in the spectra of fig. 6.2 and the energy level scheme for Be^{11} is shown in fig 6.3, together with the predictions of Talmi and Unna. In Table 6.I are listed the excitation energies of the Be^{11} levels together with their natural half-widths which were measured directly from the spectra.

As previously mentioned, states in Be^{11} above 0.53 MeV excitation may decay by neutron emission to Be^{10}. The measured natural width, Γ, for each such state therefore provides a means for estimating the neutron reduced width, θ_n^2, since the two are related [15] through a barrier penetrability factor, P_l, viz: $\theta_n^2 = \Gamma/2\ P_l$. Gove [106] has published curves relating P_l to the neutron decay energy and for neutron orbital angular momenta l = 0 to 4. These have been used to obtain estimates of θ_n^2 for the three broad levels in Be^{11} at 1.78, 2.70 and 3.41 MeV excitation. The results (in units of $\hbar^2/mR^2$ where m is the reduced neutron mass and R the nuclear radius, assumed to be 4.5 fm for Be^{11} [106]) are given in the last four columns of Table 6.I. Since the spins and parities of these states are not known the reduced widths were calculated for neutron orbital angular momenta L = 0 to 3.

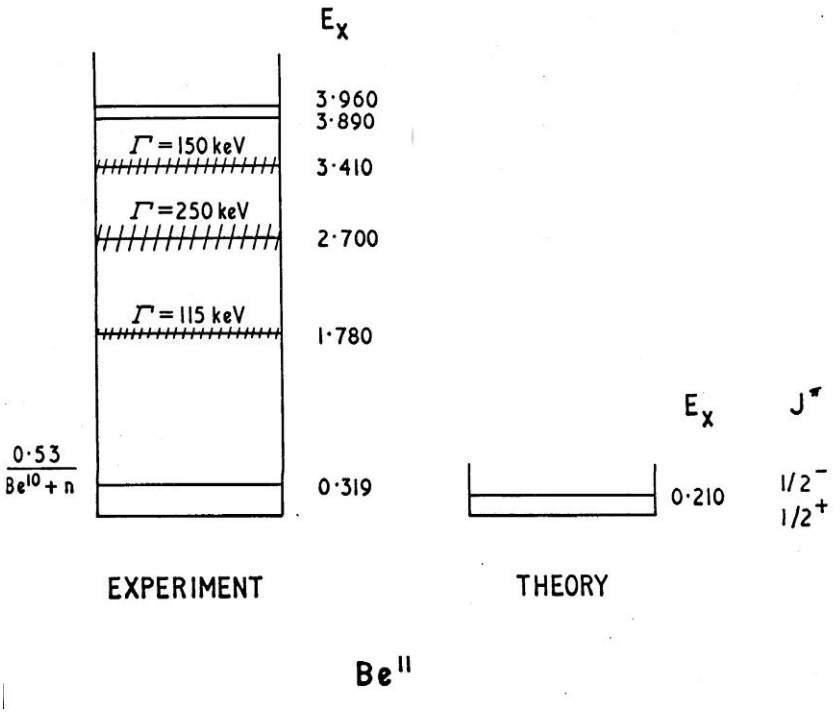

Fig. 6.3 *Level Energies for Be^{11}*

T A B L E 6.I

Natural and Neutron Reduced Widths for Levels in Be^{11}

Group	Excitation Energy (MeV ± keV)	Γ_{lab} (keV)	$\theta_n^2/\{\hbar^2/mR^2\}$			
			s	p	d	f
0	0					
1	0.319 ± 10	≤10				
2	1.780 ± 20	110 ± 15	0.028	0.051	0.40	10
3	2.700 ± 25	250 ± 20	0.046	0.080	0.31	3.6
4	3.410 ± 25	150 ± 20	0.025	0.038	0.073	0.89
5	3.890 ± 20	≤ 10				
6	3.960 ± 20	≤ 10				

6.4 Angular Distributions from $Be^{9}(t,p)\,Be^{11}$ and $C^{12}(t,\alpha)B^{11}$

Proton angular distributions from $Be^{9}(t,p)Be^{11}$ corresponding to the ground and first excited states of Be^{11} were measured at 5.96 and 10.08 MeV triton energy. These are shown in fig. 6.4. The curves were calculated from plane wave double stripping theory assuming a radius of interaction a =5.5 fm and L = 1 for the ground state, and a = 6.0 fm and L = 2 for the first excited state. Although in most cases these fit the experimental data well in the forward direction, the presence of large backward peaks in all cases suggest that double stripping may not be the predominant reaction mechanism.

Angular distributions of the alpha-particles from the $C^{12}(t,\alpha)B^{11}$ reaction were measured at an incident energy of 10.06 MeV. These are shown in fig. 6.5. The unit of cross-section is arbitrary although the observed relative cross-sections between the states have been preserved. The curves were calculated from distorted wave pick-up theory assuming the l-values given in the figure. The alpha-particle and triton optical model parameters used in the calculations are given in Table 6.II. The latter were taken from the triton elastic scattering measurements from F^{19}at 7.2 MeV (Chapter 7), and the alpha parameters from the analysis of alpha scattering measurements by Hodgson [51].

T A B L E 6.II

Optical Model Parameters from Alpha and Triton Elastic Scattering

Parameter	U (MeV)	W (MeV)	r_0 (fm)	a (fm)
Alpha	50	12	1.5	0.6
Triton	25	28	1.4	0.7

The agreement between the calculated distributions and the experimental data in fig. 6.5 is in most cases satisfactory in the region of the forward peaks. However, the theory does not reproduce at all well the detailed structure observed at large angles. The discrepancy is particularly serious for the first and second excited states where backward peaks are observed with similar intensities to the forward peaks. Nevertheless, the l-values required to describe the distributions at small angles for the ground (l = 1), 2.14 MeV (l = 1) and 4.46 MeV (l = 3) states are consistent with

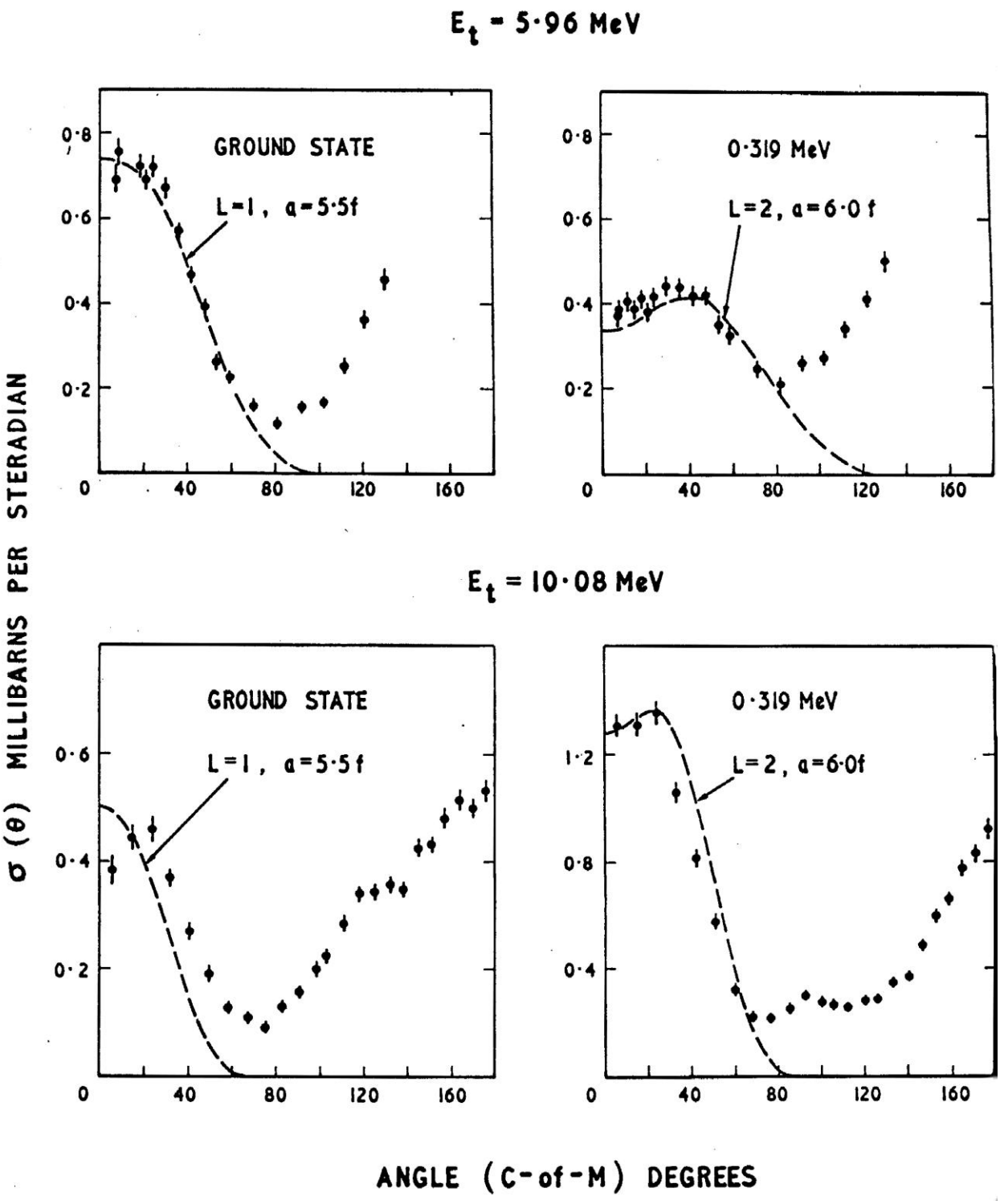

Fig. 6.4 *Proton angular distributions from Be9(t,p)Be11*

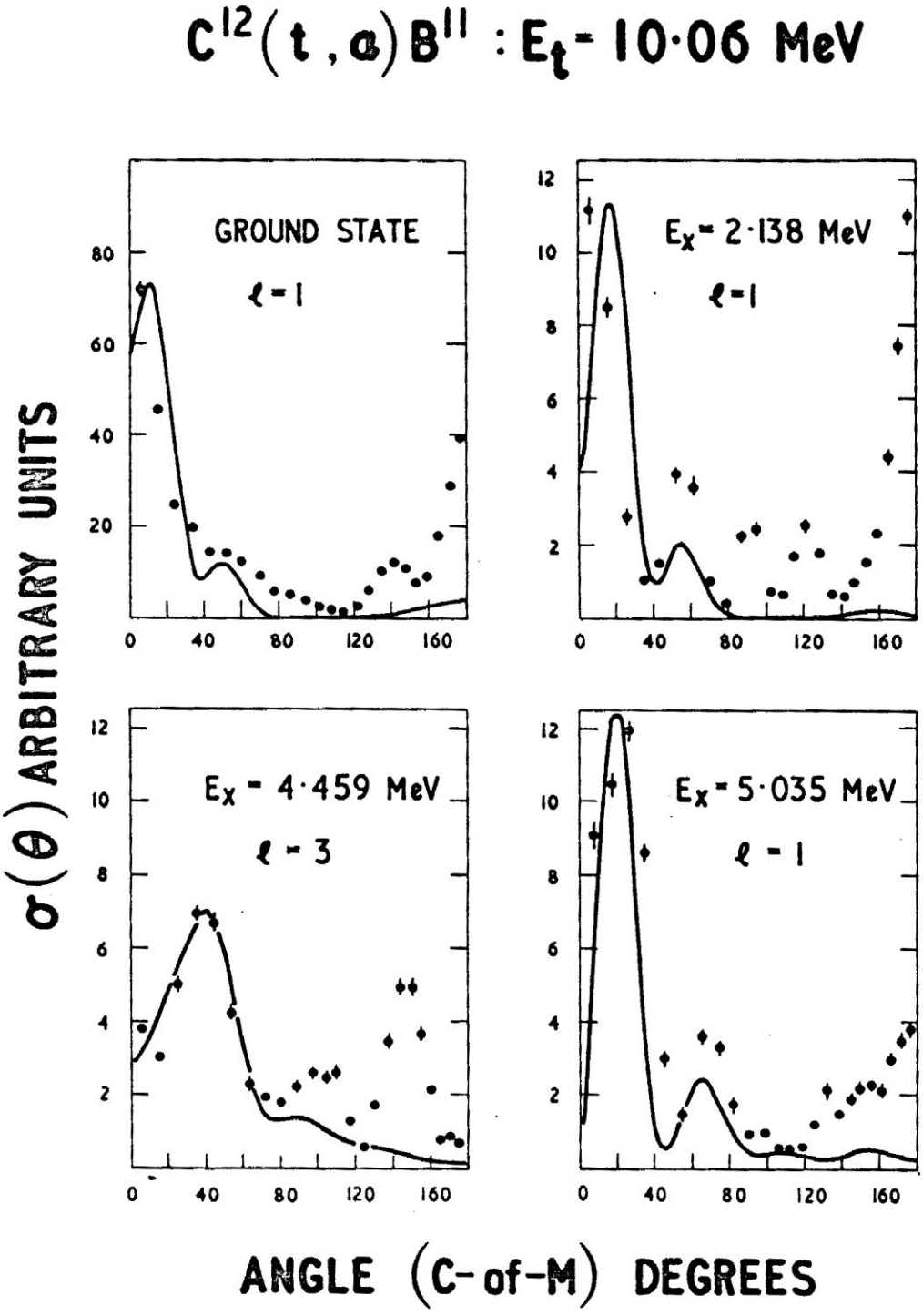

Fig. 6.5 *Alpha particle angular distributions from $C^{12}(t,\alpha)B^{11}$.*

their known spins and parities of $3/2^-$, $1/2^-$ and $5/2^-$, respectively. The agreement between pick-up theory and experiment is particularly satisfactory for the 5.04-MeV level in which an l = 1 transition has been assumed. This would require a spin-parity of $1/2^-$ or $3/2^-$ for this state.

6.5 Discussion

Plane wave double stripping theory gives a good account of the proton distributions at forward angles for the ground and first excited states of Be^{11} if L-values of 1 and 2, respectively, are assumed. Since $J = 3/2^-$ for Be^9, these L-values require $1/2^+$, $3/2^+$, or $5/2^+$ for the ground state of Be^{11} and $1/2^-$, $3/2^-$, $5/2^-$ or $7/2^-$ for the first excited state. They are therefore consistent with the values of $1/2^+$ and $1/2^-$ predicted by Talmi and Unna. Furthermore, the measured energy separation between these states (319 keV) is in excellent accord with the predicted $2s_{1/2}$ - $1p_{1/2}$ spacing of 210 keV.

Unfortunately, the spin-parity assignments based on these measurements cannot be regarded as conclusive since the large backward peaks observed in the distributions throw some doubt on the nature of the reaction mechanism. These may be due to heavy-particle stripping or simply to distortions of the incident and outgoing waves. However, the cross-sections are also rather low for a stripping process and it is possible that compound nucleus formation and decay is the predominant mechanism.

Detailed calculations of the negative parity states of Be^{11} have been made by Kurath [107]. For values of the intermediate coupling parameter a/K ranging from 3.0 to 7.0 there are only two other negative parity states within 4.5 MeV of the 1.2^- level. These are $3/2^-$ and $5/2^-$ levels which, for a/K ~ 4.5 (which is appropriate to B^{11} [57,104]), lie about 3 MeV above the $1/2^-$ level. Thus, of the seven levels in Be^{11} observed below 4 MeV excitation it appears likely that four have positive parity. Calculations are available for only one of these [103], namely the $1/2^+$ level suspected of being the ground state.

Limits to the possible spins of the three broad levels may be obtained from their reduced neutron widths. The spins of the initial and final states involved in the neutron emission are related by $\vec{J} = \vec{J}_i + \vec{l}_n + \vec{1}/2$, where l_n is the orbital angular momentum carried away by the neutron. In this case $J_f = 0^+$ and corresponds to the ground state of Be^{10}. Therefore $J_i = l_n \pm$ ½ and the initial state parity is even or odd according as l_n is even or odd. The values of θ_n^2 listed in Table 6.I suggest that f-wave neutron emission is most unlikely for the states at 1.78 and 2.70 MeV. Their

spins and parities are therefore restricted to $1/2^{\pm}$, $3/2^{\pm}$, or $5/2^{\pm}$. In the case of the 3.41 MeV state, the possibilities of $5/2^-$ or $7/2^-$ cannot be precluded. The observed upper limits on the widths for the 3.89 and 3.96 MeV states do not provide limits on their spins.

The intermediate coupling calculations assume the coupling of seven p-shell neutrons to produce the $5/2^-$ state. However, the large reduced neutron width obtained assuming $5/2^-$ for the 3.41 MeV level indicates that this would have to be nearly a single-particle state with the odd neutron in the 1f-shell. Thus, the most likely candidates for the $5/2^-$ level would therefore appear to be the 3.89 and 3.96 MeV states.

The importance of the spin-parity determination for the 5.04 MeV level in B^{11} and its association with the Be^{11} ground state parity have already been discussed. In the present study of the $C^{12}(t,\alpha)B^{11}$ reaction the alpha-particle distribution for this state can be well described by pick-up theory assuming an $l = 1$ transition, which therefore requires a spin-parity of $1/2^-$ or $3/2^-$ for this level. This would then suggest even parity for Be^{11} since the β^--ray transition to this state with $\log ft \geq 8.2$ can then be understood as a typical first-forbidden transition. However, this assignment must again be accepted with some caution, since the structure observed at large angles in the angular distributions for the lower three states in B^{11} suggest that a simple proton pick-up mechanism may not hold for these cases. The large backward peaks in particular indicate that exchange interactions may be important. It is possible that in the case of $C^{12}(t,\alpha)B^{11}$, 'cluster' exchange interactions may play an important role in the reaction mechanism (Gutsche et al. [108]). This interpretation requires that C^{12} may be well described as $\{Be^8 + \alpha\}$ and B^{11} as $\{Be^8 + t\}$. The reaction may then proceed simply by replacing the alpha-particle cluster in C^{12} with a triton cluster. Such a process could explain the forward and backward peaking observed in the distributions in terms of knock-out and heavy-particle stripping processes.

Returning finally to the problem of Be^{11}, it may be concluded that, although no single piece of experimental information seems sufficient to exclude odd-parity for this nucleus, all the available evidence taken together overwhelmingly favors it having even-parity. This is in accord with the predictions of Talmi and Unna.[103]

C H A P T E R VII

TRITON ELASTIC SCATTERING FROM LIGHT NUCLEI

In the D.W.B.A. theory of (t,p) double stripping (Rook and Mitra [30]) the distorted waves are again generated by elastic scattering optical model potentials. Since no previous measurements of elastic triton scattering had been reported, the measurements described in this chapter were undertaken to facilitate a D.W.B.A. analysis of some of the double stripping distributions described in the previous two chapters.

7.1 Procedure

Tritons elastically scattered from C^{12}, O^{16}, O^{18}, F^{19}, and Ca^{40} were magnetically analyzed in the multi-channel spectrograph. An upper limit of 7.2 MeV was placed on the triton energy owing to the limiting magnetic field strength of the spectrograph, and measurements were made at this energy and, in some cases, at 6.4 and 6.8 MeV.

Measurements on O^{16} and O^{18} were made with a natural tungsten oxide target and one enriched in O^{18}. The latter was the same target as that previously employed in the (t,p) reaction studies on O^{16} and O^{18} (Section 5.5). The carbon backing for these targets also permitted measurements to be made on C^{12}. The triton scattering from F^{19} and Ca^{40} was measured at 7.2 MeV with the calcium fluoride target previously employed in the $Ca^{40}(t,p)Ca^{42}$ reaction study (Section 5.7). Exposure strengths of 160 microcoulombs were used for the C^{12}, O^{16}, and O^{18} measurements and 60 microcoulombs for the F^{19} and Ca^{40} measurements.

7.2 Results and Analyses

(a) $F^{19}(t,t)F^{19}$ and $Ca^{40}(t,t)Ca^{40}$: The differential cross-sections for 7.2 MeV tritons elastically scattered from F^{19} and Ca^{40} are shown in fig. 7.1. The curves shown represent some best fits obtained with the optical model using the parameter search programme of Maddison (Section 3.3). The corresponding parameters are indicated in the figure.

For both F^{19} and Ca^{40} considerable ambiguity was observed in the parameters which best describe the scattering. In the case of F^{19}, a detailed analysis showed that equally good agreement

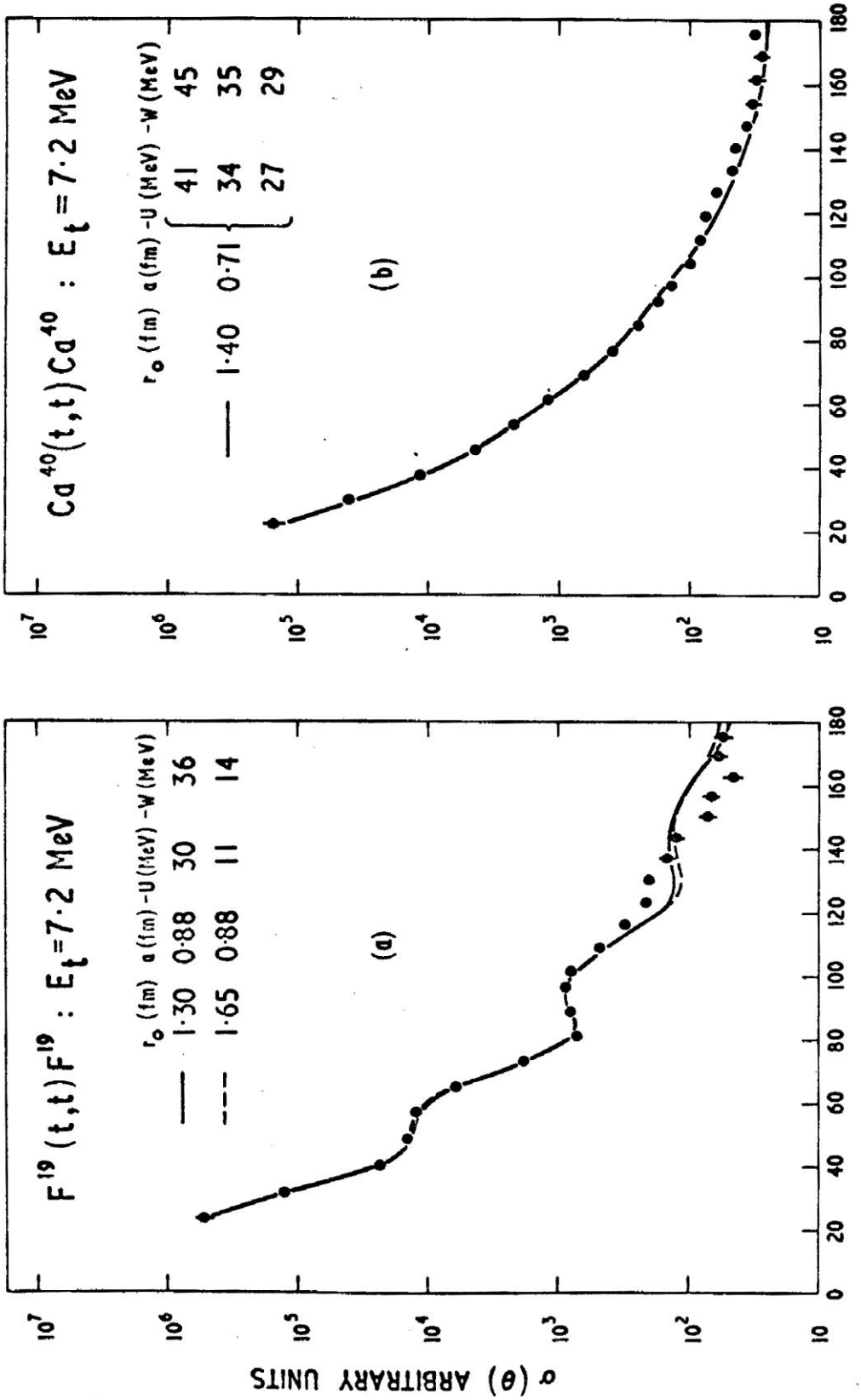

Fig. 7.1 *Triton elastic scattering from F^{19} and O^{16}.*

could be obtained with widely different sets of optical potentials, the results of two such sets being shown in fig 7.1(a). The only parameter which was well determined was the surface diffuseness, a. This was found to be 0.88 fm and the fit to the experimental result was significantly worse if this value changed by more than about 5%. A systematic variation in the radial parameter, r_o, further showed a need for keeping U and W nearly equal, although their actual values could only be determined by assuming a particular value for r_o.

This ambiguity is demonstrated in fig. 7.2 in which the values of U and W which give best agreement to the scattering from F^{19} are plotted against assumed values of r_o. The numbers against each set of points are the corresponding values of χ^2 and these indicate that departure from reasonable agreement occurs for values of r_o less than about 1.1 fm and greater than about 1.8 fm. Within this range the agreement is quite good and more or less independent of r_0.

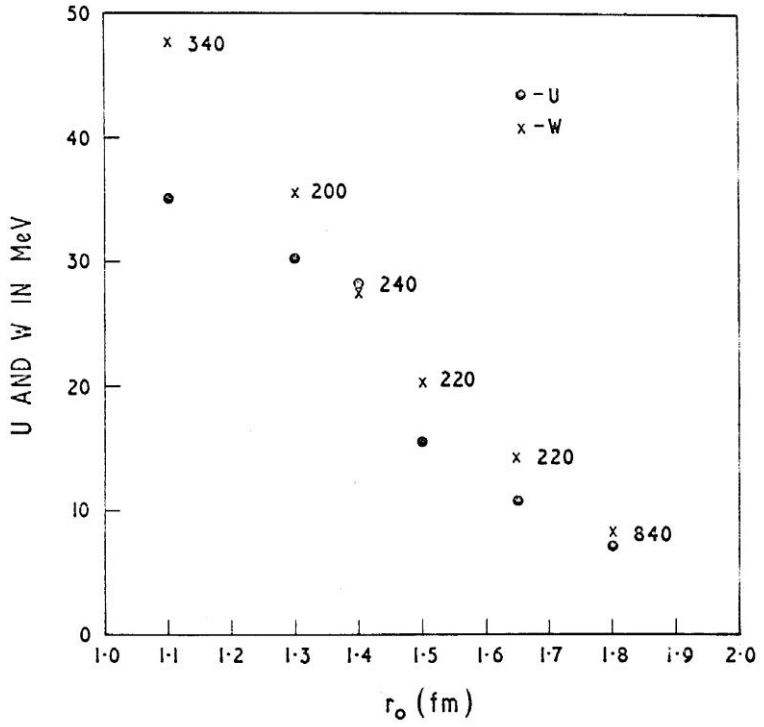

Fig. 7.2 Best-fit values of χ^2 as a function of r_0.

A similarly detailed analysis for Ca^{40} again showed the surface diffuseness to be well determined and its value was found to be 0.71 ± 0.05 fm. However, a more serious ambiguity was observed between the remaining parameters. With r_o maintained constant, equally good agreement could be obtained for different values of the potential well depths U and W. This is indicated in fig

7.1(b) where three sets of values for U and W are shown corresponding to r_o = 1.4 fm. Similar results were obtained for other values of r_o. It was, nevertheless, still necessary to keep U and W approximately equal to maintain satisfactory agreement with the observed scattering.

(b) $C^{12}(t,t)C^{12}$ and $O^{18}(t,t)O^{18}$: The triton elastic scattering results for C^{12} at 6.4 and 6.8 MeV and O^{18} at 6.4 and 7.2 MeV are shown in fig. 7.3. The curves again represent the best theoretical fits obtained with the optical model and the corresponding parameters are given in the figure.

The agreement is particularly poor in the case of C^{12} where the scattering exhibits markedly different behavior at the two triton energies. In the case of O^{18} the elastic scattering shows a backward peak at both energies, although in neither case does this rise above the Rutherford cross-section. Some success is had by the optical model in describing this structure but the agreement is less satisfactory in the forward direction where the model is expected to be more reliable.

If the experimental results at large angles were neglected in the O^{18} scattering, improved agreement out to 120^0 could be obtained with small changes in the parameters. However, as for the F^{19} and Ca^{40} results, equally good agreement could be had with several sets of parameters and in all cases the fit at large angles was considerably worse.

(c) $O^{16}(t,t)O^{16}$: In fig 7.4 the differential cross-sections are shown for tritons elastically scattered from O^{16} at 6.4, 6.8 and 7.2 MeV. (The arbitrary units are not the same in all cases.) In each case a large backward peak is observed which for the 6.8 MeV result rises to 15x the Rutherford cross-section. The broken line curve represents the best optical model fit to the data at 6.8 MeV and corresponds to a central potential with U = 68 MeV, W = 16 MeV, r_o = 1.5 fm and a = 0.6 fm. It is clear that this model is quite unable to account for the large rise in the backward direction.

Using a modified programme due to Rook [109], the effect of including an exchange term [110] of the form $(-1)^{\ell}U_{Ex}(r)$ in the scattering formalism was studied. The full line curve in fig. 7.4 illustrates the best fit which could be obtained and corresponds to a central potential with parameters U = 111 MeV, W = 23 MeV, r_0 = 1.24 fm and a = 0.6 fm and a real exchange potential U_{Ex} = 80 MeV. The same radial form was used for the exchange potential as for the central potential. Since such a term deliberately generates a backward peak, however, the improved agreement at large angles is not unexpected.

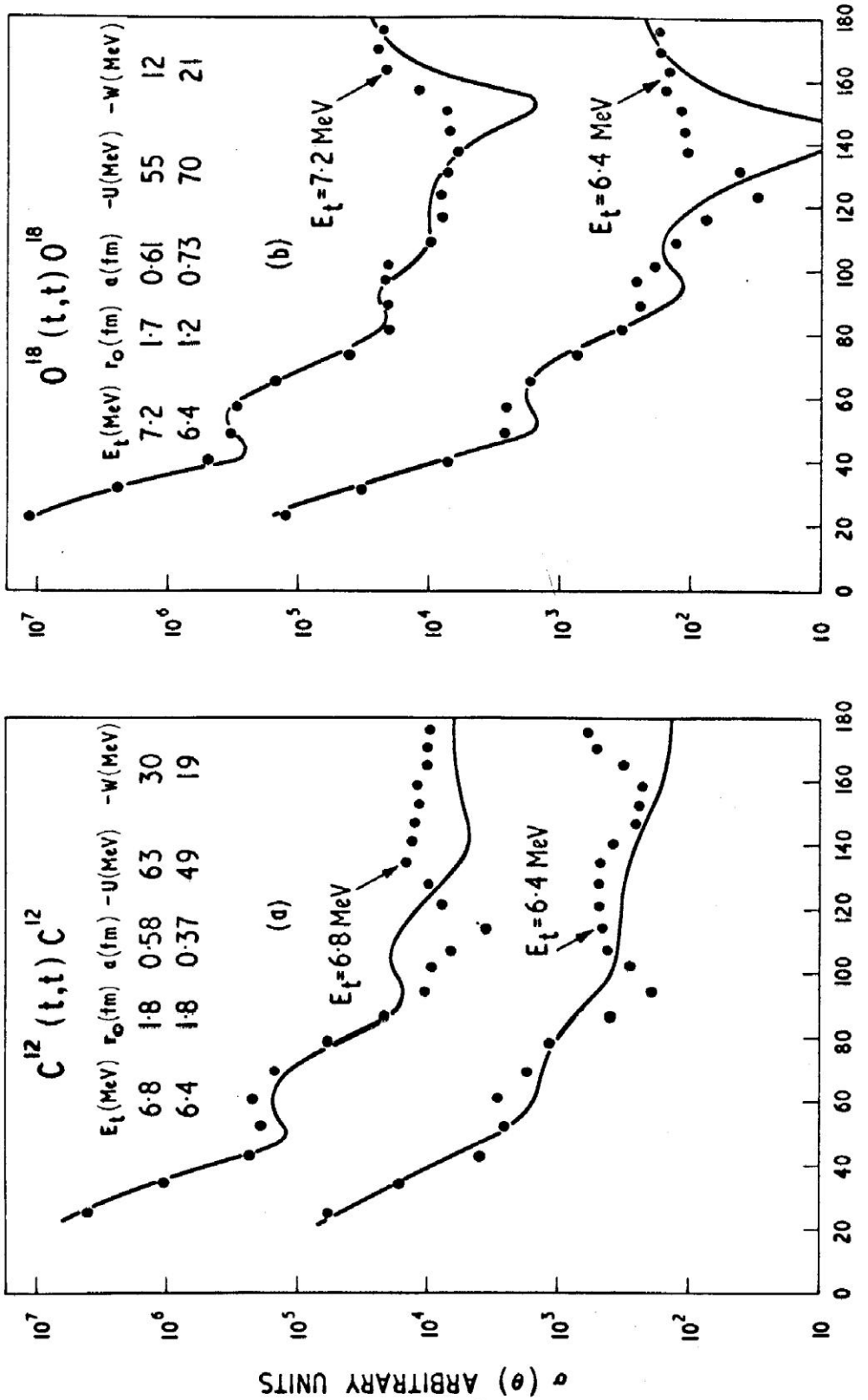

Fig. 7.3 *Triton elastic scattering from C^{12} and O^{18}.*

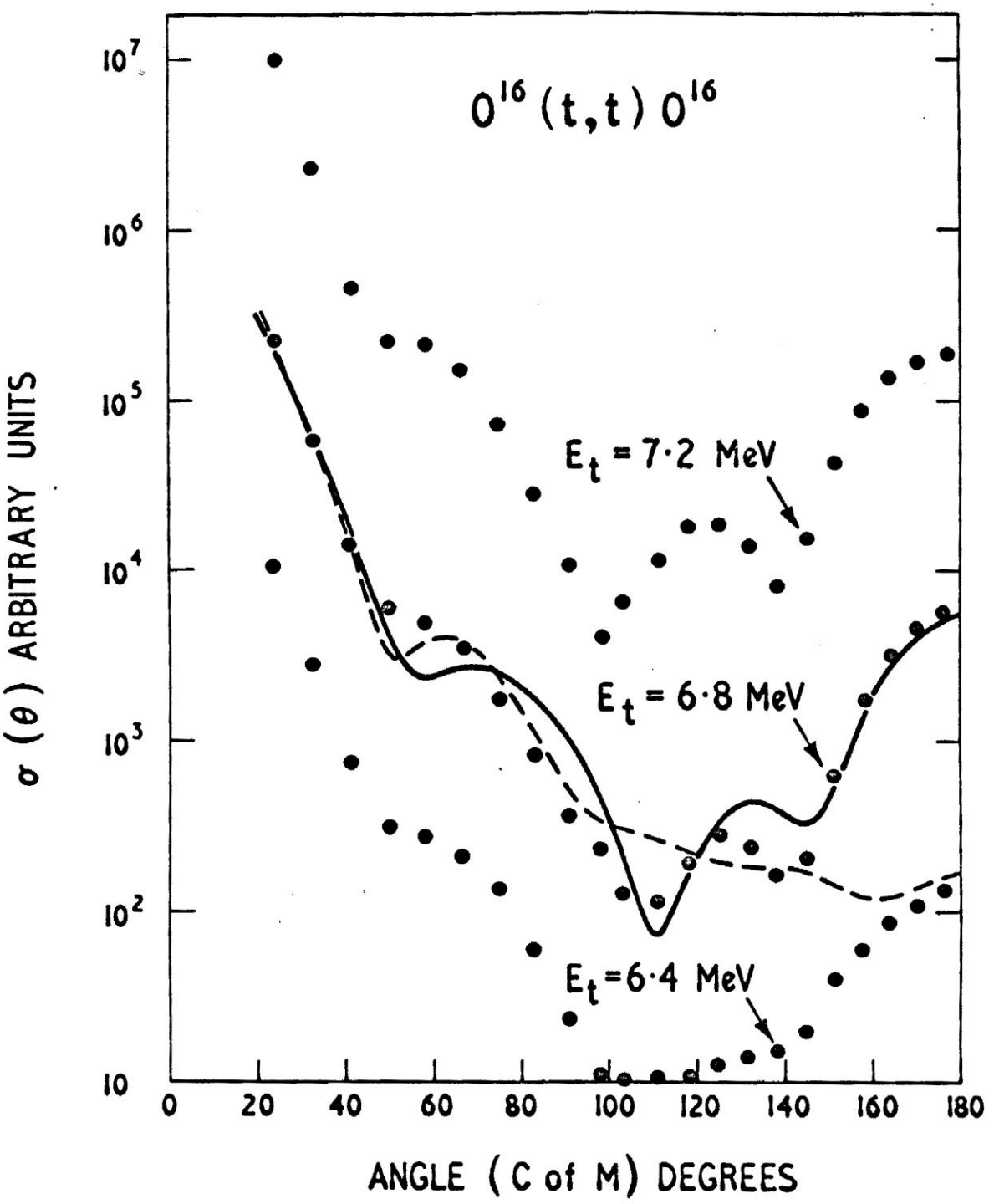

Fig. 7.4 *Effect of introducing an exchange potential (broken line) in triton scattering from* O^{16}.

7.3 Discussion

Of the cases studied in this investigation only the triton scattering from F^{19} and Ca^{40} can be satisfactorily accounted for by the optical model. Even in these cases, however, the optical parameters are ambiguous, although for F^{19} this ambiguity can be removed if a particular value for r_o is accepted. The insensitivity of the scattering from Ca^{40} to the optical potentials can probably be attributed to the predominance of coulomb scattering at 7.2 MeV.

For both F^{19} and Ca^{40} the surface diffuseness is extremely well defined. Such sensitivity may be understood if the scattering occurs predominantly in the nuclear surface region. This is certainly consistent with the large absorption potentials which are necessary to describe the scattering and which indicate a low mean free path for tritons in nuclear matter. A similar situation has been observed in the case of He^3-scattering by Hodgson [111], who further pointed out [112] that scattering at energies close to the coulomb barrier can provide useful information on the nuclear surface region. It is interesting to note that in the present analysis it was necessary to use a smaller surface diffuseness for Ca^{40} than for F^{19} which may perhaps reflect its closed-shell structure.

The failure of the optical model to account satisfactorily for the scattering from C^{12} and O^{18} may be due to significant interference from compound elastic scattering. This would also explain the marked energy variation observed in the scattering for these two cases.

Of particular interest, however, is the inability of the optical model to account for the large backward peak observed in the elastic differential cross-sections for O^{16} at these energies. Its explanation in terms of exchange scattering does not seem plausible in view of the somewhat unrealistic optical parameters required. These same parameters were also unable to account for such a rapid energy variation as that observed for the backward peak, whose magnitude at 6.8 MeV is greater by almost a factor of two than at 6.4 and 7.2 MeV. Exchange scattering would also seem physically unlikely since this implies a large triton reduced width for O^{16}, i.e., that a considerable proportion of the O^{16} ground state configuration can be represented as $\{N^{13}+t\}$. One might expect such a large reduced width to be more likely in the case of F^{19} i.e. $\{O^{16}+t\}$, in view of the 1p-shell closure in O^{16}. However, no significant backward peaking is observed in this scattering.

Calculations have also been carried out by Rook [113] with a spin-orbit term of the Thomas-Fermi form included in the scattering formalism. The results are shown in fig 7.5. With the real and imaginary depths of the spin-orbit potential varied in the range 0 to 22 MeV, the effect on the

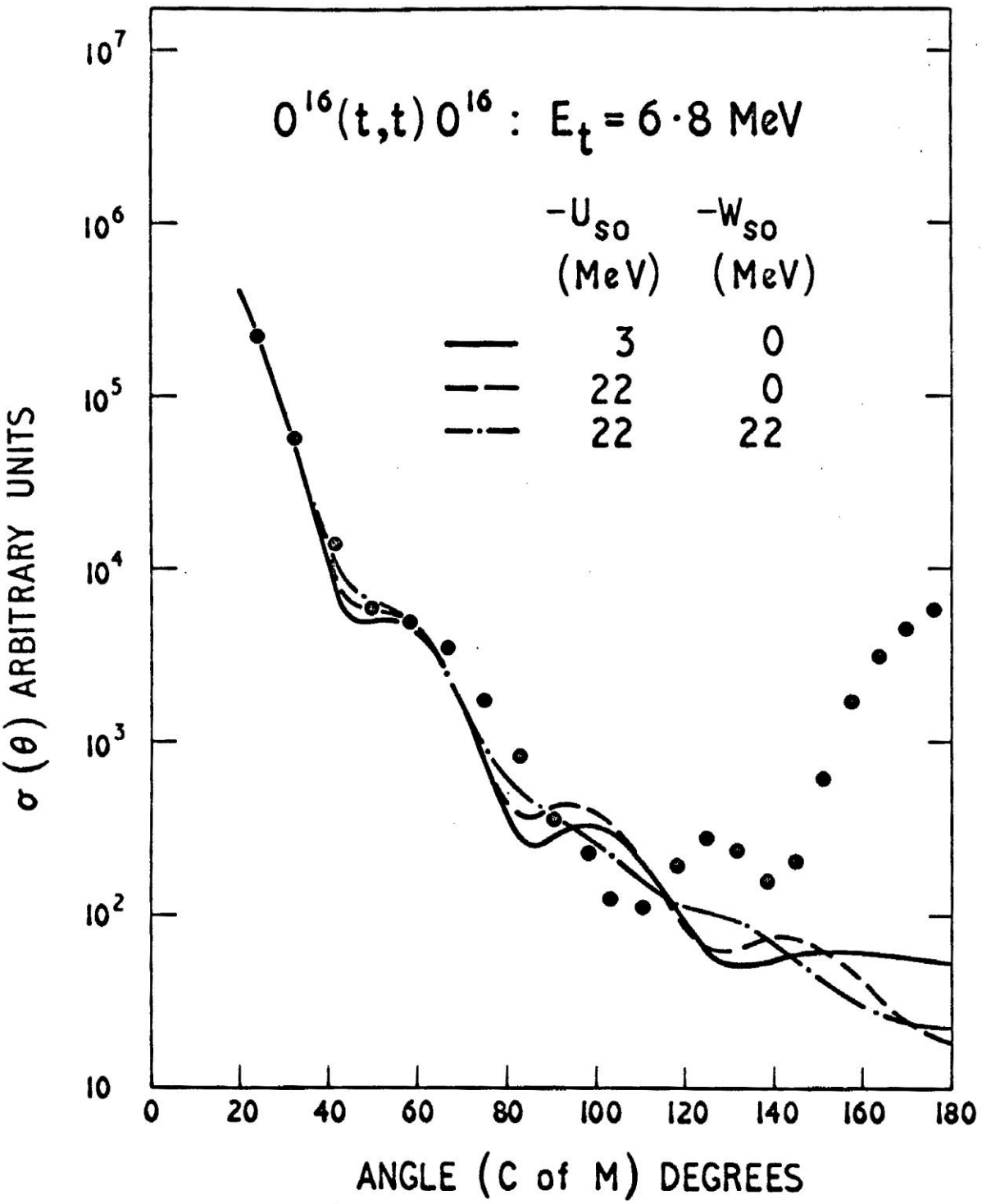

Fig. 7.5 *Effects of adding Thomas-Fermi spin-orbit terms in the scattering potential.* (The author is indebted to Dr. J.R. Rook for this figure.)

scattering is seen not to be very significant compared with the discrepancy between the observed scattering and theory and is clearly unable to explain the backward peak.

The rapid energy variation of the backward peak can be more readily understood as a consequence of compound resonance scattering. Thus, if the cross-sections observed at the extreme backward angles are assumed to be due entirely to resonance scattering, an estimate of the total resonance width, Γ, and resonance energy, E_0, can be readily obtained from the relation [114],

$$\frac{E_1\sigma_1(\theta)}{E_2\sigma_2(\theta)} = \frac{(E_2 - E_0)^2 + \Gamma^2/4}{(E_1 - E_0)^2 + \Gamma^2/4}$$

where $\sigma_n(\theta)$ is the differential cross-section at incident energy E_n. The values so determined are Γ = 0.83 MeV and E_0 = 6.87 MeV, the latter corresponding to an excitation energy of 18.6 MeV in F^{19}. Further measurements of this scattering at other energies are clearly necessary, however, before its nature may be fully understood [a].

[a] Triton elastic scattering measurements from O^{16} have recently been extended to energies up to 13 MeV by Glover and Jones (private communication). They observe marked fluctuations in the excitation function between 9 MeV and 13 MeV although the backward peak appears to persist at all energies. Its explanation in terms of a single resonance in F^{19} may not therefore be valid.

A P P E N D I X A

PREPARATION OF C^{14} TARGETS.

Fabrication of the C^{14} targets was adapted from one used by Douglas et al.[115] and Moore[116]. In this technique an electrical discharge is passed through an atmosphere of acetylene gas, the major effect of which is to partially ionize the acetylene molecule which subsequently deposits on to the electrodes. If an a.c. discharge is used, approximately equal amounts of carbon are deposited on each electrode.

In the present case the gas discharge apparatus of fig. A1 was used and the targets were obtained by placing gold or nickel foils, approximately 1 mg cm^{-2} in thickness, over the electrodes. The polymer deposit was limited to a circular area, 1 cm in diameter, by the pyropholite insulators shown in the figure. Both electrodes were adjustable from outside and a separation of about 1 cm was generally found most suitable. The wall of the chamber was of perspex glass, so making visual observation of the discharge possible. The ends of the chamber were of brass and the vacuum seals were provided by 'O'-rings as shown. Acetylene enriched to 44% in C^{14} was used [1].

The targets were produced as follows. The target backing foils were assembled on the electrodes and the discharge apparatus attached by a valve unit to the gas cell, backing pump and oil manometer. The general arrangement is shown in fig. A2. After evacuating the system through to the gas cell, the pump was isolated and the acetylene admitted slowly to the chamber until a pressure of about 10 mm Hg was reached. The gas cell was then isolated and a radiofrequency discharge applied by means of a Tesla coil. The discharge was then continued until the depositing process was complete. Fairly uniform targets were obtained in this way and the target thicknesses were estimated by direct weighing to be about 150 μgm cm^{-2}. The deposit was yellow-brown in colour but gradually turned black under the beam bombardment. The overall efficiency of this

[1] Obtained from U.K.A.E.A. Radiochemical Centre, Amersham, Bucks.

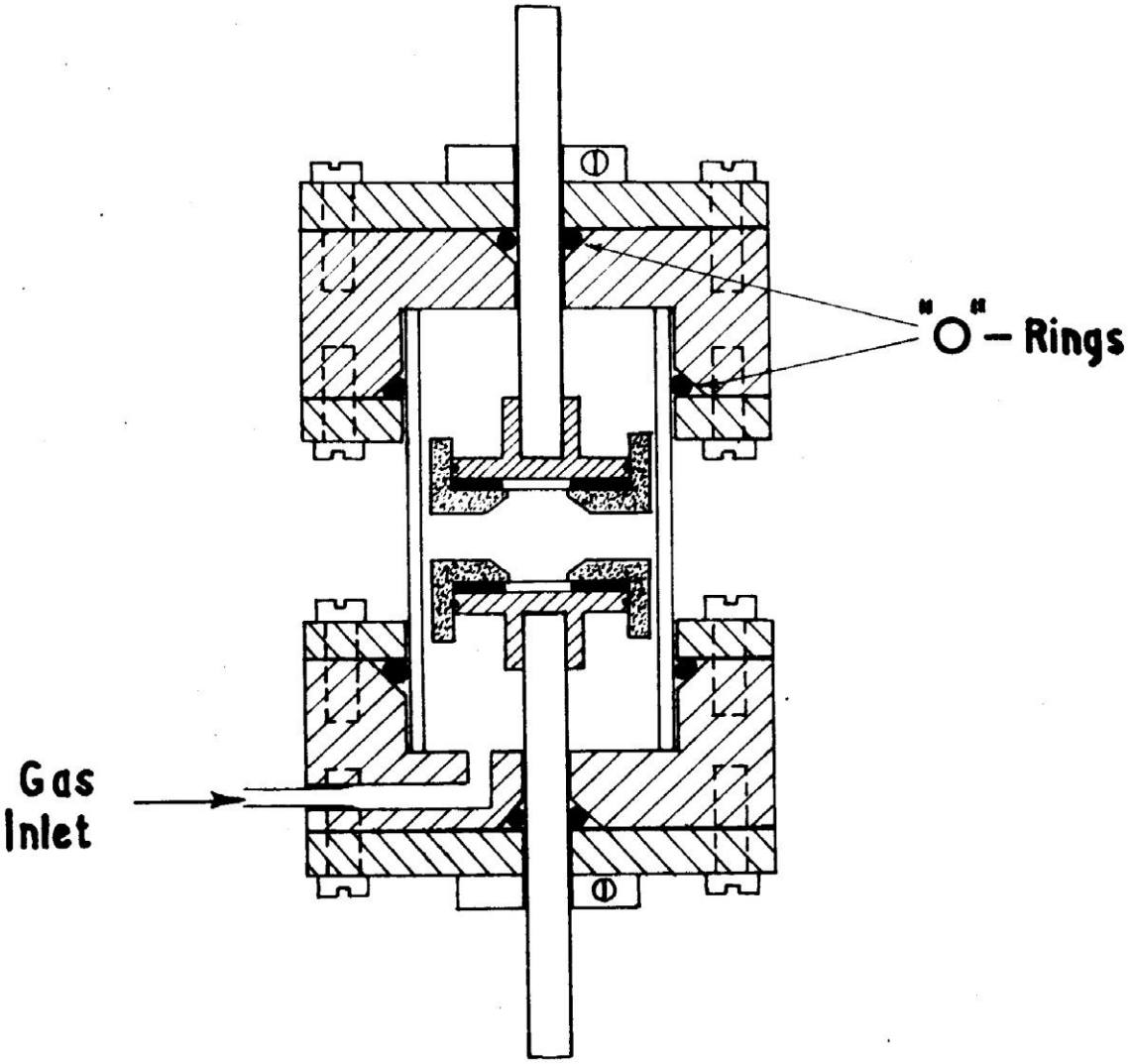

Fig. A1 *Schematic of gas discharge tube for fabricating C^{14} targets.*

method of preparation was about 60%, most of the loss being due to an appreciable amount of acetylene being deposited on the insulators and adjacent parts of the chamber.

The best discharge condition was determined by several trial runs using commercial grade acetylene. These natural carbon targets also proved useful later in the identification of reaction particle groups arising from target contaminants. The first targets were prepared with nickel backings. Although satisfactory for the low-energy reaction studies, these did not prove suitable for the investigations at higher energies owing to particle groups arising from reactions with the nickel. The later targets were therefore prepared with gold backings.

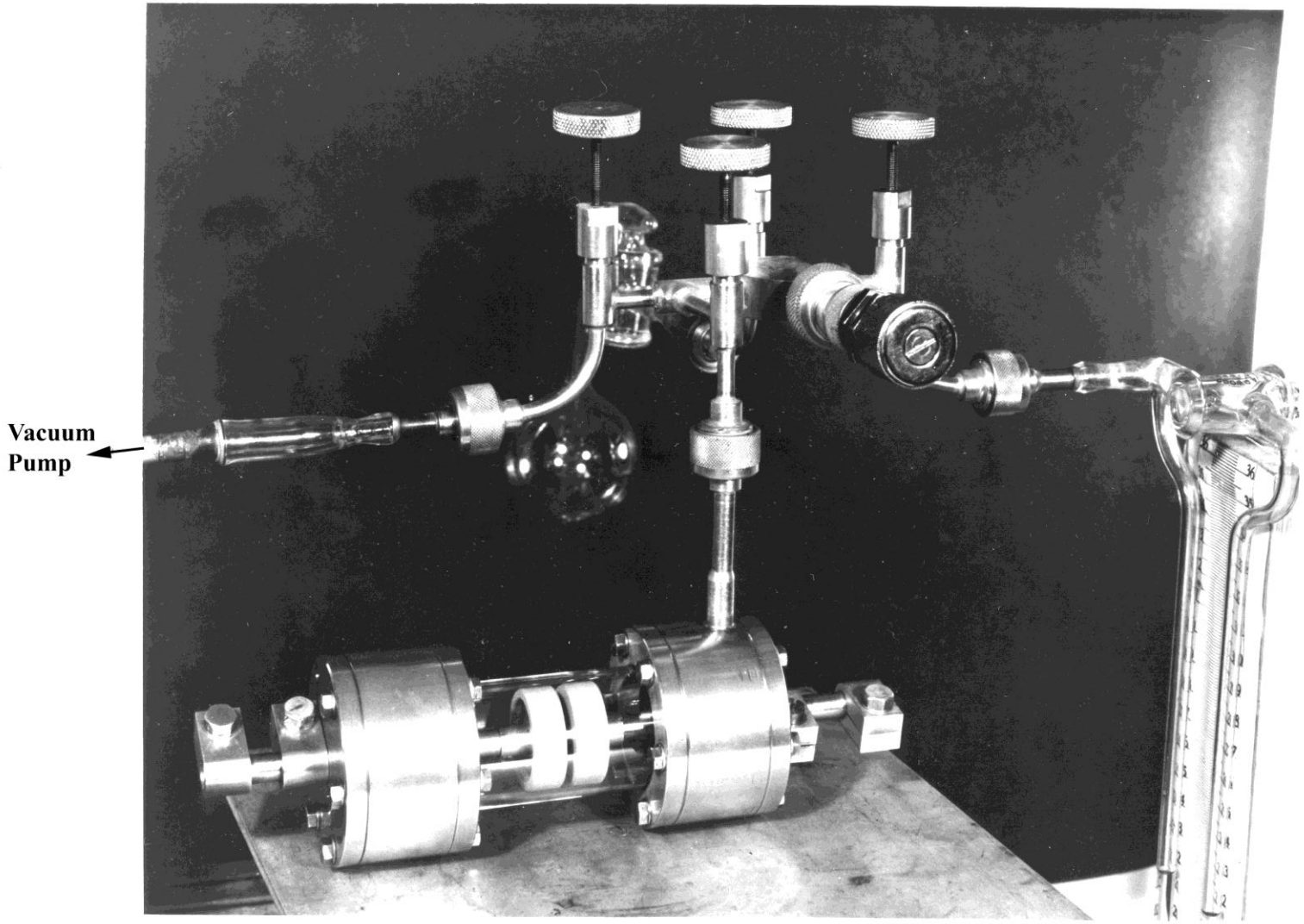

Fig A2. *General arrangement showing gas discharge tube and manifold.*

APPENDIX B

NEW ISOTOPE OF CARBON: C^{16}

S. Hinds and R. Middleton
Atomic Weapons Research Establishment, Aldermaston, Berkshire, England

and

A. E. Litherland* and D. J. Pullen
Clarendon Laboratory, Oxford, England
(Received December 30, 1960)

Estimates of the neutron binding energies of a number of neutron-rich light nuclei have been made recently by Zel'dovich.[1] In particular, from these estimates the $C^{14}(t,p)C^{16}$ reaction was expected to have a Q value lying between -3 and -4 Mev. This reaction has now been observed and the measured Q value is -3.014 ± 0.016 Mev. In addition, the decay of C^{16} has been studied and the measured half-life is 0.74 ± 0.03 second.

A 6-Mev triton beam from the Aldermaston electrostatic generator was used to bombard a thin C^{14} target and the emitted protons were analyzed with a broad-range magnetic spectrograph.[2] The targets were prepared by polymerizing acetylene gas containing 33% C^{14} directly onto nickel backing foils. Several exposures were made with the spectrograph using different magnetic field strengths and at angles ranging from 15° to 65°. On five of these an intense proton group was observed which could not be accounted for by the known target impurities. Further analysis established that this group varied in energy characteristically of a mass-14 target nucleus and probably corresponded to the formation of C^{16} in its ground state. The kinematics of the reaction, however, do not allow the $C^{14}(t,p)C^{16}$ reaction to be distinguished from either the $C^{14}(He^3,p)N^{16}$ or the $N^{14}(t,p)N^{16}$ reactions. The He^3 contamination of the ion beam was measured to be less than 0.1% by observing the elastically scattered particles and was therefore unlikely to give rise to significant reaction groups. It was also noted that, although several intense groups were observed arising from the $C^{12}(t,p)C^{14}$ reaction, none could be attributed to the $C^{12}(He^3,p)N^{14}$ reaction. To eliminate the possibility of the $N^{14}(t,p)N^{16}$ reaction, two exposures were made with a target containing nitrogen. No group was observed with the same energy as the group ascribed to C^{16}. Also no proton groups were observed corresponding to the known lower excited states of N^{16} in the spectra obtained with the C^{14} target, and only a weak continuum of protons was observed from a typical nickel target backing.

The energy of the incident triton beam was determined in terms of the Q value of the $C^{12}(t,p)C^{14}$ reaction[3] and from this the Q value of the $C^{14}(t,p)C^{16}$ reaction was calculated to be -3.014 ± 0.016 Mev. This is consistent with a C^{16} mass excess of 13.694 ± 0.017 Mev and a mass of 16.014702 ± 0.000017 mass units, both referred to the scale on which the mass excess of C^{12} is zero.

An energy level diagram showing the possible modes of decay of C^{16} is shown in Fig. 1.[4-6] As a change of parity is required for the high-energy beta transitions, the beta decay of C^{16} was expected to leave N^{16} in neutron-unstable 1+ states. This expected delayed-neutron emission has been observed experimentally and used to determine the half-life of C^{16}.

A one-microampere triton beam from the electrostatic generator was interrupted by a mechanical shutter some 20 feet away from the neutron detector which was a block of polystyrene, 45 cm long by 45 cm in diameter, containing five BF_3 counters. A hole of 10-cm diameter through the polystyrene block allowed the C^{16} nuclei to be formed at the center of the assembly. The efficiency of the detector was between 1 and 2%. The pulses from the neutron detector and associated electronic equipment were fed into a circuit which converted their time of arrival into a pulse height. The time distribution of the pulses could then be displayed on a 100-channel pulse-amplitude analyzer immediately after the interruption of the beam. The time scale of the analyzer was calibrated using the 50-cps mains frequency.

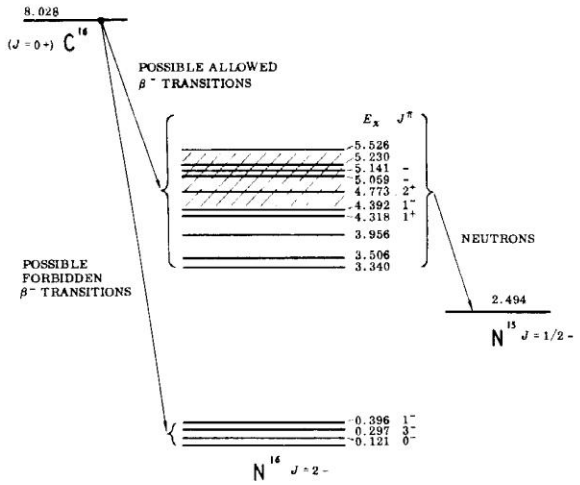

FIG. 1. An energy level diagram showing the possible modes of decay of C^{16}.

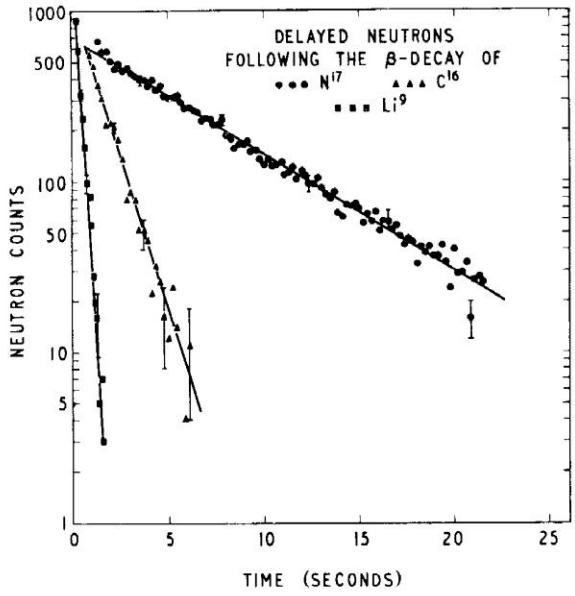

FIG. 2. A logarithmic plot of the decay of the delayed-neutron intensity from C^{16}. Also shown are the decay curves for the other two delayed-neutron emitters Li^9 and N^{17}.

Targets containing Li^7, C^{14}, and O^{18} were bombarded by the 6-Mev triton beam for periods between 2 and 10 seconds. The delayed neutrons from, respectively, Li^9, O^{16}, and N^{17} were displayed in the time-analyzer for periods ranging from 2 to 25 seconds. A fraction of a second delay between the end of each beam pulse and the start of the counting period was provided manually. No delayed neutrons were observed from the target backings though there was a very small background which was thought to arise from the triton beam striking the mechanical shutter. Figure 2 shows the decay of the delayed neutrons following the $Li^7(t,p)Li^9$, the $C^{14}(t,p)C^{16}$, and the $O^{18}(t,\alpha)N^{17}$ reactions. The half-lives of Li^9 and N^{17} were found to be 0.17 ± 0.01 and 4.20 ± 0.08 seconds, respectively, and these are in good agreement with the published values.[4] The half-life of C^{16} was found to be 0.74 ± 0.03 second.

The measured mass of C^{16} implies that the first $T = 2$ state in O^{16} is at approximately 23.0 Mev. In the future it would be interesting to determine the neutron-unstable states of N^{16} to which C^{16} decays and to determine the beta-ray branching ratio to the low-lying negative-parity states of N^{16}.

We wish to thank Dr. K. W. Allen and Professor

D. H. Wilkinson for their interest in this work and several helpful discussions.

---

*Seconded from Atomic Energy of Canada, Chalk River, Ontario, Canada.

[1]Ya. B. Zel'dovich, J. Exptl. Theoret. Phys. U.S.S.R. 38, 1123 (1960)[translation: Soviet Phys. - JETP 11, 812 (1960)].

[2]S. Hinds and R. Middleton, Proc. Phys. Soc. (London) 74, 196 (1959).

[3]F. Everling, L. A. Konig, J. H. E. Mattauch, and A. H. Wapstra, Nuclear Phys. 18, 529 (1960).

[4]F. Ajzenberg-Selove and T. Lauritsen, Nuclear Phys. 11, 1 (1959).

[5]C. P. Sikkema and R. Van Wageningen, in Proceedings of the International Conference on Nuclear Structure, Kingston, edited by D. A. Bromley and E. W. Vogt (University of Toronto Press, Toronto, Canada, 1960), p. 513.

[6]N. Jarmie, M. G. Silbert, and D. B. Smith (private communication).

APPENDIX C

DISTORTED WAVE ANALYSIS OF $Ca^{40}(t,p)Ca^{42}$

The proton angular distributions from the $Ca^{40}(t,p)Ca^{42}$ reaction (Section 5.7) have recently been analyzed by Rook and Mitra [30] using a distorted wave formalism for double stripping. The calculations have been described in detail in ref (30) and only a brief description of some of the results obtained is given here. The optical parameters U = 23 MeV, W = 28 MeV, r_o = 1.4 fm and a = 0.7 fm were assumed for the triton potential (taken from the elastic scattering measurements of Chapter 7), and for the proton potential the parameters U = 50 MeV, W = 8 MeV, r_o = 1.25 fm and a = 0.55 fm were assumed.

In fig. C1 are shown some fits obtained for the ground and first three excited levels of Ca^{42}. In these calculations the zero-range approximation was made for the triton and no cut-off radius was employed. The theoretical cross-section has been arbitrarily normalized to the ground state experimental value and the normalization factors for the excited levels are indicated in the figure. It is interesting to note that the excited states are not so strongly excited as the single-particle model would suggest. The two neutrons were assumed to be captured into a combination of 2p and 1f shell model states. The values of θ shown for each level are the relative spectroscopic factors for some of the possible configurations arising from these states which give best agreement with experiment. These fits are superior to those obtained assuming pure configurations and the distributions were found to be quite sensitive to the configuration mixture. This is in contrast to the situation observed with plane wave theory which gives a good account of the experimental distributions near the stripping peaks with only one adjustable parameter, apparently independent of the final state configurations. Although improved agreement is undoubtedly had with distorted wave theory the fit to the detailed structure is nevertheless still rather unsatisfactory.

Rook and Mitra also investigated the effect of including a finite range for the triton and showed that this could be simulated by a cut-off radius extending just beyond the nuclear surface. In fig. C2 a comparison is made between the experimental and theoretical

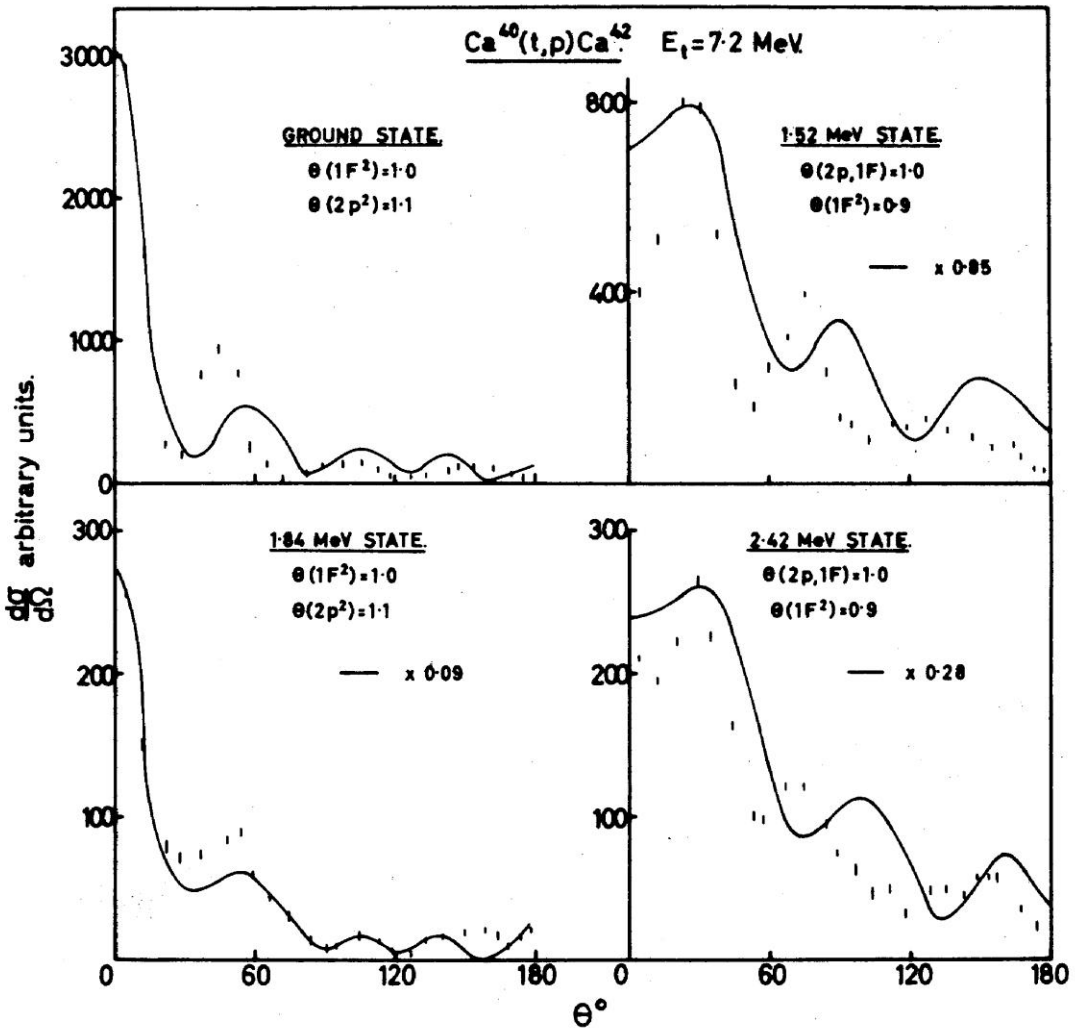

Fig. C1 *Two-nucleon DWBA stripping fits to $Ca^{40}(t,p)Ca^{42}$ reaction* [30].

(The author is indebted to Drs. J.R. Rook and D. Mitra for this figure and Fig. C2.)

results for the ground and first excited levels of Ca^{42} with a sharp cut-off at 5.5 fm. The overall agreement is seen to be somewhat better than that obtained previously without cut-off and in particular the calculated distributions exhibit sharper peaks than before. This effect is similar to the plane wave result. These calculations further showed the angular distributions to be relatively insensitive to the detailed configurations of the final states which thus explains the success of plane wave theory with only one parameter.

It is apparent from these investigations by Rook and Mitra that finite range effects are by no means negligible, and that their inclusion by means of a cut-off radius can lead to improved

agreement with the observed distributions. Unfortunately, however, it does not appear that cut-off theory will be able to yield detailed information on the final state configurations.

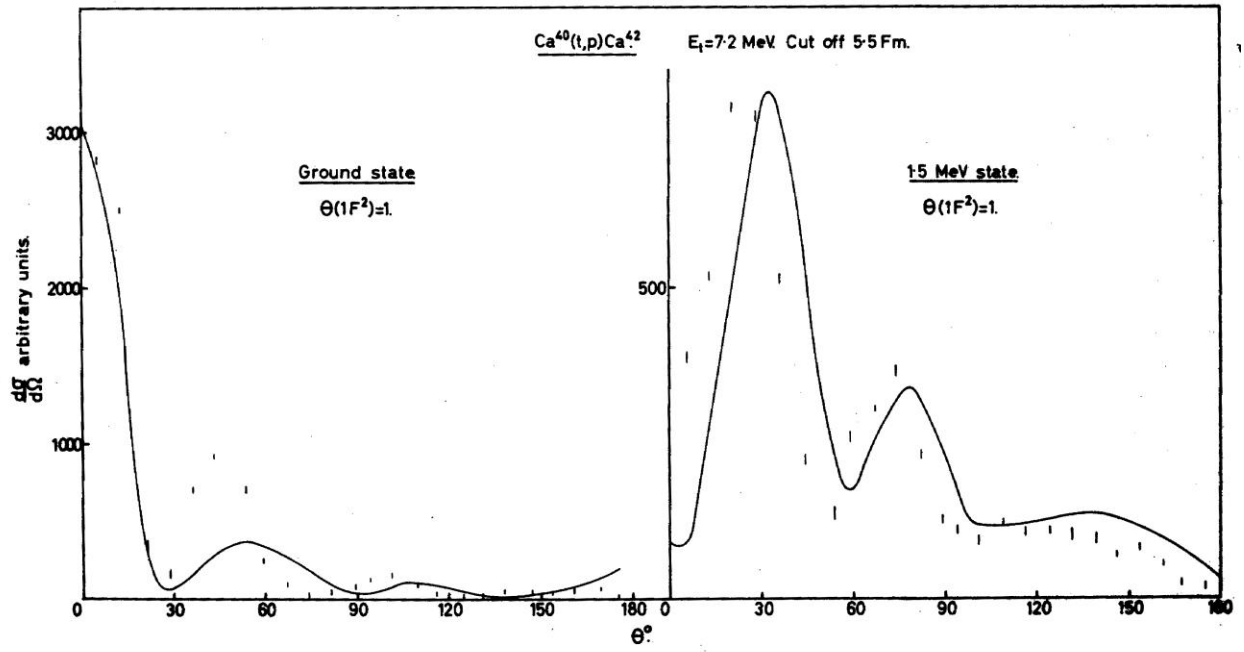

Fig. C2 *Effect of 5.5 fm cut-off radius to DWBA fits of $Ca^{40}(t,p)Ca^{42}$ reaction.*[30]

REFERENCES

1. M. B. Mayer, Phys. Rev. 75, (1949) 1969(L); and 78,(1950) 16.
2. O. Haxel, J. H. D. Jensen and H. E. Suess, Phys. Rev. (L) 75, (1949) 1766.
3. A. M. Lane and D. H. Wilkinson, Phys. Rev. 97, (1955) 1199.
4. D. R. Inglis, Rev. Mod. Phys. 25, (1953) 390.
5. A. M. Lane, Proc. Phys. Soc. A66, (1953) 977, A67, (1954) 167, A68, (1955) 189,197.
6. D. Kurath, Phys. Rev. 101, (1956) 216.
7. J. P. Elliot and B. H. Flowers, Proc. Roy. Soc. A229, (1955) 536.
8. A. Bohr and B. R. Mottelson, in *Nuclear Spectroscopy*, p.1009, Ed. F. Ajzenberg-Selove (Academic Press, New York, 1960).
9. S. G. Nillson, K. Danske Vidensk. Selsk. mat. fys. Medd. 29(1955) No.16.
10. A. E. Litherland, H. McManus, E. B. Paul, D. A. Bromley and H. E. Gove, Canad. J. Phys. 36, (1958) 378; 37 (1959) 53.
11. E. B. Paul, Phil. Mag. 2, (1957) 311.
12. S. T. Butler, Proc. Roy. Soc. A208, (1951) 559, also with O. H. Hittmair, in *Nuclear Stripping Reactions* (Wiley and Sons, New York, 1957).
13. A. B. Bhatia, K. Huang, R. Huby and H. C. Newns, Phil. Mag. 43, (1952) 485.
14. G. Gamow and C. L. Critchfield, *Theory of Atomic Nucleus*, p.11 (Oxford University Press, 1949)
15. e.g., J. M. Blatt and V. F. Weisskopf, *Theoretical Nuclear Physics*, Chapter 8, (Wiley and Sons, New York, 1952).
16. J. E. Bowcock, Proc. Phys. Soc. A68, (1955) 512.
17. J. A. Kuehner, E. Almqvist and D. A. Bromley, Nucl. Phys. 21, (1960) 555.
18. R. D. Amado, Phys. Rev. Letts. 2, (1959) 399.
19. M. H. MacFarlane and J. B. French, Rev. Mod. Phys. 32, (1960) 567.
20. A. P. French, Phys. Rev. 107, (1957) 1655.
21. N. T. S. Evans and A. P. French, Phys. Rev. 109, (1958) 1272.
22. G. E. Owen and L. Madansky, Phys. Rev. 105, (1957) 1766.
23. D. H. Wilkinson, in *Proc. Int. Conf. on Nuclear Structure*, p.20, Ed. D. A. Bromley and E. W. Vogt (North Holland, Amsterdam, 1960).

24. N. K. Glendenning, Nucl. Phys. 29, (1962) 109.
25. D. H. Wilkinson, Phil. Mag. 3, (1958) 1185.
26. R. G. Thomas, Phys. Rev. 100, (1955) 25.
27. W. Tobocman and M. H. Kalos, Phys. Rev. 97, (1955) 132.
28. R. Huby, M. Y. Refai and G. R. Satchler, Nucl. Phys. 9, (1958) 94.
29. B. Buck and P. E. Hodgson, Phil. Mag. 6, (1961) 1371.
30. J. R. Rook and D. Metra, Nucl. Phys. (in print).
31. B. E. F. Macefield, unpublished (private communication).
32. H. Feshbach, C. Porter and V. F. Weisskopf, Phys. Rev. 96, (1954) 448.
33. F. Bjorklund and S. Fernbach, Phys. Rev. 109, (1958) 1295.
34. S. Hinds, R. Middleton and D. J. Pullen, Phys. Letts. 1, (1962) 12.
35. B. E. F. Macefield, R. Middleton and D. J. Pullen, Nucl. Phys. (in print) 44, (1963) 309.
36. S. Hinds and R. Middleton, Proc. Phys. Soc. A74 (1959) 762, A75 (1960) 754.
37. S. Hinds and R. Middleton, Proc. Phys. Soc. A74 (1959) 196.
38. H. W. Fulbright, W. Parker-Alford, O. M. Bilaniuk, V. K. Deshponde and J. W. Verba, N.Y.O.-10034 (1962).
39. D. A. Bromley, E. Almqvist, H. E. Gove, A. E. Litherland, E. B. Paul and A. J. Ferguson, Phys. Rev. 105, (1957) 957/
40. M. El. Nadi, Proc. Phys. Soc. A70, (1957) 62, A73, (1959) 705.
41. H. C. Newns, Proc. Phys. Soc. A76, (1960) 489.
42. D. J. Pullen, A. E. Litherland, S. Hinds and R. Middleton, Nucl. Phys. 36 (1962) 1.
43. D. H. Wilkinson and D. E. Alburger, Phys. Rev. 113, (1959) 563.
44. R. Middleton and S. Hinds, Nucl. Phys. 34, (1962) 404.
45. K. T. Bainbridge, in *Experimental Nuclear Physics*, Part V, Ed. E. Segre (Wiley and Sons, New York, 1952).
46. C. P. Brown and W. W. Buechner, Rev. Sci. Inst. 27, (1956) 899.
47. C. W. Snyder, S. Rubin and W. A. Fowler and C. C. Lauritsen, Rev. Sci. Instr. 21, (1950) 852.
48. E. K. Warburton and L. F. Chase, Phys. Rev. 120, (1960), 2095.
49. J. P. F. Sellshop, Phys. Rev. Letts. 3, (1959) 346; Phys. Rev. 119, (1960) 251.
50. V. M. Rout, W. M. Jones and D. G. Waters, Nucl. Phys. 34, (1962) 628.
51. P. E. Hodgson, *Optical Model of Elastic Scattering* (Oxford University Press, 1963).

52. A. H. R. Muggleton and F. A. Howe, Nucl. Inst. and Methods 13, (1961) 211.
53. R. N. Maddison, Proc. Phys. Soc. 79, (1962) 264.
54. F. Ajzenberg-Selove and T. Lauritsen, Energy Levels of Light Nuclei, in *Landolt-Bornstein Tables*, Vol. I (Springer, Berlin, 1961).
55. B. Buck, Oxford University Nucl. Phys. Computing Group, Report No.6.
56. P. E. Hodgson, *Proc. Int. Symp. on Direct Nucl. Interactions*, Ed. E. Clementel and C. Villi, (Gordon and Breach, New York, 1963).
57. O. M. Bilaniuk and J. C. Hensel, Phys. Rev. 120, (1960) 211.
58. S. Hinds and R. Middleton, Nucl. Phys. 38, (1962) 114.
59. A. J. Ferguson, H. E. Gove, J. A. Kuehner, A. E. Litherland, E. Almqvist and D. A. Bromley, Phys. Rev. Letts. 1, (1958) 414.
60. P. F. Donovan, J. V. Kane, R. E. Pixley and D. H. Wilkinson, Phys. Rev. 123, (1961) 589.
61. N. T. S. Evans and W. C. Parkinson, Proc. Phys. Soc. A67, (1954) 684.
62. D. H. Wilkinson, Phys. Rev. 105, (1957) 666.
63. J. R. Holt and T. N. Marsham, Proc. Phys. Soc. A66, (1953) 1032.
64. E. Kondaiah and C. Badrinathan, Nucl. Phys. 15 (1960) 254.
65. W. E. Moore and J. N. McGruer, Bull. Amer. Phys. Soc. 4 (1959) 17.
66. D. E. Alburger, A. Gallmann and D. H. Wilkinson, Phys. Rev. 116, (1959) 939.
67. E. C. Halbert and J. B. French, Phys. Rev. 105, (1957) 1563.
68. E. Baumgartner and H. W. Fulbright, Phys. Rev. 107, (1957) 219.
69. G. R. Satchler, private communication via J. R. Rook.
70. F. Everling, L. A. Konig, J. H. E. Mattauch and A. H. Wapstra, Nucl. Phys. 18, (1960) 529.
71. K. Way, N. B. Gove, C. L. McGinnis and R. Nakasima, in Energy Levels of Nuclei in *Landolt-Bornstein Tables*, Vol I. (Springer, Berlin, 1961).
72. W. C. Rutledge, J. M. Cork, S. B. Burson, Phys. Rev. 86 (1952) 775.
73. R. G. Girgis, R. A. Ricci and R. van Lieshout, Nucl. Phys. 13, (1959) 485.
74. B. L. Saraf, J. Varma and C. E. Mandeville, Phys. Rev. 91 (1953) 1216.
75. G. M. Temmer and N. P. Heydenburg, Phys. Rev. 104, (1956) 567.
76. H. A. Bethe and S. T. Butler, Phys. Rev. (L) 85, (1952) 1045.
77. D. A. Bromley, E. Almqvist, H. E. Gove, A. E. Litherland, E. B. Paul and A. J. Ferguson, Phys. Rev. 105, (1957) 957.
78. H. D. Holmgren, L. Bullock and W. E. Kunz, Phys. Rev. 104, (1956) 1446.

79. R. L. Johnston, H. D. Holmgren, E. A. Wolicki and E Geer-Illsley, Phys. Rev. 107, (1958) 884.
80. D. A. Bromley and E. Almqvist, *Reports on Progress in Phys.* 23, (1960).
81. H. D. Holmgren and E. A. Wolicki, *N.R.L. Quarterly on Nucl. Science and Technology*, January 1961.
82. A. A. Jaffe, F. de S. Barros, P. D. Forsyth, J. Muto, I. J. Taylor and S. Ramavataram, Proc. Phys. Soc. A76, (1960) 914.
83. A. H. F. Muggleton and F. A. Howe, Nucl. Inst. and Methods, 12, (1961) 192.
84. C. K. Bockelman, D. W. Miller, R. K. Adair and H. H. Barschall, Phys. Rev. 84, (1957) 69.
85. J. Muto, F. de S. Barros and A. A. Jaffe, Proc. Phys. soc. A75, (1960) 929.
86. G. C. Morrison and J. A Galey, Phys. Rev. 116, (1959) 1583.
87. A. Marques, A. J. P. L. Policarpo and W. R. Phillips, Nucl. Phys. 36(1962)45.
88. E. K. Warburton and H. J. Rose, Phys. Rev. 109, (1958) 1199.
89. H. A. Cohn, J. K. Bair and H. B. Willard, Phys. Rev. 122, (1961) 534.
90. S. Hinds, R. Middleton, A. E. Litherland and D. J. Pullen, Phys. Rev. Letts. 6, (1961) 113.
91. S. Hinds. and R. Middleton, Proc. Phys. Soc. A75, (1960) 745.
92. R. Middleton, *Proc Int. Symp on Direct Interactions*, Ed. E. Clementel and C Villi (Gordon and Breach, New York, 1963).
93. S. Hinds, H. Marchant and R. Middleton, Nucl. Phys. 38, (1962) 81.
94. N. Jarmie and M. G. Silbert, Phys. Rev. 120, (1960) 914.
95. I. Talmi and I. Unna, Nucl. Phys. 30, (1962) 280.
96. D. Wilmore, *Proc. Rutherford Jubilee Int. Conf.* p.785, Ed. J. B. Birks (Heywood and Co., London 1961).
97. M. Harvey, Phys. Letts. 3, (1963) 209.
98. P. M. Endt and C. Van der Leun, Nucl. Phys. 34, (1962) 1.
99. C. M. Braams, Thesis, University of Utrecht, (1956) (unpublished).
100. H. Morinaga, N. Matsuro and M. Sugawara, Phys. Rev. 114, (1959) 1146.
101. J. D. McCullen and J. J. Kraushaar, Phys. Rev. 122, (1961) 555.
102. H. E. Mitler, Nucl. Phys. 23, (1961) 200.
103. I. Talmi and I. Unna, Phys. Rev. Letts. 4. (1960) 469.
104. P. F. Donovan, J. V. Kane, R. E. Pixley and D. H. Wilkinson, Phys. Rev. 123, (1961) 589.
105. S. Hinds and R. Middleton, Proc. Phys. soc A74, (1959) 775; A75, (1960) 444.

106. H. E. Gove, in *Nuclear Reactions I,* p.259, Ed. P. M. Endt and M. Demeur (North Holland, Amsterdam, 1959).

107. D. Kurath, private communication.

108. G. D. Gutsche, H. D. Holmgren, L. A. Cameron and R. L. Johnston, Phys. Rev. 125, (1962) 648.

109. J. R. Rook, private communication.

110. e.g. J. L. Gamel and R. M. Thaler, Phys. Rev. 109, (1958) 2041.

111. P. E. Hodgson, Nucl. Phys. 21, (1960) 28.

112. P. E. Hodgson, Nuclear Phys. 23, (1960) 28.

113. D. J. Pullen, J. R. Rook and R. Middleton, Nucl. Phys. (in print).

115. R. A. Douglas, B. R. Gasten and A. Mukerji, Canad. J. Phys. 34, (1956) 1097.

116. W. E. Moore, Thesis, University of Pittsburgh (1959) (unpublished).

117. K. Yagi, Y. Nakajima, K. Katori, Y. Auraya and M. Fujioka, Nucl. Phys. 41,(1963)584.

(Yagi et al. have studied the $O^{17}(d,p)O^{18}$ reaction and observe a strong l= 1 transition leading to the 4.45 MeV level. This state must therefore have odd parity which rules out the suggested 3^+ assignment. Also, since the state is strongly excited by (d,p) stripping it is unlikely to have the Harvey configuration $(1p)^{-1}$ $(2s,1d)^3$. A possible configuration is $(1d_{5/2},2p_{3/2})$ and since the state is not excited by (t,p) stripping this would suggest $J^\pi = 2^-$ or 4^-).